



Titre: Laser machining of cutting tool materials
Title:

Auteur: Dong Xiao Yu
Author:

Date: 2007

Type: Mémoire ou thèse / Dissertation or Thesis

Référence: Yu, D. X. (2007). Laser machining of cutting tool materials [Mémoire de maîtrise, École Polytechnique de Montréal]. PolyPublie.
Citation: <https://publications.polymtl.ca/7953/>

 **Document en libre accès dans PolyPublie**
Open Access document in PolyPublie

URL de PolyPublie: <https://publications.polymtl.ca/7953/>
PolyPublie URL:

Directeurs de recherche: Marek Balazinski, & Daniel Therriault
Advisors:

Programme: Non spécifié
Program:

UNIVERSITÉ DE MONTRÉAL

LASER MACHINING OF CUTTING TOOL MATERIALS

DONG XIAO YU

GÉNIE MÉCANIQUE

ÉCOLE POLYTECHNIQUE DE MONTRÉAL

MÉMOIRE PRÉSENTÉE EN VUE DE L'OBTENTION
DU DIPLÔME DE MAÎTRISE ÈS SCIENCE APPLIQUÉES
(GÉNIE MÉCANIQUE)

AVRIL 2007

© DONG XIAO YU, 2007



Library and
Archives Canada

Bibliothèque et
Archives Canada

Published Heritage
Branch

Direction du
Patrimoine de l'édition

395 Wellington Street
Ottawa ON K1A 0N4
Canada

395, rue Wellington
Ottawa ON K1A 0N4
Canada

Your file *Votre référence*
ISBN: 978-0-494-29260-0
Our file *Notre référence*
ISBN: 978-0-494-29260-0

NOTICE:

The author has granted a non-exclusive license allowing Library and Archives Canada to reproduce, publish, archive, preserve, conserve, communicate to the public by telecommunication or on the Internet, loan, distribute and sell theses worldwide, for commercial or non-commercial purposes, in microform, paper, electronic and/or any other formats.

The author retains copyright ownership and moral rights in this thesis. Neither the thesis nor substantial extracts from it may be printed or otherwise reproduced without the author's permission.

AVIS:

L'auteur a accordé une licence non exclusive permettant à la Bibliothèque et Archives Canada de reproduire, publier, archiver, sauvegarder, conserver, transmettre au public par télécommunication ou par l'Internet, prêter, distribuer et vendre des thèses partout dans le monde, à des fins commerciales ou autres, sur support microforme, papier, électronique et/ou autres formats.

L'auteur conserve la propriété du droit d'auteur et des droits moraux qui protègent cette thèse. Ni la thèse ni des extraits substantiels de celle-ci ne doivent être imprimés ou autrement reproduits sans son autorisation.

In compliance with the Canadian Privacy Act some supporting forms may have been removed from this thesis.

Conformément à la loi canadienne sur la protection de la vie privée, quelques formulaires secondaires ont été enlevés de cette thèse.

While these forms may be included in the document page count, their removal does not represent any loss of content from the thesis.

Bien que ces formulaires aient inclus dans la pagination, il n'y aura aucun contenu manquant.


Canada

UNIVERSITÉ DE MONTRÉAL
ÉCOLE POLYTECHNIQUE DE MONTRÉAL

Ce mémoire intitulé :

LASER MACHINING OF CUTTING TOOL MATERIALS

Présenté par : YU Dong Xiao

En vue de l'obtention du diplôme de : Maîtrise ès sciences appliquées

a été dûment accepté par le jury d'examen constitué de :

M. DAOUD Ahmed, président

M. BALAZINSKI Marek, Ph.D., membre et directeur recherche

M. TERRIAULT Daniel, Ph. D., membre et codirecteur de recherche

M. SONGMENE Victor, Ph.D., member

DEDICATION

*To my wife, Wen Fang
To my children, Zong Lin and Jessica*

ACKNOWLEDGEMENTS

I would like to express my sincere appreciation to Professor Marek Balazinski, my thesis director, for his guidance and constant encouragement throughout this research. His support and understanding give me a great courage to complete my M.Sc. thesis at École Polytechnique de Montréal. I would like to thank Professor Daniel Therriault for his helpful advices on the organization of my thesis.

I also wish to thank Mr. Francois Menard for his help for measuring the roughness of machined workpieces.

Thanks also go to Mr. Sylvain Simard for his help in solving problems on the DML 40SI laser machine when I started to use the machine.

I am indebted to Mr. Aurélien Riou and Mrs. Josée Dugas for his help in chapter “Condensé en Français”

Thanks also go to my classmate Mr. Victor Calatoru for his help in taking some photos for the machined samples and my friend Mr. Huo Li Guo and Mrs. Ren Qun for their advices on my thesis.

Finally, I want to thank the technical support of Lasertec Company.

During my study and research at École Polytechnique, personnel in Department of Mechanical Engineering gave me enthusiastic support. I would like to express my acknowledgement for their help.

ABSTRACT

This thesis focuses on applying laser micro-machining technology to machine cutting tool materials. The effects of laser parameters on cemented carbide were investigated in the thesis. Laser machined cutting edge and other micro-geometries were presented in the thesis also. This thesis is one of the explorations of cutting tool manufacturing technology.

During laser machining, the laser light is used as a high energy heating source to melt and/or vaporize the volume of the material to be removed. It is a non-contact process. Combined with modern control and CAD technologies, the machining rate and precision are high.

Metal cutting is an important field in modern manufacturing domain where the cutting tool is a key element. Development of metal cutting theory, tool technology, ultra-precision and nano-machining technology push the research on cutting tool unceasingly advance. Cutting edge is a geometry form of cutting tool. It is very important for optimizing the quality of machined surface and improving the life of cutting tool. The traditional ways to prepare cutting edge are time and money costing, the precision of obtained geometry form is also not satisfying.

In this thesis, laser was investigated to make cutting edge on cutting tool. Heating effect on cemented carbide is researched. The effect of laser machining parameters, the roughness of machined surface and the quality of machined geometry were also investigated. During research, DML40 SI laser machine was used to do experiment. The machining results show that the profile of micro geometry is satisfied when it is above 0.1mm order. The roughness of machined surface is less than 3 μ m. Finally, using laser to prepare cutting edge is concluded as a feasible method. This method can be a new member of family of cutting edge preparing methods and can be used to process most of cutting tool materials.

CONDENSÉ EN FRANÇAIS

INTRODUCTION

Dans ce mémoire, on présente l'arrière-plan de la technologie du laser et la technologie d'usinage. Puis, on va présenter le problème dans la recherche d'outil de coupe. Finalement, on explique la technologie d'usinage par laser pour les matériaux d'outil de coupe. Cette nouvelle approche pour l'usinage d'outil de coupe est explorée et une étude sur la rugosité de la surface usinée est faite.

CHAPITRE 1: LITTÉRATURE

Première partie : revue de littérature sur l'usinage par laser

Le laser est une lumière amplifiée par l'émission du rayonnement stimulé. Il traite le monochromatisme, la cohérence, la diffraction et le rayonnement. Ces propriétés rendent le rayon laser utile pour beaucoup d'applications dans les communications, la mesure et le traitement des matériaux. L'usinage par laser appartient à la grande famille de l'usinage par enlèvement de matière. Pendant l'usinage par laser, la lumière du laser travaille comme une source de chaleur d'énergie élevée et enlève les matériaux grâce à un mécanisme thermique, un mécanisme photochimique ou les deux pour fondre et/ou vaporiser le volume du matériau. C'est un traitement sans contact.

Par la manipulation de la condition de traitement telle que la densité de puissance, la longueur d'onde, l'impulsion ou continue le mode d'laser, le diamètre du rayon laser et la vitesse de déplacement, un laser simple peut exécuter plusieurs fonctions. En combinant les paramètres du rayon laser et de la matière, le résultat d'usinage obtenu peut différer.

En raison de l'intensité de grande énergie et de la contrôlabilité du rayon laser, le laser est très approprié pour l'usinage des matériaux difficiles à usiner, tels que les métaux durcis, la céramique, les composites et les polymères. Avec le développement de la technologie de commande numérique et de métrologie, un champ réussi de l'usinage par laser est le domaine de micro-usinage par laser. Récemment, les besoins croissants du marché ont poussé les personnes à rechercher de nouveaux domaines d'applications du laser. L'usinage par laser a assurément un avenir.

Deuxième partie: revue de littérature sur la technologie d'usinage

L'usinage des matériaux en pratique a occupé l'activité humaine depuis la préhistoire. Pendant de nombreuses années, les besoins civils et militaires poussent la technologie de *l'usinage de métal* à développer l'une des méthodes les plus importantes dans *la famille de l'usinage*, qui se compose de processus chimiques et électrochimiques, de traitements thermiques et de traitements mécaniques. Les matériaux des outils de coupe et les matériaux usinés sont développés à partir de matériaux non-métalliques aux matériaux en métal, en fer, du cuivre à l'acier, de l'acier rapide au métal dur, la céramique, le diamant synthétique. La précision d'usinage du métal peut être de l'ordre du nanomètre (10^{-6} millimètres).

Généralement, on considère que la technologie d'usinage moderne a débuté vers les années 1850. Toutes les recherches dans ce domaine peuvent être généralisées comme l'optimisation de technologie d'usinage dans le sens large :

- théorie d'optimisation usinage;
- optimisation de l'application de fluide ou près sec;
- optimisation de la fragmentation du copeau et de la qualité de la surface usinée;
- optimisation de la machine-outil;
- optimisation de la conception d'outil et la technologie de fabrication pour l'outil.

Les carbures frittés sont un groupe de matériaux durs. Ils sont résistants à l'usure et difficiles à usiner. Ils sont fabriqués à partir de particules dures de carbure et de métaux mous et malléables. Comparé aux conditions de fonctionnement de l'outil en acier rapide, qui sont principalement limitées par leur résistance au recuit, leur dureté à haute température et leur résistance à la chaleur pendant l'usinage. Pour les conditions d'usinage différentes, les géométries différentes sont usinées sur les outils de coupe, comme la géométrie de l'arête, l'angle primaire de râtelier, deuxième angle de râtelier et terre de contact, etc. Dans ces géométries, la géométrie de l'arête est la plus difficile à usiner à cause de la taille ultraprécise et de la géométrie variée.

La géométrie de l'arête inclut habituellement le type de l'arête, la dimension de l'arête arrondie ou l'arête chanfreinée, la tolérance de l'arête, la qualité extérieure de la surface de l'arête, etc. Le microsoufflage et la rectification sont les deux méthodes traditionnelles pour préparer l'arête. Ces méthodes de transformation sont coûteuses en temps, en travail peu efficace et peu précises.

Cet article présente une étude sur l'emploi de la technologie de l'usinage par laser pour préparer l'arrondi de l'arête. L'exécution de l'outil en carbure fritté préparé par laser est également étudiée.

CHAPITRE 2 : EFFETS THERMIQUES RAYON LASER SUR LES MATÉRIAUX D'OUTIL DE COUPE

Pendant le processus d'usinage par laser, le matériau est enlevé par un changement de phase provoqué par le rayon laser intense, fonte ou vaporisation. En raison des gradients énormes de la température qui sont développés dans la surface usinée, beaucoup d'effets secondaires concernant la qualité extérieure se produiront pendant l'usinage par laser, tel que la microfissuration, la formation d'une zone affectée par le chauffage et la formation

des striations. Par conséquent, il est important de comprendre le mécanisme de transfert thermique pendant l'usinage par laser.

Afin de commander le processus d'usinage par laser, nous développons un modèle général 3D de transfert thermique pour le processus d'usinage par laser. Dans le modèle, on s'attend à ce que la relation simple entre la profondeur de la coupe et les variables de processus soit donnée, telles que la puissance de rayon laser, la vitesse déplaçant du rayon laser, etc. La définition physique de notre modèle est la suivante :

- 1) Le rayon laser a une distribution gaussienne de l'intensité. Il cause la chaleur s'accumulant sur la surface du matériau, qui est absent d'une source chaleur extérieure. La chaleur se transfère dans la partie intérieure du matériau.
- 2) L'objet traité est considéré comme objet avec la géométrie de demi infinité parce que le rayon laser est trop petit comparé à l'objet soumis à un traitement thermique. $-\infty < x < \infty$, $-\infty < y < \infty$, $0 < z < \infty$.
- 3) La conductivité thermique, la densité et la chaleur spécifique des matériaux usinés sont indépendantes de la température.
- 4) Des pertes de chaleur par rayonnement et convection sont négligées.
- 5) La réflectivité est considérée comme nulle quand la température excède le point d'ébullition.
- 6) Quand n'importe quel endroit excède la température d'ébullition, le matériau est considéré comme vaporisé.
- 7) On admet que n'importe quel matériau fondu est entièrement enlevé par un gaz voyageant en jet et n'affecte pas l'interaction de faisceau-matériau.
- 8) L'effet des différences dans les conductivités thermiques entre le liquide et le solide n'est pas considéré.

L'équation diffusion est :
$$\frac{\partial T}{\partial t} - D \nabla^2 T = \frac{I}{C_p}$$

L'équation Green est :

$$G(x, y, z, t | x', y', z', t') = \frac{1}{8(\pi D \tau)^{\frac{3}{2}}} * \exp\left[-\frac{(x-x')^2 + (y-y')^2}{4D\tau}\right] * \left\{ \exp\left[\frac{-(z-z')^2}{4D\tau}\right] - \exp\left[\frac{-(z+z')^2}{4D\tau}\right] \right\}$$

L'équation de la distribution de température est :

$$T = \frac{P}{C_p \rho} \int_0^{\infty} \frac{\exp\left[-\frac{(x+vt')^2 + y^2}{2r_0^2 + 4Dt'} - \frac{z^2}{4Dt'}\right]}{(\pi^3 Dt')^{\frac{1}{2}} \cdot (2r_0^2 + 4Dt')} dt'$$

(Cline H.E. et al., 1977)

Après calcul, nous constatons que l'effet thermique sur la plaquette en carbure fritté par propriété mécanique est très négligeable.

CHAPITRE 3 : EFFETS DES PARAMÈTRES DU RAYON LASER SUR LE CARBURE CIMENTÉ

Au chapitre II, nous avons vu que l'effet thermique sur la surface du carbure est très faible. Par conséquent, dans ce chapitre, nous allons employer la technologie du micro-usinage par laser pour usiner le carbure fritté.

Dans ce chapitre, on présente l'objectif d'expérience, la procédure d'expérience, le matériau d'expérience, les paramètres de DML 40SI laser machine.

CHAPITRE 4 : ANALYSE DE TEXTURE DE LA SURFACE USINÉE PAR LASER

Dans ce chapitre, nous présentons la technologie de micro-usinage par laser pour usiner le carbure fritté. Pendant notre expérience, nous avons modifié la fréquence de fermeture de Q-commutateur, la vitesse de rayon laser, l'ouverture pour le rayon laser, en gardant constant les autres paramètres d'usinage. Les influences des paramètres du rayon laser seront recherchées.

D'abord, nous employons un paramètre d'usinage différent pour usiner le carbure fritté. Puis, nous utilisons le microscope pour observer la surface usinée et utilisons la Formtracer SV-C3000/4000 pour mesurer la rugosité de la surface usinée. Finalement, on va analyser la rugosité selon le standard ANSI/ASME B46.1-1985.

En conclusion, l'application de la technologie micro-usinage par laser sur l'outil de carbure cimentée sera évaluée.

CHAPITRE 5 : ANALYSE DE LA GÉOMÉTRIE MICRO-USINÉE PAR LASER

D'abord, nous utilisons une géométrie détaillée différente. Puis, nous analysons la géométrie usinée et trouvons la taille minimum satisfaisante de la géométrie qui peut être faite par DML40.

En conclusion, l'application de la machine DML40SI sera évaluée.

CHAPTER 6 CONCLUSION DE LA RECHERCHE ET PERSPECTIVE

L'utilisation de la technologie de micro-usinage pour usiner l'arête est une méthode faisable. Quand le rayon de l'arête tranchante est plus grand que 100 μm ou la taille du T-chanfrein est plus grande que 100 μm , la machine laser DML40SI peut faire le traitement. Si nous choisissons autre laser plus précis, des tailles plus petites pourraient être réalisées.

TABLE OF CONTENTS

DEDICATION	iv
ACKNOWLEDGEMENTS.....	v
ABSTRACT	vi
CONDENSÉ EN FRANÇAIS.....	vii
TABLE OF CONTENTS.....	xiv
LIST OF FIGURES.....	xix
LIST OF TABLES	xxiii
LIST OF ABBREVIATIONS AND SYMBOLS	xxiv
LIST OF APPENDIX	xxvi

INTRODUCTION

1.1 Background of laser technology.....	1
1.2 Background of cutting tool technology.....	2
1.3 Problem definition.....	3
1.4 Research objectives	3
1.5 Methodology	4
1.6 Thesis structure.....	4

CHAPTER 1- LITERATURE REVIEW

Part one. Literature review on laser technology

1.1 Basic notions of laser	5
----------------------------------	---

1.1.1 Introduction of laser	5
1.1.2 Properties of laser light.....	6
1.1.3 Basic mechanisms of laser system	6
1.1.4 Laser applications.....	8
1.2 Basic notions of laser machining technology	10
1.2.1 Mechanisms of laser machining.....	11
1.2.2 Characteristics of laser machining	12
1.2.3 Categories of laser machining	13
1.2.4 Components of laser machining system	18
1.3 Effects of laser machining parameters	19
1.3.1 Effects of beam properties.....	19
1.3.2 Effects of material properties of workpiece	21
1.3.3 Effects of transport properties	21
1.4 Summary of literature review on laser technology	22
Part two. Literature review on metal cutting technology	
1.5 Basic notions of metal cutting.....	23
1.6 Introduction of modern metal cutting technology	24
1.7 Introduction of geometry of cutting tool.....	25
1.7.1 Terms and definitions.....	25
1.7.2 Introduction of cutting edge	26
1.7.3 Importance of cutting edge.....	27

1.7.4 Preparing methods for cutting edge	28
1.8 Introduction of material of cutting tool	30
1.9 Introduction of cemented carbide.....	31
1.10 Summary of literature review of metal cutting technology	32
CHAPTER 2 HEATING EFFECTS OF LASER BEAM ON CUTTING TOOL MATERIAL	
2.1 Introduction	34
2.2 Generalized model for laser machining	35
2.3 Three dimension conduction model of laser machining.....	36
2.3.1 Fundamental of conduct heat transfer	36
2.3.2 Thermal model of melting material.....	37
2.3.3 Physical definition of the process to be modeled.....	37
2.3.4 Heat transfer of moving laser beam	38
2.4 Calculation example	43
2.5 Conclusion.....	47
CHAPTER 3 LASER MACHINING EXPERIMENTS ON CEMENTED CARBIDE INSERTS	
3.1 Introduction	49
3.2 Objectives of experiment	49
3.3 Materials and equipment	49

3.4 Parameters of DML 40SI laser machine.....	51
3.5 Experimental procedures.....	52
 CHAPTER 4 ROUGHNESS ANALYSIS OF LASER MACHINED SURFACES	
4.1 Laser spot overlapping rate	56
4.2 Effects of laser power.....	57
4.3 Effects of the aperture size	64
4.4 Effects of the engraving speed.	68
4.5 Effects of servo feed rate.....	72
4.6 Effects of track distance	72
4.7 Thickness of machined layer per pulse	73
4.8 Conclusion.....	74
 CHAPTER 5 ANALYSIS OF LASER MACHINED MICRO GEOMETRIES	
5.1 Machining of micro-geometries.....	76
5.2 Conclusion.....	83
 CHAPTER 6 CONCLUSION AND RECOMMENDATIONS	
6.1 Recommendations	86
 REFERENCES.....	 89

APPENDIX..... 97

LIST OF FIGURES

Figure 1.1 Comparison between ordinary light and laser light	5
Figure 1.2 (a) Photons in initial random states. (b) Photons in amplified and coherent state.	7
Figure 1.3 Basic construction of a laser cavity (a) stable cavity (b) unstable cavity	7
Figure 1.4 Schematic of laser beam interact with workpiece.....	11
Figure 1.5 Schematic of laser beam temporal modes (left: continuous, right:pulsed).....	14
Figure 1.6 Schematic of One, Two and Three-Dimensional machining (George Chryssolouris, 1991).....	14
Figure 1.7 Schematic of two types laser cutting (a) cutting through all (b) no cutting through (George Chryssolouris, 1991).....	15
Figure 1.8 Schematic of components of a Laser Machining System (George Chryssolouris, 1991).....	18
Figure 1.9 Schematic of laser application as a function of laser power density vs. interaction time	19
Figure 1.10 Schematic of laser spatial modes.....	20
Figure 1.11 Schematic of machine area. (Johan Meijer, 2002).....	22
Figure 1.12 Cutting tool schematic. Probable forms of ancient cutting implements (left) and modern metal cutting tool (right).....	23
Figure 1.13 Schematic of wood pieces made by ancient turning tool driven by arc and cord in the era of king Perse Darius 1 st . (Balazinski M.).....	24
Figure 1.14 Summary of researches on modern metal cutting technology.....	25
Figure 1.15 Terms and definitions of single point cutting tool (Machinery Handbook Edition 26 th).....	26
Figure 1.16 Tool with rounded cutting edge in orthogonal turning operation.....	27
Figure 1.17 Zone around the tool tip during machining.....	27

Figure 1.18 Cutting edges after surface blasting as well as after surface and focused on the cutting edges blasting. (K.-D Bouzakis et al., 2003	29
Figure 1.19 Micro-blasting effect on cemented carbide (HM) substrates (K.-D Bouzakis et al., 2001)	29
Figure 1.20 The variation of edge radius along the four cutting edges of inserts from set A (50.8 μ m), set B (101.8 μ m), and set C (152.4 μ m). (Willam J. Endres. 2002).	30
Figure 2.1 Heat transfer and fluid mechanics occurring during laser machining	34
Figure 2.2 Schematic of laser beam moving in the x direction at a constant velocity.....	38
Figure 2.3 Surface temperature distribution function f along the x axis which is the path of the laser beam for different scanning velocity. (Cline. E. et al., 1977). R: laser beam diameter; D: thermal diffusivity; Z: depth; V: laser beam scanning speed	42
Figure 2.4 The effect of laser beam velocity on the temperature distribution f at different depths below the surface of laser spot, (0, 0, z). (Cline. E. et al., 1977).....	42
Figure 2.5 Temperature distribution f at different depths below the surface at a constant scanning velocity. (Cline. E. et al., 1977)..	43
Figure 2.6 Temperature distributions at center point (0, 0, 0.002).....	45
Figure 2.7 Temperature distributions at center point (0.1, 0, 0.002).....	46
Figure 2.8 Temperature distributions at center point (0.0, 0, 0.004).....	47
Figure 3.1 (a) DML 40SI laser machine. (b) Diagram of components of DML 40SI laser machine for beam generation and beam switch. (Manuel of Laser 3D).....	50
Figure 3.2 Test of making microstructure on cemented carbide insert. (a) Micro-rectangular grooves. (b) Micro-semi circular profile grooves. (c) Micro-cylindrical pockets. (d) Micro-square pockets. (e) Micro-mould for micro-drill.....	53
Figure 3.3 (a) Olympus BX61 microscope. (b) Formtracer SV-C3000/4000.....	54
Figure 4.1 Diagram of the laser generating system of the DML 40SI machine	55
Figure 4.2 Overlapping ratio O_{ratio}	56

Figure 4.3 Schematic of the Q-switch function. (Manual of Laser 3D, Lasertec Co.)	58
Figure 4.4 Effects of Q-switch closing frequency on cemented carbide (a) 4 kHz (b) 50 kHz (O_{ratio} is 0.33, track distance is 0.01mm, laser spot diameter is 30 μ m).	59
Figure 4.5 Profile of machined surface of cemented carbide. (a) 4 kHz (b) 50 kHz.	59
Figure 4.6 Self-correlation of machined surface of cemented carbide. (a) 4 kHz (b) 50 kHz	60
Figure 4.7 3D model of surface texture after laser scanning with $O_{ratio}=0.33$	60
Figure 4.8 Schematic of temperature distribution during laser machining.	61
Figure 4.9 Schematic of laser machine with a) 4 kHz and b) 50 kHz laser spot.....	61
Figure 4.10 Effects of Q-switch frequencies on surface roughness, spot size 30 μ m.....	63
Figure 4.11 25 kHz Q-switch laser machined surface (a) optical microscope image (b) profile (c) self-correlation.....	63
Figure 4.12 100W laser energy distribution $P = 100 \cdot \exp\left(\frac{-r^2}{r_{spot}^2}\right)$ (W) (a) 30 μ m spot (b) 80 μ m spot.	64
Figure 4.13 Effects of aperture size (a) 30 μ m spot (b) 80 μ m spot. Other laser beam parameters is: f=4kHz, $O_{ratio} = 1/3$	65
Figure 4.14 4 kHz Q-switch laser machined surface of cemented carbide (a) 30 μ m spot (b) 80 μ m spot	65
Figure 4.15 Self-correlation of 4 kHz Q-switch laser machined surface of cemented carbide. (a) 30 μ m spot (b) 80 μ m spot	66
Figure 4.16 Schematic of laser machine with a) small aperture b) big aperture sizes.	66
Figure 4.17 Effects of aperture size on surface roughness, O_{ratio} is 0.33.	67
Figure 4.18 Schematic of engraving speed. ($O_{ratio}=1$)	68
Figure 4.19 Schematic of different spaces between two neighbor spots (s1, s2, s3) and two neighbor-scanning tracks (t1, t2).....	69
Figure 4.20 Schematic of laser hatching mode.....	69
Figure 4.21 Schematic of different laser engraving speed when f=30kHz, spot size 30 μ m.70	

Figure 4.22 Effects of engraving speed on surface roughness, spot size 30 μ m.....	71
Figure 4.23 Schematic of track distance.....	73
Figure 4.24 Schematic of the machined layer thickness.....	73
Figure 4.25 Diagram of I-O _{ratio} for cutting tool material X..	74
Figure 5.1 Round cutting edge machined by DML40SI laser machine, desired radius=0.5mm (a) positive cutting edge (b) negative cutting edge.....	76
Figure 5.2 Comparison of laser machined cutting edge to desired cutting edge.....	77
Figure 5.3 Semi-circular profile micro-groove laser machined using DML40SI machine. Desired radius=0.10mm.	78
Figure 5.4 Schematic of side burning.	79
Figure 5.5 Relation of width and depth of machined microstructure.....	79
Figure 5.6 Rectangular micro grooves, desired width=0.2mm, desired depth=0.75mm.....	80
Figure 5.7 Micro-cylindrical pocket machined using DML40SI laser machine, desired radius=0.2mm, desired depth=0.3mm.....	81
Figure 5.8 Micro square pocket machined by DML40SI laser machine, 1.0 x 1.0 mm, desired depth 0.5mm.	81
Figure 5.9 Schematic of surface texture of the wall and bottom of the machined square pocket.....	82
Figure 5.10 Micro drill CAD drawing.	82
Figure 5.11 Laser machined mould for micro-drill fabrication.....	83
Figure 6.1 Laser 80 fine cutting technology (Lasertec Company).....	87
Figure 6.2 Illustration of 3D model of cutting edge machined by laser.....	87
Figure 6.3 Illustration of edge wear of insert (Balazinski M.)	87
Figure 6.4 Illustration of insert of varying radius cutting edge.	88
Figure 6.5 Example of crater wear of insert (Balazinski M.)	88
Figure 6.6 Example of local strengthened insert.	88

LIST OF TABLES

Table 1.1 Categories of laser according to lasing medium (George Chryssolouris, 1991). 13	13
Table 1.2 Main applications of different laser (Singh J., 1995)	13
Table 1.3 Photon energies from different laser sources and required dissociation energies for several chemical bonds. (Johan Meijer, 2002)	17
Table 1.4 Behaviors of different materials in laser machining (Steen W.M., 2003).	21
Table 1.5 Characteristics of several types of tool materials (Milton C. Shaw, 2005).....	31
Table 1.6 Dates of carbide introduction and tool concepts (Milton C. Shaw, 2005).....	32
Table 3.1 Technical information of DML 40SI laser machine	51
Table 3.2 Machining parameters of DML 40SI laser machine.	51
Table 3.3 Value of laser machining parameters for machining cemented carbide inserts... 52	52
Table 3.4 Values of laser beam parameters for machining micro-geometries on cemented carbide inserts.	53
Table 4.1 Effects of Q-switch closing frequencies on surface roughness, spot size 30µm.. 62	62
Table 4.2 Effects of aperture size on surface roughness, O_{ratio} is 0.33.	67
Table 4.3 Effects of engraving speed on surface roughness, spot size 30µm.	71
Table 5.1 laser beam parameters for machining micro geometry on cemented carbide	76

LIST OF ABBREVIATIONS AND SYMBOLS

Nomenclature for laser part

C_p' : specific heat per m^2 per m per $^{\circ}C$. ($J/m^3/^{\circ}C$).

C_p : specific heat ($J/kg/^{\circ}C$).

D : thermal diffusivity (m^2/s).

D : track distance.

f : Q-switch closing frequency.

F : feed rate of servo of DML 40 laser machine.

HAZ: heating affected zone.

$h(\lambda)$: the function absorption depth. When $z=0$, $h(\lambda)=1$.

I : laser beam intensity on surface to $1/e$ the central value I_{max} (W/m^2).

I_{max} : maximum laser intensity.

I_{thresh} : machining stop at this intensity.

K : thermal conductivity ($J/m/s/^{\circ}C$ or $w/m/^{\circ}C$)

O_{ratio} : overlapping ratio of laser spot.

P : absorbed power of laser beam on surface (W).

ρ : density (kg/m^3).

q^m : the rate of energy conversion per unit volume by heat source from work, chemical reaction.

R : reflectivity of solid.

r_0 : the radius of laser beam in the place where the intensity equal the $0.8413 I_{max}$.

$V_{engraving}$: engraving speed.

Nomenclature for cutting tool

α : rake angle.

β : tool tip angle.

γ : clearance angle.

R : radius of cutting edge.

R_a : surface roughness. Arithmetic mean value of profile tolerance.

R_{max} : the maximum roughness depth.

R_z : height of 10 irregular points in basic measure length.

R_t : the maximum height of the profile.

t_1 : thickness of uncut chip. It is called feed rate sometimes.

t_2 : thickness of chip.

w : width of cut in orthogonal cutting.

V_c : cutting speed.

LIST OF APPENDIX

APPENDIX-A PHOTOS AND EXPERIMENTAL RESULT OF MACHINED
SURFACE FOR EXPERIMENTS DISCUSSED IN CHAPTER 4..... 97
APPENDIX-B PHOTOS OF MICRO-GEOMETRIES DISSCUSSED IN CHAPTER 5
..... 116

INTRODUCTION

It was observed during human history when a new form of energy is discovered, their quality of life is improved significantly by different applications of this new form of energy. After the laser invention 45 years ago, the research on laser and its applications never stopped. Now, the laser technology is applied in atmospheric studies, spectroscopy, photoluminescence study, photo effect, measurement and manufacturing domain, such as laser micro machining. Laser micro-machining technology is a branch of application of laser technology in manufacture domain. With the help of computer graphic technology, the CAD 3D model is transferred to the data for the micro material processes, for example *.stl document. Then, the CAM technology is used to make the designed part. In this thesis, the application of laser micro-machining technology in traditional metal cutting domain is presented.

1.1 Background of laser technology

Since the first working ruby laser made by Maiman (Maiman T. H., 1960) in 1960, optical energy at high density is now available for novel applications. Due to laser's properties -- high intensity (power) of electromagnetic energy flux and high spatial coherence, laser light can be focused on a precise area with very high heating. Hence, material processing has become one of the major applications of laser. In laser material processing, laser cutting, laser hardening and laser remelting are thermal processes. Laser remelting, laser alloying, laser cladding and laser dispersing are thermo chemical processes. The CO₂, Nd-YAG, Nd-glass diode and excimer laser are often used according to the processing conditions.

The CO₂ laser was invented by Patel C.K.N. (Patel C.K.N., 1964) in 1964 working at the Bell Laboratories. The power of this first CO₂ laser was only 1mW. Today the CO₂ laser has developed into the work family for material processing with slow flow, fast axial

flow and transverse flow lasers operating at average power up to 25 kW or even 100 kW.

The Nd-YAG (Neodymium-yttrium aluminum garnet) laser was invented in the Bell Laboratories in 1964 (Geusic et al., 1964). After then, the Nd lasers have progressed with the introduction of sophisticated pulse shaping. The peak power can reach petawatt (10^{15} W). Beam expansion and compression techniques have allowed extremely short pulses down into the femtosecond range (10^{-15} s)

The diode lasers were discovered late but are rapidly becoming the laser technology considered to have the brightest future. Basov et al. suggested the possible diode laser in 1961 (Basov et al., 1961). Soon after that, the first diode laser was demonstrated in three laboratories at the same time, GE (Hall et al., 1962); IBM (Nathan et al., 1962); MIT Lincoln Laboratory (Quist et al., 1962). From the first modern diode laser appeared in 1969, today the power of diode lasers can reach several kilowatts. Although there is a problem in beam quality, diodes are small, robust and cheap.

The excimer laser was invented in 1974 in the Avco Everett laboratories by Ewing and Brau (Ewing et al., 1974). The ultraviolet laser from Xe gas is used as “cold cutting” in electronic industry, microlithography processing.

1.2 Background of cutting tool technology

Cutting is one of the most important methods of removing unwanted material in the production of mechanical components. Development of cutting tools can be traced back to stone age where mankind made different tools from wood, bones and stones. These ancient tools were made with different geometry shapes by cutting or honing. During the entire civilization history, cutting tool were developed from copper, iron to steel, from high speed steel to hard metal, ceramic, synthetic diamond, etc. The needs of mankind introduced new material to be machined and pushed the development of cutting tool.

Modern metal cutting started in 1850s. The most popular material for cutting tool are high speed steel (HSS), cemented carbide, coated carbide, cermet, ceramic, diamond, etc. Tool materials generally have the following properties:

- Hard enough at high temperature during metal cutting to resist abrasive wear and deformation.
- High strength to resist rupture and shock.
- Chemically inert compared to work piece.
- Chemically stable to resist oxidation and dissolution.
- Good thermal conductivity to resist thermal shock.

In general, cutting tool materials are difficult to be machined due to their high hardness.

1.3 Definition of the problem

Although cutting tool materials are difficult to be machined, they have to be shaped in different geometries to satisfy the different cutting requirements. Cutting edge roundness, T-land, chip breakers are the main geometry characteristics for cutting tools. For making cutting edge roundness and T-land, the traditional ways are honing, micro blasting and heating pressing. For making chip breaker, the usual methods are grinding, pressing and sintering. These processing methods are time consuming, labor costing, low efficiency and with a low geometry precision.

1.4 Research objectives

This thesis is an exploration of using laser machining technology to machine cutting tool. The aim of this exploration is not only to introduce laser machining technology into cutting tool manufacturing field but also to solve the existing problem during using the traditional processing methods to manufacture cutting edge.

In this thesis, Q-switch laser micro-machining technology was used to make geometries on cemented carbide inserts. The effect of laser machining parameters, the temperature around the heat-affected-zone (HAZ), the roughness of machined surface, the microstructure of machined surface and the quality of machined microstructure will be presented in this thesis. This thesis will also present the previous development of laser machining and cutting tools and the perspective researches.

In our laser micro machining experiments, DML40 SI laser machine were used to process cemented carbide insert. Then, we investigated the roughness of machined surface, the tolerance of machined geometry and the microstructure of machined surface.

1.5 Methodology

In this thesis, laser micro-machining technology was used to machine cemented carbide insert. The effects of laser parameters on cemented carbide were investigated in review of roughness of machined surface. Laser micro machining technology, CAD/CAM technology and optical measuring and analysis technology were applied during research. The following are the main methodology:

1. Analyze the heating effect on cutting tool material using the theory of laser.
2. Use CAD software Catia to create 3D model of micro-geometries and convert Catia file to *.stl file for CAM software LPSWin.
3. Use LpsWin to convert *.stl file to CNC program for DML 40SI laser machine.
4. Machine cemented carbide using DML 40SI laser machine.
5. Measure surface roughness using Formtracer.
6. Observe and take photos using optical microscope and digital camera.
7. Study the effects of laser machining parameters on cemented carbide insert.

1.6 Thesis structure

This thesis includes introduction; chapter 1: literature review; chapter 2: heating effects of laser beam on cutting tool material; chapter 3: laser machining experiments on cemented carbide inserts; chapter 4: roughness analysis of laser machined surfaces; chapter 5: analysis of laser machined micro geometries; chapter 6: conclusion and recommendations; appendix a: photos and experimental results of machined surface for experiments discussed in chapter 4; appendix b: photos for micro-geometries discussed in chapter 5.

CHAPTER 1 LITERATURE REVIEW

Part one Literature review on laser technology

1.1 Basic notions of laser

1.1.1 Introduction of laser

Laser is an acronym for **L**ight **A**mplification by **S**timulated **E**mission of **R**adiation. Laser light differs from ordinary light (e.g. light bulb) because it consists of photons that are all at the same direction, frequency and phase (coherence) as shown in Fig. 1.1. It exhibits temporal, spatial and energy properties that are different from those of diffuse light. These properties make the laser beam useful for many applications such as communication, measurement and materials processing. The first working laser was designed by Maiman.

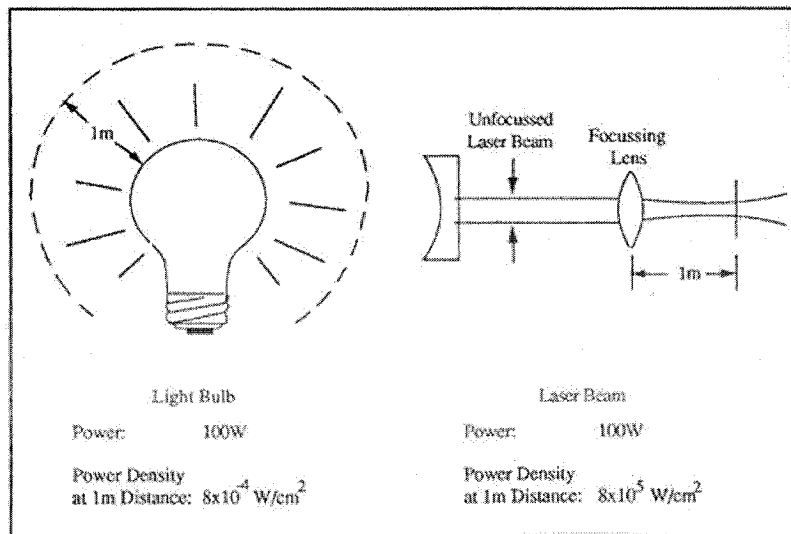


Figure 1.1 Comparison between ordinary light and laser light (George Chryssolouris, 1991).

1.1.2 Properties of laser light

Laser light shows high monochromaticity, high coherence, low diffraction and high radiance.

High monochromaticity. High monochromaticity implies that the range of frequencies emitted by the light source is small. Monochromaticity is most important in applications such as interferometry, holography, velocimetry, isotope separation and communications in which the frequency content of the laser beam is of great importance.

High coherence. Spatial and temporal coherence refer to the relationship between the electronic and magnetic components of an electromagnetic wave. When the change of phases at different points in space at a single moment is aligned, it is called *spatial coherent*. When the change of phases at a single point in space over a period time is aligned, it is called *temporal coherent*. Spatial coherent and temporal coherent is also very important for interferometry, holography, velocimetry and communication.

Low diffraction. Diffraction is the phenomenon by which lights bends around sharp-edge objects. One advantage of the laser light over ordinary light is that lasers produce beams with very a limited diffraction.

High radiance. The radiance of a light source is the value of power per unit area emitted by the light source for a given angle, i.e. W/cm^2 . Because of the diameter of laser beam is very small, laser light usually possesses extremely high radiance.

1.1.3 Basic mechanisms of laser system

The basic laser consists of two mirrors that are placed to form an optical oscillator as shown in Fig 1.2. The space between the two mirrors forms a cavity in which photons traveling back and forth between the mirrors forever, if not prevented by some mechanism such as absorption. Between the two mirrors is an active medium that is capable of amplifying the light oscillations by the mechanism of stimulated emission. One of the two mirrors is totally reflecting, the maximum reflecting rate can reach 99.999%. The other mirror is partially transparent to allow some of the photons to shoot

out. In the cavity, the photons are changed from initial random state into an amplified and coherent beam

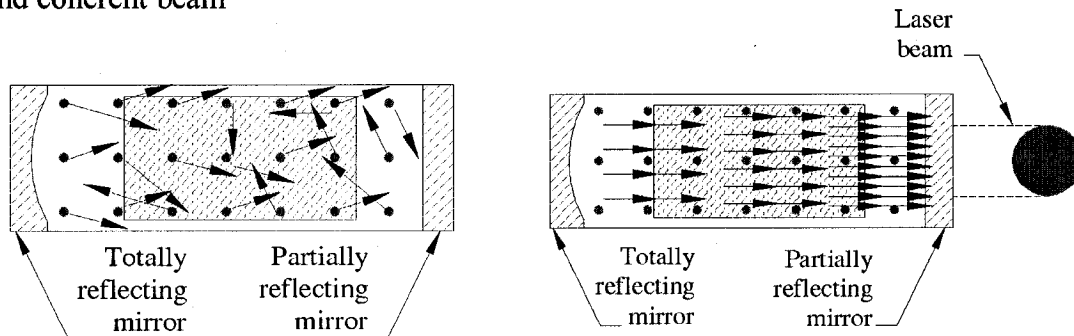


Figure 1.2 Photons in initial random states (left) and photons in amplified and coherent states (right).

Optical cavities can be classified as “stable” or “unstable” depending on whether they make the oscillating beam converge into the cavity or spread out from the cavity as illustrated in Fig 1.3.

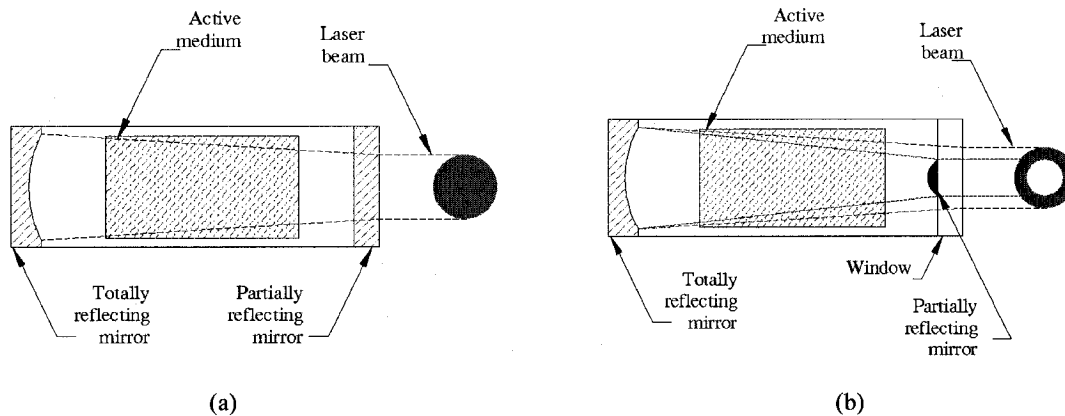


Figure 1.3 Basic construction of a laser cavity: (a) stable cavity (b) unstable cavity

In unstable cavity, each photon has only a limited lifetime and will eventually achieve an output trajectory. Unstable cavity generates doughnut mode laser, which is suitable for heat treatment. In stable cavity, each photon remains in the cavity for indefinite time in theory. Stable cavity generates gaussian mode laser, which is usually used for machining.

1.1.4 Applications of laser

Powerful light. Because of the high spatial coherence, the laser beam can have a low divergence and hence can be projected to make a bright spot. This technology can be used as laser pointers for lecturing, laser light show and LED (low emitting diode).

Alignment. Laser can be used to guide assembling of auto parts, sequencing of wiring harness, tunneling and ground leveling.

Length measurement. Because of high temporal coherence, laser can be used in length measurement. This technology can be used as laser radar.

Pollution detection. When laser beam shoot on a region of different composition, it may excite the molecules of SO_2 in that region. As this excitation decays, a Raman spectrum is revealed which indicates the concentration of the pollutant.

Velocity measurement. This is also an application of high temporal coherence property. There are two types of laser velocity meters – the laser Doppler velocimeter and the laser Doppler anemometer. The laser Doppler velocimeter measures the frequency shift in emitted radiation and the returning radiation, and then calculates the velocity of the moving target. The laser Doppler anemometer is popularly used for study fluid flow.

Holography. We can use this technology to make hologram and holographic film.

Speckle interferometry. When laser light falls down on an object, the object appears speckled due to the coherent nature of laser light forming interference patterns on the retina of eye. These patterns are a function of the roughness of the object being viewed. When we use a computer to store these patterns and play it back on a video screen, we can record any movement of the object as a fringe pattern. For example, people use this

technology to monitor the blood flow in the brain by looking at the change in shape of blood vessels.

Inspection. A laser beam can be either focused as a line or scanned over the surface of an object, if there is flaw on the surface, the recorded reflectivity is different. This technology has been used in scanning system of supermarket, fingerprint detection and scattered laser light looking for dust on semi-conductor.

Recording. The popular CD player, VCD player, DVD player use a photodetector to read reflecting signal when a low powered GaAlAs laser shoot on the aluminum coated layer of compact disc, on which the digital information is represented by pits of different length.

Communications. Low-loss optical fiber technology combined with laser technology is used in Transatlantic Fiber System. Today most transatlantic calls are made using optical fiber links as opposed to satellites.

Print. Laser printer is a product of this technology

Isotope separation. The energy levels for ionizing an isotope differ slightly from isotope to isotope. By using two frequencies shining the mixing isotope vapor will cause only one isotope to be ionized – not totally but with some level of efficiency. Then, the ionized species can be easily collected in a near vacuum chamber.

Medical. This is a big area of laser application by using laser property high intensity (power) of electromagnetic energy flux, high monochromaticity, diffraction, and radiance in micro and biological field. The main applications are the following:

the blue argon laser is used in eye surgery for welding back the detached retinas. CO₂ laser is used to treat Glaucoma. Excimer laser is used to machine cornea to treat serious

optical defects. Nd-YAG laser conducted by optical fiber allows surgical work to be done via an endoscope. The precision surgery done by Konig at Friedrich Schiller University in Jena showed the dissection of chromosomes by ultra fast pulse laser using high apertures, 170 femto second pulse at 800 nm. Laser is used in removing sun spots, age spots, freckles, tattoo, wrinkle, laser treatment of spider veins on the face or legs, skin rejuvenation. Laser is used in Photodynamic therapy. Laser is used in diagnostic tool, such as flow cytometry, diffuse optical tomography.

Heat source. Due to laser's properties -- high intensity (power) of electromagnetic energy flux and high spatial coherence, it can be focused upon a precise area with very high heating energy. Hence, it is often be used as a heat source in industry field.

Through manipulating property parameters, a single laser can perform several functions. Such as laser cutting, laser hardening, laser remelting, laser alloying, laser cladding, and laser dispersing. Laser cutting, laser hardening and laser remelting belong to thermal process. Laser remelting, laser alloying, laser cladding, and laser dispersing belong to thermochemical processes.

1.2 Basic notions of laser machining technology

Laser machining belongs to the big family of *material removing*, which consists of chemical or electro-chemical processes, thermal Process and mechanical Process. In laser machining, the laser light works as a high energy heating source by thermal ablation mechanism, photochemical ablation mechanism or both to melt and/or vaporize the volume of the material. It is a non-contact processing. Combined with modern numerical control and CAD technology, the machining rate and precision increase significantly. It is used in variety industry fields, particularly in the processing of difficult-to-machine materials such as hardened metals, ceramics and composites.

1.2.1 Mechanisms of laser machining.

From the classic physics, light shows two properties – wave property and particle property. When electromagnetic radiation strikes on a surface, some energy is reflected, some absorbed and some transmitted. The absorbed energy can be expressed by Beer Lambert' law, $I = I_0 e^{-\beta z}$, where I: absorbed radiation. I_0 : input radiation. β : absorption coefficient. Z: absorbed depth. The absorption coefficient β depends on the medium, wavelength of the radiation and the intensity of electromagnetic radiation. Because electromagnetic radiation can be represented as an electric vector field and a magnetic vector field, when it passes over a small elastically bound charged particle, it will generate electric force and the particle will be set in motion this force. Although this electric force is too small to vibrate an atomic nucleus, it can cause the electrons to vibrate. As the electron vibrates, it will either re-radiate freely or be bonded by lattice phonons (the bonding energy within a solid or liquid structure). Furthermore, the vibrating phonons will cause the structure to vibrate and this vibration will be transmitted through the structure by the normal diffusion type processes due to the linking of the molecules of the structure. The vibrations in the structure are the heating phenomena. If sufficient energy is absorbed then the vibration becomes so intense that the molecular bonding is stretched so far that it is no longer capable of exhibiting mechanical strength and the material is melting. On further heating the bonding is further loosened due to the strong molecular vibrations and the material is evaporating. The vapor continues to absorb the radiation but only slightly since it only has bound electrons. When the gas is sufficiently hot that electrons are freed from track and the gas is said to be plasma as shown in Fig 1.4.

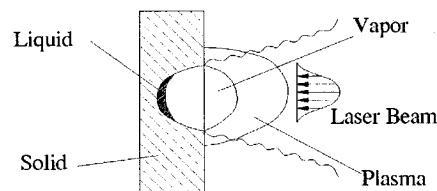


Figure 1.4 Schematic of laser beam interacting with workpiece

1.2.2 Characteristics of laser machining

- **Advantage**

Laser machining is a thermal or photochemical process. It is appropriate for hardened metals, ceramics and composites.

Laser machining is a non-contact process. There are no mechanically induced material damage, tool wear and machine vibration. Moreover, the material removal rate for laser machining is not limited by constraints such as maximum tool force, build-up edge or tool chatter.

Laser machining is a flexible process. This flexibility eliminates the workpiece transportation that is necessary for processing parts with a set of specialized machine. So, it can be used for drilling, cutting, grooving, welding, and heat-treating processes on a single machine.

- **Disadvantage**

Low energy efficiency. In most laser machining techniques, the removal of material occurs by melting or vaporizing. Laser machining needs significantly higher energy inputs and processing times than the need of mechanical process because the diameter of the laser beam is in order of micrometer.

Material damage. During laser machining metals, the temperature of the point where the laser focuses is very high. The heat conduction will create a heat-affected zone in the vicinity of the erosion front and change the surface integrity.

1.2.3 Categories of laser machining

In general, laser processing can be categorized by a number of industrial.

Categorized according to the lasing medium: Laser can be divided into three basic categories as defined by the state of the lasing material: gas, liquid, or solid as presented in Table 1.1. The applications are presented in Table 1.2.

Table 1.1 Categories of laser according to lasing medium (George Chryssolouris, 1991)

Type	Laser medium	Example
Gas laser	Neutral atom	Helium-Neon
	ion	Argon; Krypton; Xenon
	Molecular	CO; CO ₂ ; HF
	Excited dimer	Xe ₂ -F ₂ ; ArF-KrF-XeF-XeCl
Liquid laser	Large organic dye molecular	
Solid laser	Cr ³⁺	Ruby laser
	Nd ³⁺	Nd:YAG laser
		Nd: glass laser

Table 1.2 Main applications of different laser (Singh J., 1995)

Laser	Wavelength (μm)	Mode of typical operation	Power (W)	Typical application
CO ₂	10.6	CW	10000	Heat treating, welding, cutting, alloying, cladding
		Pulsed	500	Welding, material removal
Nd: YAG	1.06	CW	2800	Welding, cladding, trimming
		Pulse 5000 (Q-switched)	200	Welding, hole drilling
		Pulse		
Ruby	0.6943	Pulsed	10 ⁵	Spot welding Hole drilling
Nd:YAG	1.06	Pulsed	10 ⁶	Spot welding Hole drilling
Argon	0.4480	CW	20	Semiconductor
KrF	0.248	Pulsed	100	Semiconductor Material remove

- **Categorized according to the laser temporal mode:** Laser is divided into two modes: *continuous wave (CW)* and *pulsed wave (pulsed)* as shown in Fig. 1.5

In CW mode, the laser beam is emitted without interruption. Because the energy is charged smoothly in CW laser, the machined surface is removed continuously.

In the pulsed beam mode, laser beam is emitted periodically. The pumped energy is stored until threshold energy is reached, and then the stored energy is discharged rapid out off the laser cavity. The peak power of pulse laser is very high, so the laser can be

said “sharp”. Pulse laser is often used in deeper drilling, marking and micro machining. For other applications, such as cutting, welding and surface treatment, both pulsed and continuous mode (CW) lasers can be used. The machined surface or cutting section by pulse laser is better than that gotten by CW laser.

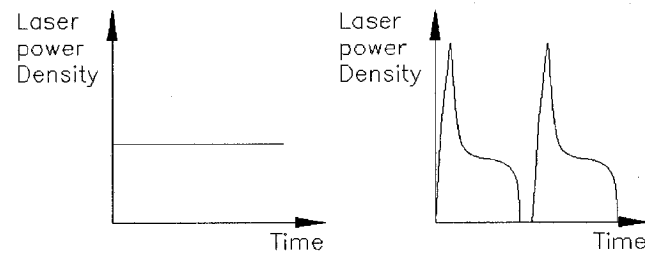


Figure 1.5 Schematic of laser beam temporal modes (left: continuous, right: pulsed)

- **Categorized according to the shape and the kinematics of the erosion front:**
In general, laser machining can be divided into *one-, two- and three- dimensional processes* as shown in Fig. 1.6.

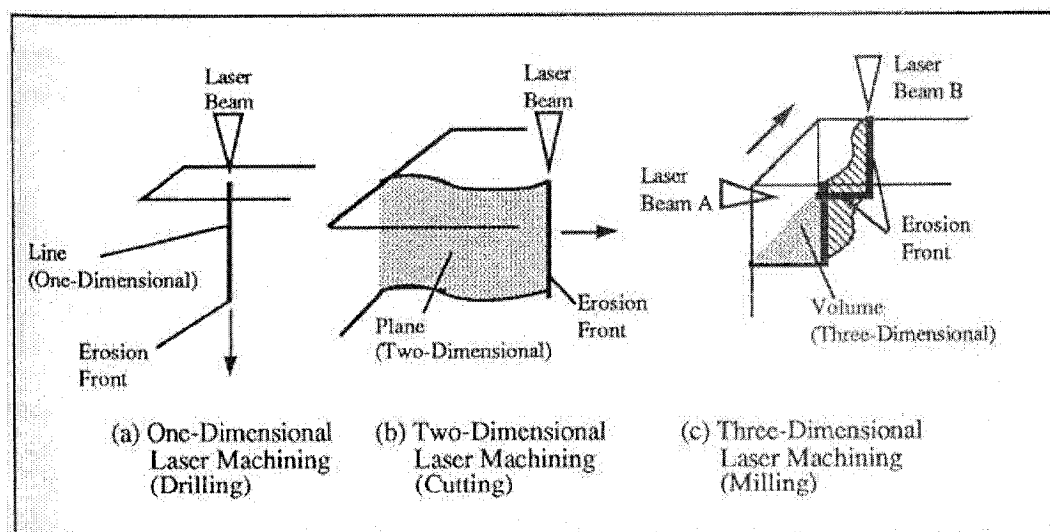


Figure 1.6 Schematic of One, Two and Three-Dimensional machining (George Chryssolouris, 1991)

In case of a *one-dimensional process* (drilling), the laser beam is stationary relative to the work piece. The erosion front, located at the bottom of the keyhole, propagates in the direction of the line source in order to remove material. The keyhole causes a sudden increase in the absorptivity due to multiple reflections and the hole deepens quickly. As it deepens, generated vapor escapes, blows ejecta out of the hole, stabilizes the molten walls of the hole and keeps the hole from being covered by the molten work piece. The heat model can be simplified as one-dimensional heat flow with zero heat conduction in other direction (William M. Steen, 2003).

In case of a *two-dimensional process* (cutting), the laser beam is in relative motion with respect to the work piece. The process can be approximately modeled as a line source moving in a direction perpendicular to the line direction, all energy enters the melt and is removed before significant conduction occurs. For laser cutting in Figure 1.7 (a), due to the presence of a bottom surface in cutting that behaves as an adiabatic boundary, the heat conduction occurs two-dimensionally (downward conduction is negligible compared to conduction in other directions). Thus, the heat model for laser cutting is usually simplified as a two-dimensional heat flow. For laser cutting in Figure 1.7 b, the process exhibits complicated characteristics, such as three-dimensional heat transfer, two material phases and a moving boundary.

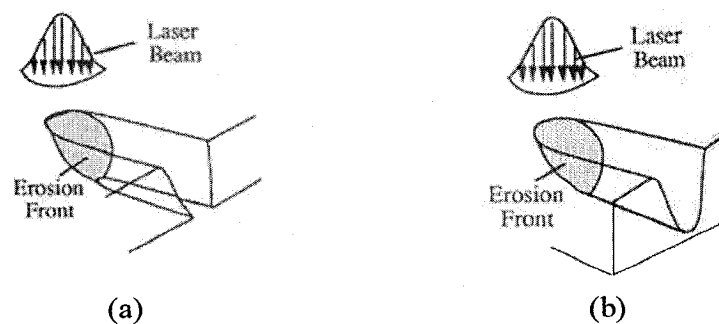


Figure 1.7 Schematic of two types laser cutting (a) cutting through all (b) no cutting through (George Chryssolouris, 1991)

For a *three-dimensional process* (milling) as shown in Fig. 1.6, two or more laser beam are used. Each beam forms a surface through relative motion with the work piece. The erosion front is located at the leading edge of each laser beam. The heat flow model is three-dimensional

- **Categorized according to the volume of machined piece.** Laser machining could be divided as *laser general machining* and *laser micro machining*. Although laser micro machining is also a material removing process, the mechanism of *laser micro machining* is different from that of the *laser general machining*. During laser micro machining, ultra short pulses of a few nanoseconds and powers up to gigawatts means that the laser can ablate material with very little heating. If we use a laser beam with Femtosecond (10^{-15} s) pulse and gigawatt power (10^9 W), the solid material will be ionized in an extremely short time of the pulse length. The heating affected zone is very little.

Although CO₂ and Nd:YAG lasers are both used in laser micro machining, Nd:YAG pulsed lasers are recently more popular due to their high energy densities and small focused spot (to 2 μ m diameter in some applications)(Bube K.R. et al., 1979)

- **Categorized according to the mechanism of the ablation of laser.** The mechanism of laser machining can be divided as laser machining with thermal ablation mechanism, laser machining with photochemical ablation mechanism or both. For example, when using CO₂ or Nd:YAG laser to machine a polymer, the polymer is rapidly heated and ejected from surface. Some polymers simply melt to char depending on the thermal resistance properties. This process is a thermal phenomenon. When using ultra short pulse laser beam for ablating materials, the mechanism is different from the simple thermal mechanism (Hess P., 1993). These processes have three different pulse grades: femtosecond ablation (10^{-15} s), picosecond ablation (10^{-12} s) and nanosecond ablation (10^{-9} s). Femtosecond ablation

has the best precision. Droplets or crater walls can be observed around the machined area in the nanosecond pulse time scale.

The physical mechanism of the material removal process for excimer laser to machine polymer is different from that of CO₂ laser or Nd:YAG laser. When the UV pulses of radiation from the excimer laser contact with the plastic workpiece surface, the UV photons are absorbed in the top layer typically of 0.2 μ m thickness, the high energy will cause the C-C or C-H bonds in a material to break. When the rate of bond breaking exceeds a critical value, the material decomposes. The material is ejected from the surface with little absorption to the surrounding material. During machining, no liquid or gaseous phases of the material are present. This process is a photochemical process. In photochemical ablation, only photons with higher energies can release the chemical bonds. For example, the machining of Teflon requires at least the photon energy as produced by the fluorine laser, like KrF laser (as shown in Table 1.3). The threshold that effects for a wide variety of plastics is about 120mJ/cm². (Johan Meijer, 2002)

Table 1.3 Photon energies from different laser sources and required dissociation energies for several chemical bonds. (Johan Meijer, 2002)

Laser	Wavelength (nm)	Photon energy (eV)	Chemical bond	Bond energy (eV)
CO ₂	10600	0.12		
Nd:YAG	1064	1.16		
XeF	351	3.53	Si-Si, Cl-Cl	1.8~3
XeCl	308	4.03	C-N, C-C	3~3.5
KrF	248	5.00	C-H, O-H	4.5~4.9
KrCl	222	5.50		
ArF	193	6.42		
F ₂	157	7.43	C=C	7

1.2.4 Components of laser machining system

Like any other machining system, laser machining system consist of a number of optical components, electrical components, numerical control components and mechanical components as illustrated in Fig 1.8.

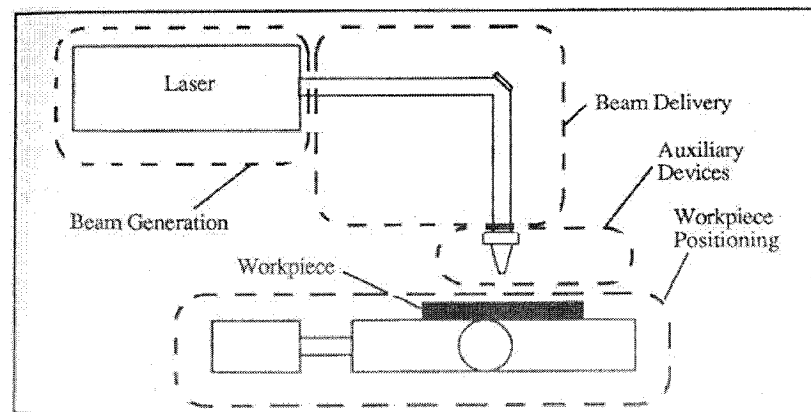


Figure 1.8 Schematic of components of a laser machining system (George Chryssolouris, 1991)

Beam delivery system includes the optical components that focus the laser beam onto the workpiece surface. They are beam polarizers, mirrors, beam splitters, focusing lenses and fiber couplings.

Workpiece positioning and laser beam positioning system is used to control the motion between the laser beam and the workpiece. For *workpiece positioning system*, workpiece can be moved in X, Y, Z direction along with the movement of working table while laser lens or nozzle remains stationary. *Workpiece positioning system* allows a high degree of accuracy and high scanning speed. For *laser beam positioning system*, the shooting angle of laser beam can be changed using translational and rotational stages while the workpiece are fixed. *Laser beam positioning system* allows the machining of more intricate details and complex shapes, due to the more flexible kinematics of the nozzle compared to *Workpiece positioning system*.

Auxiliary components include equipment that is not used to direct the laser beam or position the workpiece, such as gas jet nozzles, safety equipment, etc. These components are used in support of the laser machining process.

1.3 Effects of laser machining parameters

Through manipulation of processing condition such as power density, wavelength, pulse or continuous wave (CW), beam diameter, and traverse speed, a single laser can perform several functions as shown in Fig. 1.9. Combining the parameters of laser beam and material of workpiece, different machining results can be obtained.

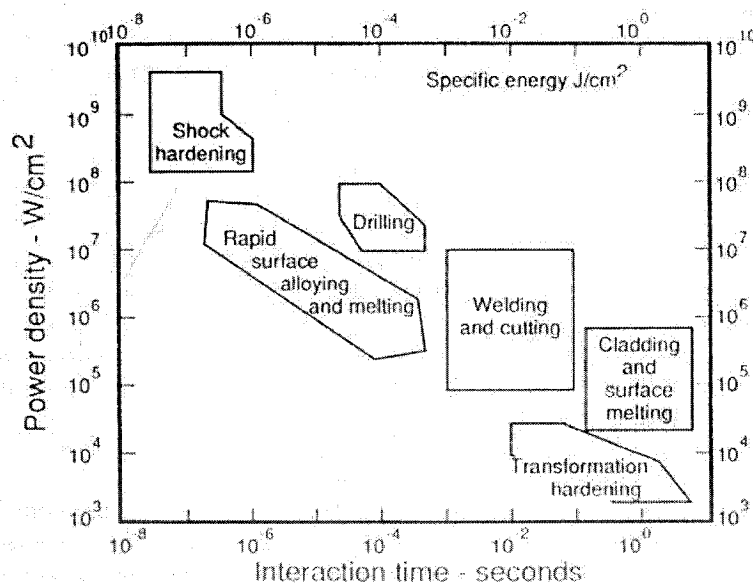


Figure 1.9 Schematic of laser application as a function of laser power density vs. interaction time. (Singh J., 1995)

1.3.1 Effects of beam properties

Power, Output power is the most basic characteristic of a laser beam. The overall effect of increasing the output power is to allow cutting at faster speeds and/or greater depths.

The potential disadvantage of increasing the power is that it will cause a wider kerf, burn side that spoils the edge finish and change sharp corners to rounded corners.

Pulsed or CW. In general, CW lasers can keep high material removal rate. Pulsed lasers can get smoother cutting surface and can get higher penetrating depth and smaller HAZ. Because the output energy of CW laser is constant, the machining result fine structure is not possible. When using pulsed laser, it is possible adjust the pulse rate in line with the cutting speed to control the overall heating. Thus, pulse laser are often used in cutting fine shapes. For example, in order to reduce the side burning and corner rounding, some laser machining system will change from the CW mode to pulsed mode near a corner.

Pulse duration. Laser with pulse length in millisecond range can be applied for micro welding. Laser with pulse length in nano-, pico- and femtosecond time scale can be applied for ablation of materials.

Wavelength. Short wavelength laser light is more difficult to be reflected. Hence, the certain lasers will be more suitable for the processing of different classes of materials. For example, aluminum and copper have higher reflectivity at the wavelength of $10.6\mu\text{m}$ than at the wavelength of $1.06\mu\text{m}$. So, Nd:YAG laser with $1.06\mu\text{m}$ wavelength is more suitable than CO_2 laser to machining Al and Cu. For laser micro machining, wavelengths vary from $10.6\mu\text{m}$ for the CO_2 to 157nm for fluorine excimer laser can be used.

Spot size and mode. The smaller the spot size will lead to higher power density and smaller cutting width. TEM00 (Transverse *Electromagnetic Mode* 00) has Gaussian spatial distribution and is usually considered the best mode for the laser machining because the phase front is uniform and there is a smooth drop off radiance from the beam center. TEM01 mode laser is usually used for heat treatment.

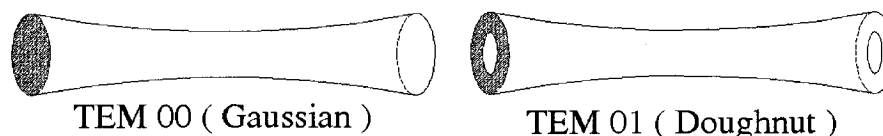


Figure 1.10 Schematic of laser spatial modes

1.3.2 Effects of workpiece properties

The workpiece optical properties such as reflectivity greatly affect the laser machining process. It is more difficult to cut higher reflectivity material. Reflectivity is not only a function of the material but also surface roughness, the surface shape, the surface coating, the surface plasma and the power intensity of laser beam.

In addition, the absorptivity affects the laser heating. Besides the reflectivity and the absorptivity, melting point of materials or oxide formed tendency, char tendency and crack tendency associated with the coefficient of thermal expansion affect laser machining also. Table 1.4 shows the behaviors of different materials in laser machining.

Table 1.4 Behaviors of different materials in laser machining (Steen W.M., 2003)

Property	Material
High reflectivity	Gold, silver, copper, aluminum, brass
Medium/high reflectivity	Most metals
High melting point	W, Mo, Cr, Ta, Ti, Zr
Low melting point	Fe, Ni, Sn, Pb
High oxide melting point	Cr, Zr
Low reflectivity	Most non-metal
Organics	
Tendency to char	PVC, leather, wood, rubber, wool, cotton, epoxy
Less tendency to char	Acrylics, polythene, polypropylene, polycarbonate
Inorganics	
Tendency to crack	Glass, natural stone
Less tendency to crack	Quartz, alumina, china, asbestos, mica

1.3.3 Effects of transport properties

Engraving speed. The faster the cutting the less time is left for the heat to diffuse sideways and will decrease the area of HAZ and the kerf. When using Gaussian laser

beam to machining, there is a “sharp pencil” effect that as the speed of laser increase, there is only sufficient energy at the tip of the Gaussian curve and not at the root to cause melting.

Focal position. The surface spot size determines the surface power intensity and whether penetration will occur. Laser cutting practice shows that optimum cutting may be obtained by having the minimum spot size below surface (Steen W.M., 2003) in order to using machine area efficiently as shown in Fig. 1.11. According to laser machining parameters, focal position should be controlled less than 1mm under surface for obtaining a satisfied machined result. (Mazumder J., 1983; Wilgoss R.A. et al., 1979; Seaman F.D., 1977).

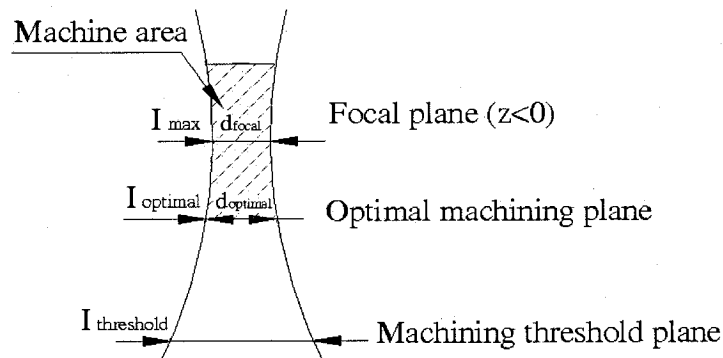


Figure 1.11 Schematic of machine area.

In the focal area the process is mainly drilling. Maximum laser intensity is at a focal plane. Smooth micro machining is obtained at a optimal machining plane. Machining stops at machining threshold plane. According the practical machined condition and result, operator should adjust the position of focal plane.

1.4 Summary of literature review on laser technology

Laser machining is a material removing technology by using high energy laser beam as cutting tool. It is a thermal processing. Compared to traditional metal cutting technology, it has a lot of advantages, such as non-contact, flexible, no tool wear, etc.

During laser machining, it is important to adjust some laser parameters to obtain optimum cutting result, such as the beam's power, temporal mode (CW mode or pulsed mode), focal spot size, engraving speed, feed rate of laser beam, frequency of pulse, etc. Because of high-energy intensity and controllability of laser beam, laser is suitable to machine materials, such as hardened metals, ceramics, composites and polymers. With the development of numerical control technology and metrology, a successful field of laser machining is the area of *laser micro machining*. Recently, continuously growing market requirement push people to look for new area of applications for laser. Laser machining undoubtedly has a bright future.

Part two: literature review on metal cutting technology

1.5 Basic notions of metal cutting

Cutting technology is one of the most ancient methods (as shown in Fig. 1.12, Fig. 1.13) in *material removing family*, which consists of Chemical and Electro-Chemical Processing, Thermal Processing, Mechanical Processing. The material of cutting tool and the work piece are developed from copper, iron to steel, from high speed steel to hard metal, ceramic and synthetic diamond. The precision of metal cutting can even reach to nanometer (10^{-6} mm) grade (Balazinski M.).

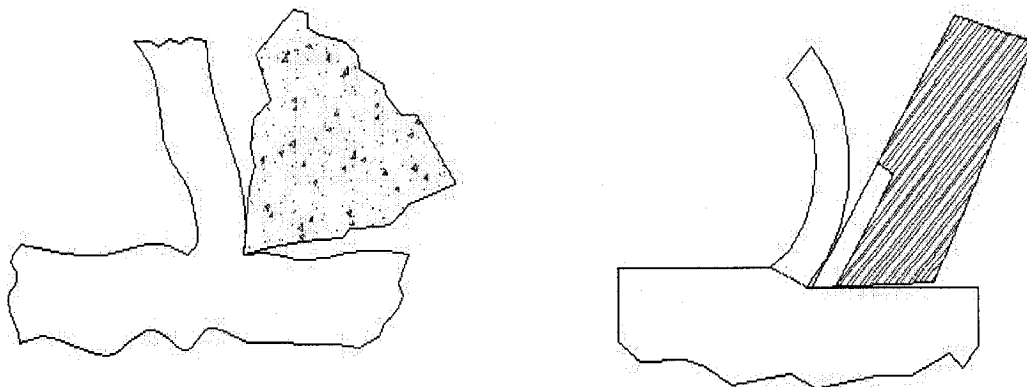


Figure 1.12 Cutting tool schematic. Probable form of ancient cutting implement (left) and modern metal cutting tool (right).

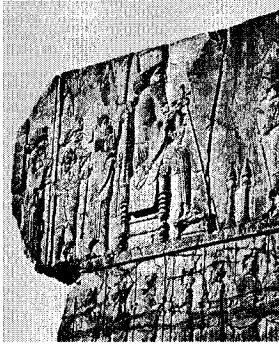


Figure 1.13 Schematic of wood pieces made by ancient turning tool driven by arc and cord in the era of king Perse Darius 1^{er}. (Balazinski M.)

1.6 Introduction of modern metal cutting technology

Modern cutting technology began in the mid of 19th century. Over the past 150 years, thousands of researchers have done research on cutting technology from different points of views. (e.g. analytical method, experimental method, mechanistic and numerical method). All of these researches can be generalized as optimization of cutting technology in broad sense as shown in Fig. 1.14.

- **optimization of cutting theory.** The works include Merchant's model (Merchant, M.E., 1944), Albrecht's model (Albrecht P., 1960, 1965).
- **optimization of application of cutting fluid, near dry cutting or dry cutting.** The works include Hand, D.M. et al. (Hands D.M., 1996), Gunter K. L. et al. (Gunter K.L. et al.).
- **optimization of chip breakability and machined surface quality.** The works include Nakayama K. (Nakayama, K., 1962, 1992, 2004), Jawahir I.S. (Jawahir I.S., 1991; Jawahir I.S. et al., 1993).
- **optimization of machining-tool system.** The works in optimization of machining condition include Jawahir I.S. (Jawahir I.S., 1991; Jawahir I.S. et al., 1993), Balazinski M. (Balazinski M., 1993; Balazinski M., et al., 1995), etc.
- **optimization of tool design and manufacturing technology.** The works include Klopstock H. (Klopstock H., 1925), Shehata G. H. et al. (Shehata G. H. et al., 1991, 1993).

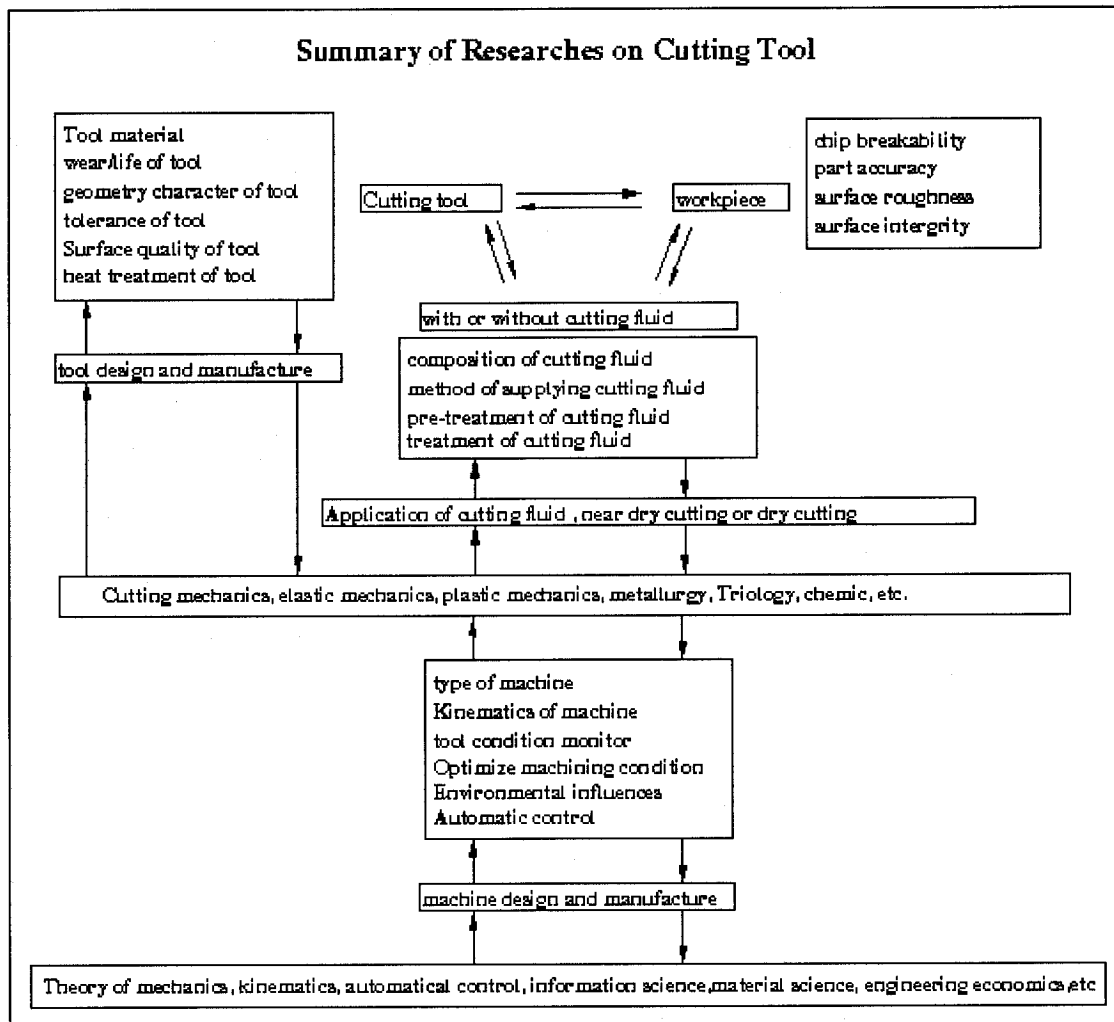


Figure 1.14 Summary of researches on modern metal cutting technology

1.7 Introduction of geometry of cutting tool

1.7.1 Terms and definitions

Fig.1.15 is an example of the single point cutting tool. Although the terms and definitions vary among different cutting tool, some terms and definitions are similar, such as cutting edge and nose radius.

According to different cutting condition, people can make cutting edge to honed cutting edge, chamfered cutting edge and make the chip breaker with different geometry form on the side rake face.

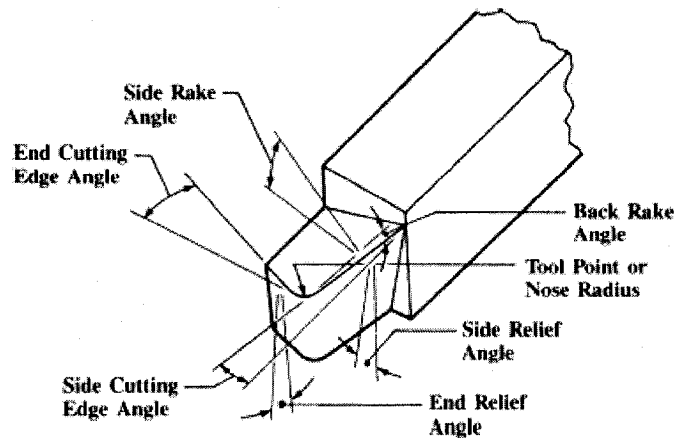


Figure 1.15 Terms and definitions of single point cutting tool (Machinery Handbook, Edition 26th)

1.7.3 Introduction of cutting edge

Cutting edge geometry is one of Tool Tip Geometry (the others are primary rake angle, second rake angle, contact land, etc). The cutting edge properties usually include the type of cutting edge, the dimension of the rounded cutting edge or chamfered cutting edge, the tolerance of the cutting edge and the surface quality of the surface of the cutting edge, etc.

In practical operation, the “cutting edge” is regarded as “a straight line surrounded by money”. Even small optimizations can result in significantly higher productivity and tool cost savings through minimizing machine downtime and sustaining production at highest practical cutting speed and feed. So, it is worthy of investing more time and energy to improve the knowledge of cutting edge not only in theory and but also in practical application. Fig. 1.16 and Fig. 1.17 show the machining with round cutting edge cutting tool and zone around the tool tip during machining.

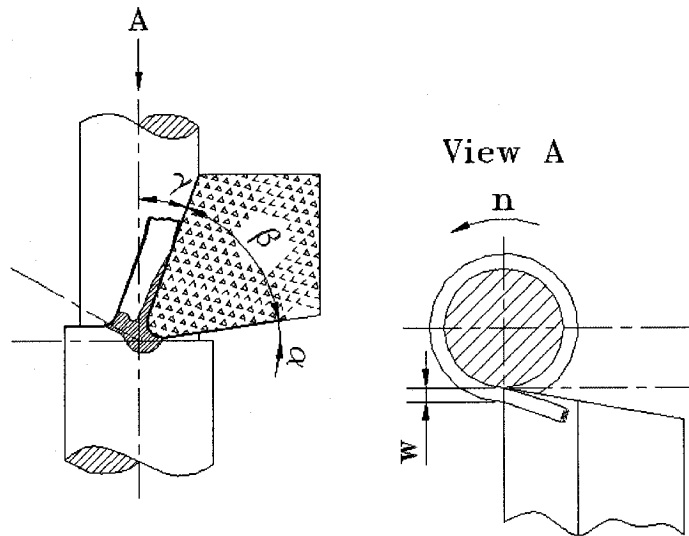


Figure 1.16 Tool with rounded cutting edge in orthogonal turning operation.

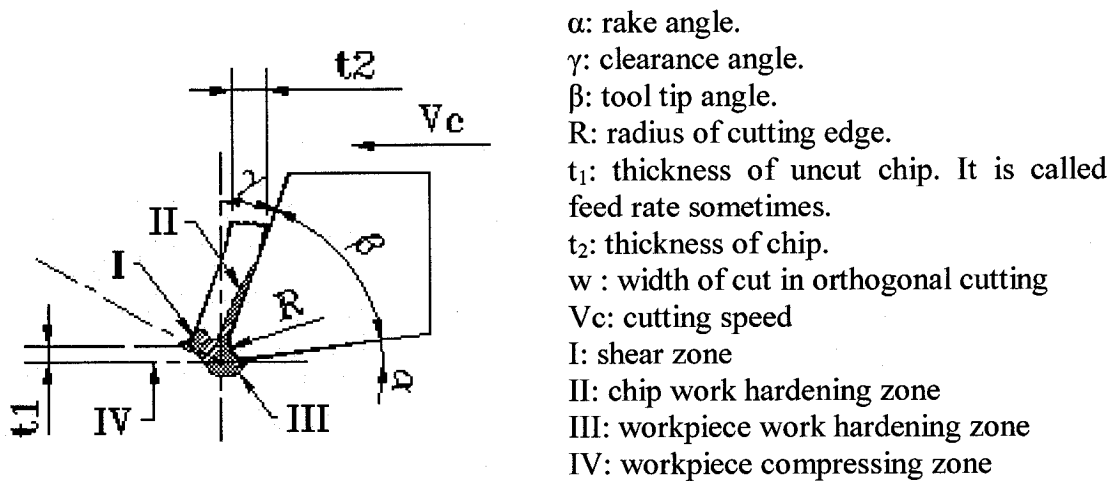


Figure 1.17 Zone around the tool tip during machining.

1.7.4 Importance of cutting edge

Following applications show the necessary of cutting edge preparation.

I. When tool is used under interrupted cutting condition or is used to cut ferrous metal or the uncut chip thickness is small, like hard machining and drilling. Proper rounded

cutting edge can prevent the damage caused by unusually hard work material such as surface scale or shock loading and delay cratering, chipping, and outright breakage.

II. Coated carbide is widespread in turning. 80% of all indexable tips are CVD (chemical vapor deposition) coated carbide. During researching on coating process technology, like carbide coating by CVD method, a brittle “ η phase” is found creating at the coating/substrate interface because of the high processing temperature. η phase (W_6Co_6C , W_3Co_3C) is a carbon-deficient brittle zone that forms in the carbide substrate just below the coating. “ η phase” is usually one or two microns thick. This brittle zone will reduce the transverse rupture strength of the cemented carbide by 30%. In order to reduce the possibility of fracture at the η -phase-weakened edge, tool manufacturers always hone most tool edges before CVD coating.

1.7.5 Preparing methods for cutting edge

In production plant operation, when the honed, chamfered or negative ground cutting edge are considered to be used, the faced big problems are large time and money cost of the traditional processing methods, like honing or micro-blasting method.

1. Cutting edge radii, manufactured by micro-blasting method

Micro-blasting method is widely used to treat surface of cemented carbide inserts, to reduce high roughness peaks, to obtain low mean spacing between roughness profile peaks, to remove the binding material Co (cobalt) and to improve hereby the coating adhesion. However, focused micro-blasting can cause local removals on the cutting edge. In these failed regions of the cutting edge, the cobalt concentration is elevated. (as shown in Fig. 1.18, Fig. 1.19). This phenomenon will cause the more rapid propagation of the coating fracture in coated carbide insert. Another disadvantage of micro-blasting is that the obtained edge radii can not be controlled in small tolerances.

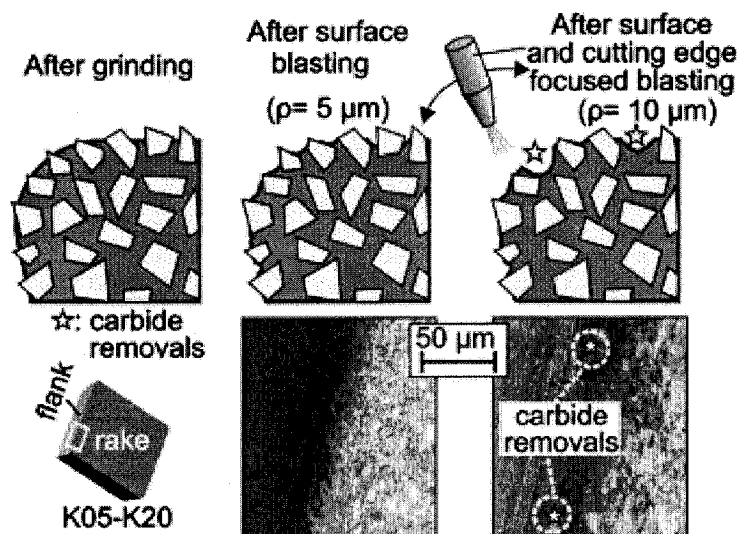


Figure 1.18 Cutting edges after surface blasting as well as after surface and focused on the cutting edges blasting. (K.-D Bouzakis et al., 2003)

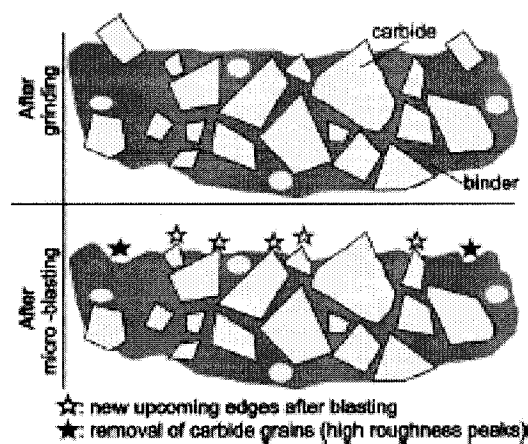


Figure 1.19 Micro-blasting effect on cemented carbide (HM) substrates (K.-D Bouzakis et al., 2001)

2. Cutting edge radii manufactured by honing method

Edge hones are commonly used for edge preparation in many situations, where increased edge strength is desired. Applying a honed edge can protect cutting edge from chipping and increase tool life.

In the brush honing process, inserts are mounted on a rotary carrier. When the carrier slowly rotate about their inscribed-circle axis, the inserts are polished while be fed through the rotating carrirer. By varying the time and depth of contact between the brush and the cutting edge, different edge radii can be obtained. However, the commercial brush honing process will cause the radius value varying along the cutting edge, as parabolic pattern as shown in Fig. 1.20 (Roy J. Schimmel, Jairam Manjunathaiah, Willam J. Endres, 2000). So, the flank wear vary along the cutting edge too. (Willam J. Endres. 2002)

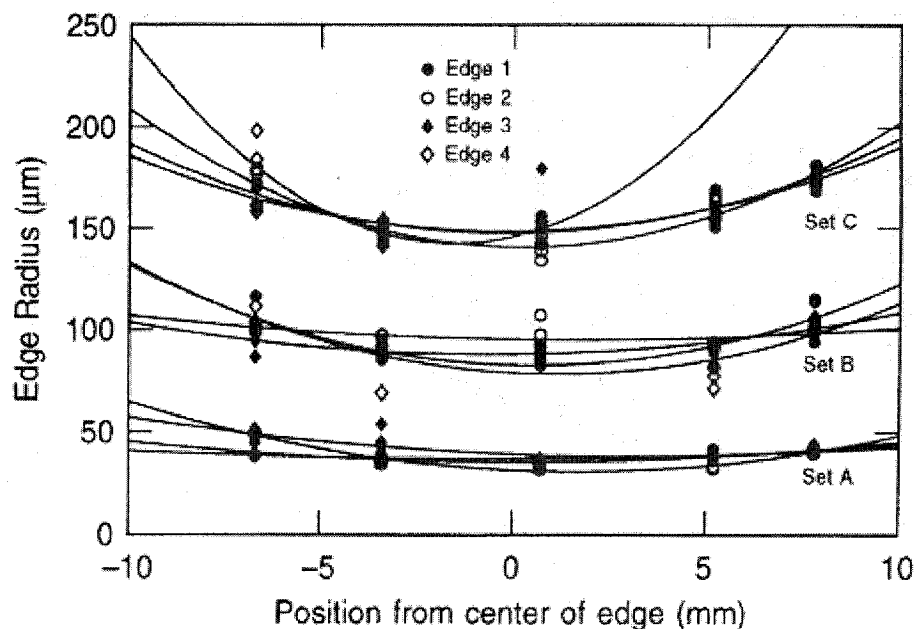


Figure 1.20 The variation of edge radius along the four cutting edges of inserts from set A ($50.8\mu\text{m}$), set B ($101.8\mu\text{m}$), and set C ($152.4\mu\text{m}$). (Willam J. Endres. 2002)

1.8 Introduction of cutting tool materials

Modern metal cutting started from 1850s. The most popular materials for cutting tool are high speed steel (HSS), cemented carbide, coated carbide, cermet and ceramic, diamond as shown in Table 1.5.

Table 1.5 Characteristics of several types of tool materials (Shaw M. C., 2005)

Material	Hardness			Typical Transverse Rupture Strength (Mpa)	Young's Modulus E (x 10 ⁶ Mpa)
	Room Temperature	535°C	736°C		
HSS	63-70R _C	50-58 R _C	Very low	4140	0.207
	85-87R _A	77-82 R _A			
Cast alloy	60-65R _C	48-58 R _C	40-48 R _C	2070	0.207
	82-85R _A	75-82 R _A	70-75 R _A		
Carbide	89-94R _A	80-87 R _A	70-82 R _A	1724	0.414-0.621
Ceramic	94R _A	90 R _A	87 R _A	586	0.414
Diamond	7000 knoop	7000 knoop	7000 knoop	276	>0.621

1.9 Introduction of cemented carbide

Cemented carbides are a group of hard, wear-resistant and difficult-to-machine materials. They are made from hard carbide particles that are cemented by a soft and ductile metal binder. Compared to operating conditions of High Speed Steel tools, which are primarily restricted by their annealing resistance, hot hardness and hot wear resistance, operating condition of cemented carbide inserts are mainly limited by their toughness, resistance to abrasion, diffusion and oxidation.

The cause of carbide failure and more demanding interrupted cut conditions continue to imply a need for improved toughness and wear resistance of carbide inserts (Table 1.6 presents the history of carbide and market needs). One key area is to using coating technology, which will not be discussed in this paper. Another area is to ameliorate the cutting conditions between the substrates and the workpiece by optimizing the geometry of insert, microstructure of material of inserts, etc.

Carbides were first developed in Germany in the early 1920s in response to requirements of a high resistant die material for drawing tungsten incandescent filament to replace the expensive diamond dies then in use.

The first cemented carbide to be produced was tungsten carbide (WC) with cobalt by French chemist Herri Moissan in 1890s (Moissan H., 1904). Since Schröeter created the power metallurgy techniques to produce the consolidated product in 1923 (Schroeder K., 1925), the basic WC-Co material has been modified to produce a variety of cemented carbides, which are used in a wide range of applications, including metal cutting, mining, construction, rock drilling, metal forming, structural components and wear parts. Approximately 50% of all carbide production is used for metal cutting applications.

Table 1.6 Dates of carbide introduction and tool concepts (Shaw M. C., 2005)

Date	Material	Manufacture market evolution
1928~1930s	Sintered tungsten carbide (WC, K type)	Aircraft
1940s~1950s	Sintered tungsten carbide (WC, P type)	World War II
	Clamped carbide inserts	Nuclear industry
	Indexable “throw away” inserts	CNC
1960s	Titanium carbide (TiC)	Jet engine program
	Improved tungsten carbide (WC)	Space program
	Coated carbide	

1.10 Summary of literature review of metal cutting technology

Because cutting edge is such an important factor in optimization of metal cutting, how to improve the precision of prepared cutting edge and how to prepare the cutting edge according to engineer's design is a valuable and attractable job.

This thesis presents a study on using laser micro machining technology to prepare the cutting edge roundness of cemented carbide insert. The effects of the laser cutting parameters are also investigated.

In chapter II, the thermal effect of laser beam on cemented carbide is analyzed. The negligible heating effect is expected that the machined cemented carbide, ceramic, cermet or HSS materials can maintain the strength, hardness and surface integrity changes in acceptable range.

CHAPTER 2 HEATING EFFECTS OF LASER BEAM ON CUTTING TOOL MATERIAL

2.1 Introduction

During laser machining process, material is removed instantly through a phase change caused by intense laser, either melting or vaporization. Due to the tremendous temperature gradients that are developed in the machined surface, many of secondary effects relating to surface quality will occur during laser machining, such as micro-cracking, formation of a heated-affected zone and formation of striations. Hence, it is important to understand heat transfer mechanism during laser machining.

Figure 2.1 presents an example of heat transfer and fluid mechanics occurring during laser machining.

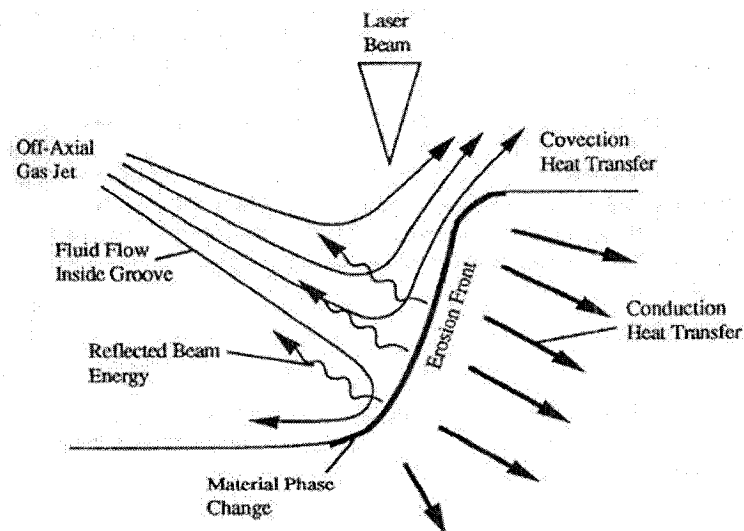


Figure 2.1 Heat transfer and fluid mechanics occurring during laser machining. (George Chryssolouris, 1991)

The laser beam can be modeled as an high density energy beam with a prescribed spatial and temporal intensity distribution. When the laser beam impinges on the surface of the erosion front, parts of this radiant energy may be reflected back to the environment, absorbed by the surface or transferred into the solid interior. Radiation heat transfer is influenced by the reflectivity R of the machined surface. R can be evaluated by the Fresnel formulas. It depends on the state of the surface (roughness of the surface, grade of the finishing, the presence of an oxide film). R decreases when the radiation flux density increases.

The absorbed laser beam energy cause the effected zone temperature raising. The energy transmits from high temperature zone to low temperature zone. Convection heat transfer is influenced by the thermal conductivity K (J/m/s/°C or W/m/°C) or thermal diffusivity D (m²/s). The relation of thermal conductivity and thermal diffusivity D is $D=$

$$\frac{K}{\rho C_p} \text{ (m}^2\text{/s) . } \rho \text{ is density (kg/m}^3\text{). } C_p \text{ is specific heat (J/kg/°C).}$$

Thermal energy may also be dissipated from the erosion front surface to the environment under the influence of fluid flow, such as the coaxial or off-axial gas jet used during laser machining. Convection heat transfer is influenced by the fluid mechanics of the gas flow near the erosion front, which is related to the gas jet pressure, jet orientation with the erosion front and the type of gas used.

2.2 Generalized model for laser machining

In order to control the laser machining process, a general model should be developed for the laser machining process. In the model, simple relations between the depth of cut and process variables, such as laser beam power and moving velocity of laser beam are known.

Because the heat transfer during laser machining is very complex, such as three dimension heat transfer, multi material phases (e.g. solid, liquid, vapor, plasma), a

moving boundary, a spatially distributed heat source, etc. Simplified analysis will be used according to different situation.

For instance, in laser drilling, the drilling direction is dominant over other directions, the heat flow is often assumed as one-dimensional heat flow whose heat conduction is zero. In laser cutting, due to the presence of a bottom surface in cutting that behaves as an adiabatic boundary, the heat conduction occurs two-dimensionally (downward conduction is negligible compared with conduction in other direction). In laser grooving, laser beam does not cut through the entire work piece. The heat flow is three-dimensional.

2.3 Three dimension conduction model of laser machining

2.3.1 Fundamental of conduction heat transfer

Considering that conduction heat transfer during laser machining is three-dimensional If thermal conductivity K is a constant, heat transfer equation should be written as:

$$\frac{\partial T}{\partial t} - D \nabla^2 T = \frac{q^m}{C_p \cdot \rho} \quad (2.1)$$

In order to research the effect of heat distribution on surface, we use other variables to rewrite the equation (2.2):

q^m : The rate of energy conversion per unit volume by heat source from work, chemical reaction. (J/m³/s)

C_p : Specific heat (J/kg/°C).

ρ : Density (kg/m³).

I : Power intensity of heat source on surface (W/m²)

C_p' : Specific heat per m² per m per °C. (J/m³/ °C)

The equation 2.8 can be rewritten as:

$$\frac{\partial T}{\partial t} - D \nabla^2 T = \frac{I}{C_p} \quad (2.2)$$

2.3.2 Thermal model of melting material

The analyses of the heating effect of laser beam on material are a very complicated work because of the many variables, such as heat loss from the heated surface by radiation and convection and heats of phase transition (melting, crystallization, evaporation). The analytical and numerical methods are the two main methods to be used in research on temperature distribution induced by the laser radiation.

In this paper, Green function method is used. Green function method is a well-known analytical method. It is the most universal method for analyzing the three-dimensional problems of heating semi-infinite bodies for any period of heating. It is quite attractive because it leads to the temperature field in the material without losing the physical aspects involved in the heating process.

When the intensity of laser beam is high enough, the existence of the second stage is very short. The material is vaporized directly. The high intensities are not totally absorbed at the surface. The part of the energy is removed out of the laser-affected zone with the vaporized material. Considering this point, we just model the temperature in laser-affected zone with the melting material ($T_{\text{melt}} < T < T_{\text{boil}}$).

2.3.3 Physical definitions of the process to be modeled

- 1) Laser beam has a Gaussian intensity distribution. It causes the heat accumulating on the surface of the material, which is absent of an external heat source. The heat transfers into the inner part of the material freely.

- 2) The treated object remains stationary relative to earth, it is considered as an object with semi-infinite geometry because the laser beam is small compared to the heat-treated object. $-\infty < x < \infty$, $-\infty < y < \infty$, $0 < z < \infty$.
- 3) The thermal conductivity, density and specific heat are independent of temperature.
- 4) Heat losses by radiation and convection are neglected.
- 5) When any location exceeds the boiling temperature, the material is considered to have been evaporated.
- 6) Any molten material is assumed to be entirely removed by a gas jet and does not affect the beam-material interaction.
- 7) The effect of differences in the thermal conductivities between the liquid and solid is not considered.

2.3.4 Heat transfer of moving laser beam

We assume that the laser beam is circular in (x, y) plane perpendicular to the direction of laser propagation (z). We assume a Gaussian laser intensity distribution on both direction, x and y.

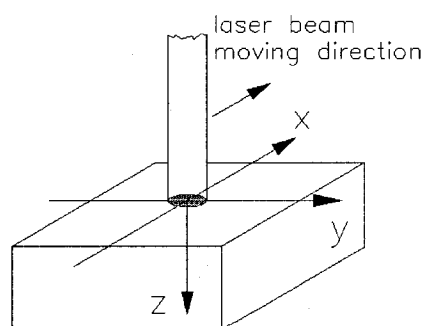


Figure 2.2 Schematic of laser beam moving in the x direction at a constant velocity

Absorbed laser power in workpiece can be expressed by equation 2.3.

$$P = (1 - R) \cdot P_{laser} \quad (2.3)$$

Gaussian power distribution is

$$I = \frac{\text{Energy}}{\text{Area}} = \{p \cdot \exp[-\frac{(x-vt)^2 + y^2}{r^2}]\} / (\pi r^2)$$

r : The radius of laser beam in the place where the intensity equal the $\frac{I_{\max}}{e}$. It is radius of focal spot (John F. R., 1971).

In heating calculation, it is better to use r_0 , which is the radius of laser beam in the place where the intensity equal the $\frac{1}{\sqrt{e}} I_{\max}$ to replace r . $r = \sqrt{2} r_0$

Thus, the power intensity of laser beam with Gaussian power distribution on surface is given as:

$$I_{\text{surface}} = \frac{P}{2\pi r_0^2} \cdot \exp[-\frac{(x-vt)^2 + y^2}{2r_0^2}] \quad (2.4)$$

The power intensity of laser beam with Gaussian power distribution in solid with the absorption depth λ :

$$I_{\text{inner}} = \frac{1}{h(\lambda)} \cdot \frac{P}{2\pi r_0^2} \cdot \exp[-\frac{(x-vt)^2 + y^2}{2r_0^2}] \quad (2.5)$$

P : Absorbed power of laser beam on surface (W).

R : Reflectivity of solid.

r_0 : The radius of laser beam in the place where the intensity equal the $\frac{1}{\sqrt{e}} I_{\max}$.

P_{laser} : The given laser beam power is actually equal 0.8413 total laser power.

$h(\lambda)$: the function absorption depth, when $z=0$, $h(\lambda)=1$.

When the temperature at (x, y, z) at the time t is due to the instantaneous point source of strength unity generated at the point $P(x', y', z')$ by a laser beam at the time t' , the laser beam shoot at $(x', y', 0)$, heat flow from $(x', y', 0)$ to (x, y, z) at the later time t .

If the heat loss through the surface to the ambient is assumed to be negligible and the ambient temperature is chosen as ($z=0$, $T=0$ °C)

The Green's function as source function for the diffusion equation

$$\frac{\partial T}{\partial t} - D\nabla^2 T = \frac{I}{C_p}$$

at the surface is (Carslaw H. S. et al., 1959):

$$G(x, y, z, t | x', y', z', t') = \frac{1}{8(\pi D \tau)^{\frac{3}{2}}} * \exp\left[-\frac{(x-x')^2 + (y-y')^2}{4D\tau}\right] * \left\{ \exp\left[-\frac{(z-z')^2}{4D\tau}\right] - \exp\left[-\frac{(z+z')^2}{4D\tau}\right] \right\} \quad (2.6)$$

The solution of equation $\frac{\partial T}{\partial t} - D\nabla^2 T = \frac{I}{C_p}$ is given by:

$$T(x, y, z, t) = \frac{1}{C_p} \int_{-\infty}^{\infty} \int_{-\infty}^{\infty} \int_{-\infty}^{\infty} \int_{-\infty}^{\infty} I(x', y', z', t') \cdot G(x', y', z', t' | x, y, z, t) dx' dy' dz' dt' \quad (2.7)$$

Considering that the function (2.13) regards that the solid is continuous in all direction and take a equal sink, we can carry out the integration over z' from $-\infty$ to $+\infty$ by taking twice its value from mirror image in order to account for the discontinuity at $z=0$.

Then the Green function becomes

$$G(x, y, z, t | x', y', z', t') = \frac{1}{4(\pi D \tau)^{\frac{3}{2}}} * \exp\left[-\frac{(x-x')^2 + (y-y')^2 + (z-z')^2}{4D\tau}\right] \quad (2.8)$$

D: thermal diffusivity (m² / s)

τ : t-t'. t is earlier than t'. When t = 0, $\tau = -t'$ means that the initial position of laser beam is at x', y'.

Integrate over x', y', z', then

$$T = \frac{P}{C_p} \int_0^{\infty} \frac{\text{Exp}\left[-\frac{(x+vt')^2 + y^2}{2r_0^2 + 4Dt'} - \frac{z^2}{4Dt'}\right]}{(\pi^3 Dt')^{\frac{1}{2}} \cdot (2r_0^2 + 4Dt')} dt' \quad (2.9)$$

(Cline H.E. et al., 1977)

By transformation to dimensionless variables, the equation (2.9) is simplified as :

$$T(x, y, z) = \frac{P}{C_p \cdot D \cdot r_0} \cdot f(x, y, z, v) \quad (2.10)$$

(Cline H.E. et al., 1977)

$f(x, y, z, v)$: Distribution function.

$$f = \int_0^{\infty} \frac{\text{Exp}(-H)}{(2\pi^3)^{\frac{1}{2}} \cdot (1+u^2)} du$$

$$H = \frac{\left(X + \frac{\rho}{2u}\right)^2 + Y^2}{2(1+u^2)} + \frac{Z^2}{2u^2}, \quad u^2 = \frac{2Dt'}{r_0}, \quad \rho = \frac{r_0}{DV}, \quad X = \frac{x}{r_0}, \quad Y = \frac{y}{r_0}, \quad Z = \frac{z}{r_0}$$

Using temperature distribution function $f(x, y, z, v)$ in equation 2.10, we can calculate the temperature distribution function along x axis or z axis as shown in Fig.2.3, Fig.2.4 and Fig. 2.5.

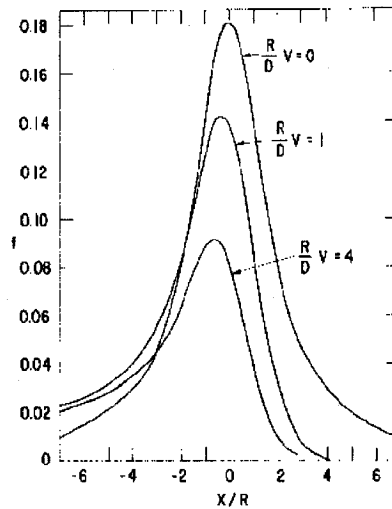


Figure 2.3 Surface temperature distribution function f along the x-axis that is the path of the laser beam for different scanning velocity. (Cline. E. et al., 1977). R: laser beam diameter; D: thermal diffusivity; Z: depth; V: laser beam scanning speed.

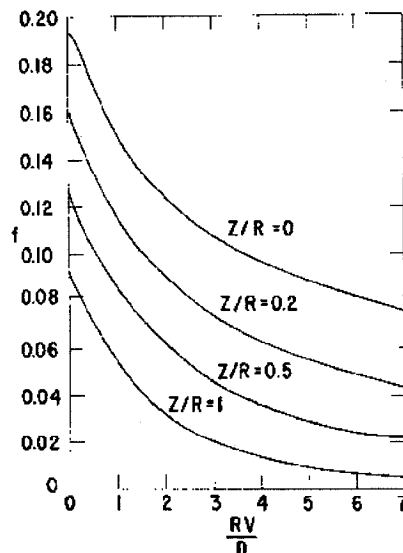


Figure 2.4 The effect of laser beam velocity on the temperature distribution f at different depths below the surface of laser spot, $(0, 0, z)$. (Cline. E. et al., 1977).

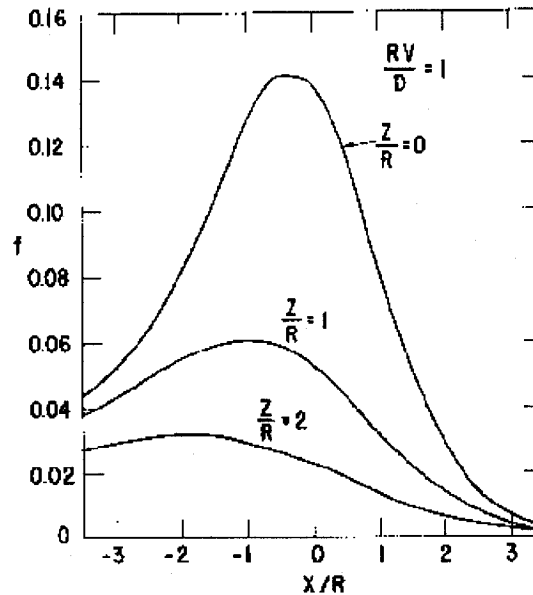


Figure 2.5 Temperature distribution f at different depths below the surface at a constant scanning velocity. (Cline, E. et al., 1977).

2.4 Calculation example

Cemented carbide is a widely used cutting tool material. It is important to know whether laser could machine the material? How the material composition of burned location would be changed? How large is the effect of HAZ? Calculation result will be used to estimate burning result, evaluate the feasibility of this method and drive us to think about whether other type of laser or cutting tool material (e.g. high speed steel, ceramic) could be used.

In the calculation, 100W laser will be used, which will be used in later machine experiment too.

Using 100 Laser beam to scan tungsten carbide insert, the parameters are following:

Laser beam	
Power P	100 W
Scanning speed V	8 cm/s
Spot diameter r_0	0.005 cm
Tungsten carbide	
Thermo conductivity k	41.84 W /m /°C
Density ρ	15600 kg/m ³
Specific heat capacity C_p	184 J/ kg /°C
Absorptivity	0.5

- Calculate C_p' : specific heat per m² per m per °C. (J/m³/ °C)

$$C_p' = C_p \cdot \rho = 184 \times 15600 \times 1 = 2870400 \text{ (J/m}^3 \text{/ } ^\circ\text{C)}$$

$$= 2.8704 \text{ (J/cm}^3 \text{/ } ^\circ\text{C)}$$

- Calculate thermal diffusivity D

$$D = \frac{k}{\rho C_p} = \frac{41.84}{15600 \times 184} = 1.458 \times 10^{-5} \text{ (m}^2 \text{/s)} = 0.1458 \text{ (cm}^2 \text{/s)}$$

- **Example 1.1:** calculating the point directly under laser spot, below workpiece

surface. $x=0, y=0, z=2 \mu\text{m}$ ($\frac{r_0}{DV} = 4.29 \times 10^{-3}$, $\frac{Z}{r_0} = 0.04$). (Figure 2.6)

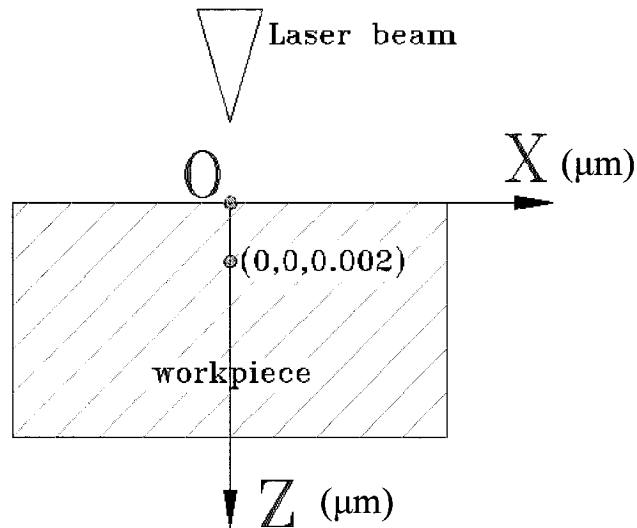


Figure 2.6 Temperature distributions at center point (0, 0, 0.002)

From function $f(x, y, z, v)$, we get

$$f(x, y, z, v) = 0.1914$$

$$T(x, y, z) = \frac{P \times a}{C_p \cdot D \cdot r_0} \cdot f(x, y, z, v) = \frac{100 \times 0.5}{2.8704 \times 0.1458 \times 0.005} \times 0.155 = 4827^\circ\text{C}$$

- **Example 1.2:** calculating the point around the centre point and below the workpiece

surface, $x=0.1\text{mm}$, $y=0$, $z=2\mu\text{m}$, $\frac{r_0}{DV} = 4.29 \times 10^{-3}$, $\frac{x}{r_0} = 2$, $\frac{Z}{r_0} = 0.04$. (Figure 2.7)

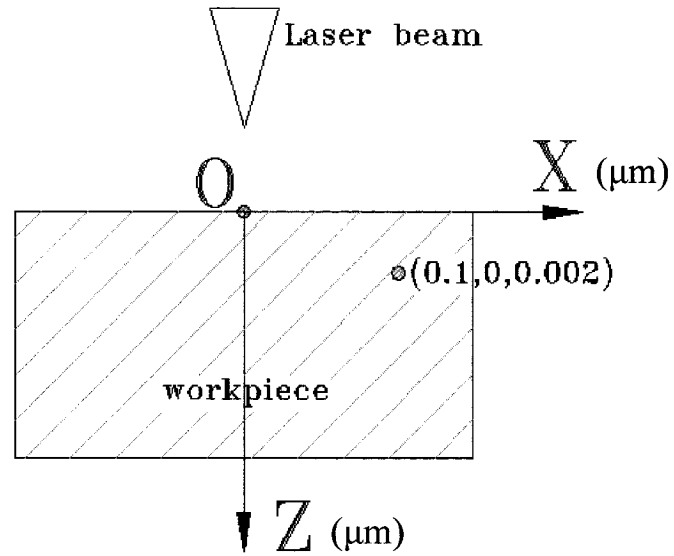


Figure 2.7 Temperature distributions at point (0.1, 0, 0.002)

From function $f(x, y, z, v)$, we get

$$f(x, y, z, v) = 0.04127$$

$$T(x, y, z) = \frac{P \times a}{C_p \cdot D \cdot r_0} \cdot f(x, y, z, v) = \frac{100 \times 0.5}{2.8704 \times 0.1458 \times 0.005} \times 0.08 = 986 \text{ } ^\circ\text{C}$$

- **Example 1.3:** calculating the point directly under laser spot, below workpiece

surface. $x=0, y=0, z=50 \text{ } \mu\text{m}$ ($\frac{r_0}{DV} = 4.29 \times 10^{-3}, \frac{x}{r_0} = 0, \frac{Z}{r_0} = 1$) (Figure 2.8).

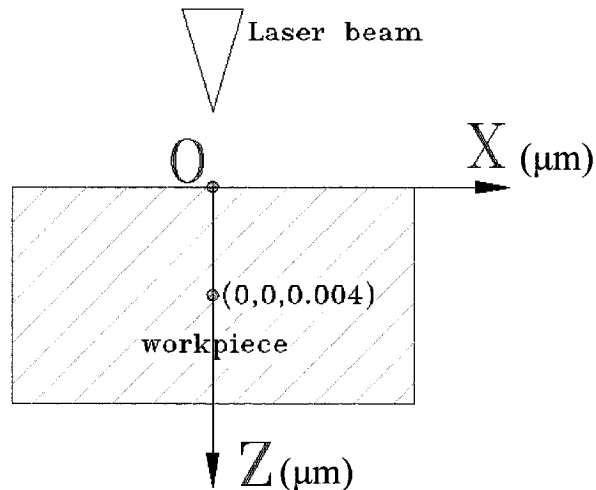


Figure 2.8 Temperature distributions at point (0, 0, 0.004)

From function $f(x, y, z, v)$, we get

$$f(x, y, z, v) = 0.1043$$

$$T(x, y, z) = \frac{P \times a}{C_p \cdot D \cdot r_0} \cdot f(x, y, z, v) = \frac{100 \times 0.5}{2.8704 \times 0.1458 \times 0.005} \times 0.08 = 2492 \text{ } ^\circ\text{C}$$

2.5 Conclusion

The melting point of Co is about 1495 °C, the melt point of WC or W₂C is about 2780-2860 °C. According to the previous calculations result, the following conclusion can be given:

Using laser to machine cemented carbide is a feasible method. The material removing rate is depending on the quantity of absorbed energy. When using laser to scanning the tungsten carbide, Cobalt should be preferentially vaporized, this phenomena will lead the concentration of Co in the machined surface of tungsten carbide insert will be decreased. The machined surface will include some melting and decomposition of surface compounds (i.e., Co oxide partly decomposes to metallic Co, the oxidised

tungsten carbide component decomposes to metallic tungsten and to tungsten oxide).

There will be a “melting effect” on the insert surface morphology.

When the absorbed energy per unit time can be controlled, the HAZ is very small. This method could be used on other cutting tool materials. Nano-, pico- and femtosecond pulse laser could be used also because of their smaller heating effects.

CHAPTER 3 LASER MACHINING EXPERIMENTS ON CEMENTED CARBIDE INSERTS

3.1 Introduction

The analytical thermal analysis of chapter 2 estimated the temperature distribution in cemented carbide materials during laser machining. In this chapter, the objectives of experiment, experimental material and equipment, parameters of DML 40SI laser machine and experimental procedures are introduced.

3.2 Objectives of experiment

The first objective of the experiments is to explore and verify the influences of the laser beam parameters in review of surface roughness of the machined surface of cemented carbide inserts

The second objective is to measure the dimensions of the laser machined geometries machined using the DML40 SI apparatus to qualify the machining performance on cemented carbide inserts.

3.3 Materials and equipment

Workpieces

Although the application of cemented carbide is very popular, its composition and performance greatly vary according to the application. In our experiments, we will use P25 and K20 cemented carbide inserts. These two types inserts are widely used in metal cutting process.

P25: This grade is used for turning, copying, milling (medium cutting speeds and chip sections) and planing with small chip sections. Machinable materials are steel, steel casting and malleable cast iron with long chips.

K20: This grade is used for turning, milling, planing, boring and broaching when demanding very tough carbide. Machinable materials are gray cast iron up to 220 HB, nonferrous metals, copper, brass and aluminum.

DML 40SI laser machine

The DML 40SI laser machine (as shown in Fig. 3(a), model 40SI, Lasertec Co.) is designed to produce precise mould and engraving/punch. This machine allows the direct machining of materials that are difficult to machine such as ceramics or hard metals. This technology does not only reduce manufacturing time and cost but also protect the environment compared to erode process.

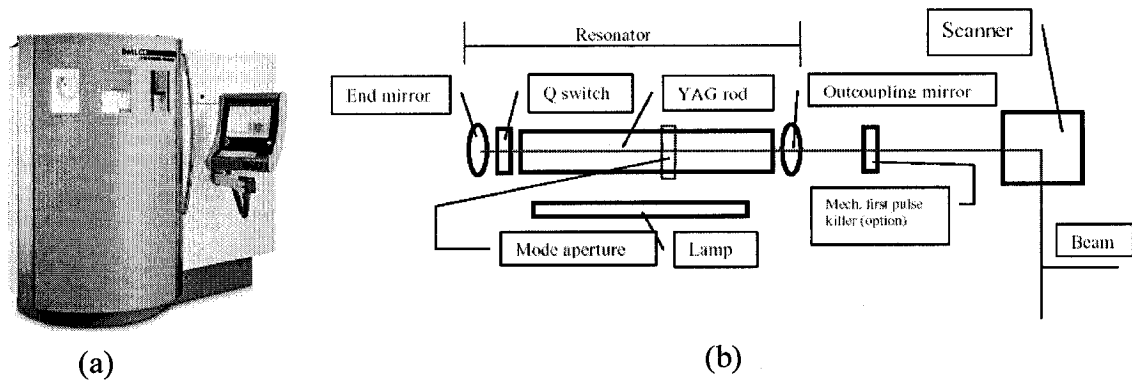


Figure 3.1 (a) DML 40SI laser machine. (b) Diagram of components of DML 40SI laser machine for beam generation and beam switch. (Manuel of Laser 3D)

Fig. 3.1(b) is the diagram of laser beam generating system of DML 40SI laser machine. It consists of YAG crystal rod (yttrium aluminum garnet) with active medium Nd^{3+} ions (neodymium), flash pump, Q-switch and mirror and Mode aperture. This is a solid laser system. The technical characteristics of the DML 40SI are listed in table 3.1.

Table 3.1 Technical information of DML 40SI laser machine.

Laser type	Nd:YAG laser, continuous pumped with pulse boost.
Laser class	4
Wave length	1.064 μm
Pulse boost	Q-switch
Continue wave output power	Min. 100 W
Feedrate	X, Y axis output <20000 mm/min
	Z axis output <12000 mm/min
Resolution	X,Y,Z axis : 0.001mm
Positioning tolerance	X,Y,Z axis : 0.001mm
Travelling distance	X axis: 400mm; Y axis: 300mm; Z axis : 500mm

3.4 Parameters of DML 40SI laser machine

With the DML40 SI laser machine, it is possible to obtain different quality of machined surfaces through the manipulation of processing condition such as Q-switch closing frequency, engraving speed, aperture mode (beam diameter), Q-switch opening time, machined layer thickness per shoot, track distance and current intensity. Their allowable range is presented in table 3.2.

Table 3.2 Machining parameters of DML 40SI laser machine.

Parameter	Range	
	Min	Max
Q-switch closing frequency (KHz)	4	50
Engraving speed (mm/s)	0	NA
Feed rate (mm/min)	0	20000
Aperture mode	small	big
beam diameter (μm)	30	70 ~ 90
Machined layer thickness per shoot (μm)	2	<50
Track distance (μm)	0	NA
Current intensity	0	100%

As shown in table 3.2, the range of laser machining parameters is large. A well-machined surface (i.e., smooth and precise) is only achievable when the laser beam parameters are adjusted according to the material properties.

3.5 Experimental procedures

The experimental procedure consists to combine CAD and CAM technologies to perform microstructure manufacturing on cemented carbide inserts. Optical microscope will be used to observe the surface texture of the machined surfaces and to measure the dimensions of the micro geometries through digital image analysis.

Phase 1: Before the laser machining, we used a CAD software (CATIA V5 R10, Dassault system), to draw the designed 3D geometries. Then, we converted the CAD model to *.Stl (stereo lithography) file. We used a CAM software (LpsWin, Lasertec Co.) to read the *.Stl document and generated the desired program for the DML40 SI laser machine.

Phase 2A: During the laser machining, we investigated the surface roughness and analysed the influences of laser beam parameters on the machined surface of cemented carbide inserts. The values of the experimental parameters tested are listed in table 3.3.

Table 3.3 Values of laser machining parameters for machining cemented carbide inserts.

Experiment number	Parameters studied	Appendix ID	Independent variable			Constant			
			Q-switch closing frequency (kHz)	Engraving speed (mm/s)	Laser spot overlapping ratio	Aperture Mode (diameter of focal spot)	Machined layer thickness (μm)	Track distance (mm)	Current intensity
1	Q-switch closing frequency	a1	4	40	$O_{ratio x}=0.33$	Small (30 μm)	0.002	0.01	25% Max
		a2	15	150					
		a3	25	250	$O_{ratio y}=0.33$				
		a4	30	300					
		a5	40	400					
		a6	50	500					
2	Engraving speed	b1	30	180	$O_{ratio y}=0.33$				
		b2	30	225					
		b3	30	300					
		b4	30	450					
		b5	30	900					
		b6	30	1350					
3	Q-switch closing frequency	A1	4	107	$O_{ratio x}=0.33$	Big (70-90 μm)	0.002	0.01	25% Max
		A2	15	400					
		A3	25	667	$O_{ratio y}=0.125$				
		A4	30	800					
		A5	40	1067					
		A6	50	1333					
4	Engraving speed	B1	30	480	$O_{ratio y}=0.125$				
		B2	30	600					
		B3	30	800					
		B4	30	1200					
		B5	30	2400					
		B6	30	3600					

Phase 2B: Another group of experiments was done to laser machine micro-geometry of different dimensions as shown in Fig. 3.2. The values used for the laser machining are presented in table 3.4. These values are chosen according to the geometry size, material property and machining rate, etc.

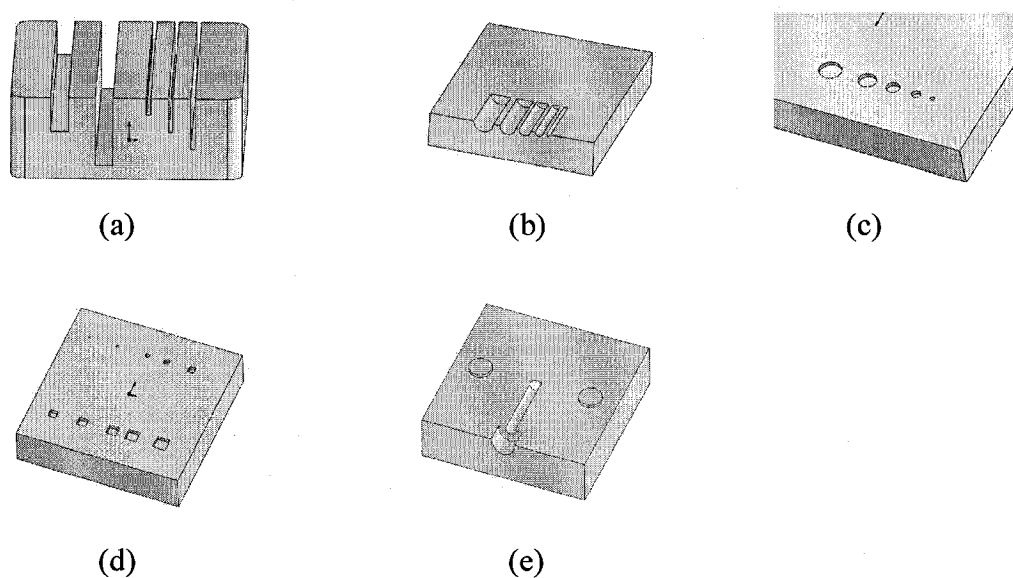


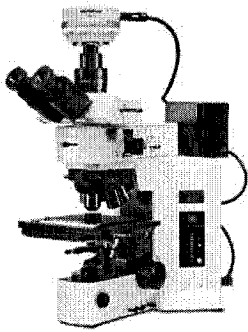
Figure 3.2 Laser machined micro-geometries on cemented carbide insert. (a) Micro-rectangular grooves. (b) Micro-semi circular profile grooves. (c) Micro-cylindrical pockets. (d) Micro-square pockets. (e) Micro-mould for micro-drill.

Table 3.4 Values of laser beam parameters for laser machining micro-geometries on cemented carbide inserts.

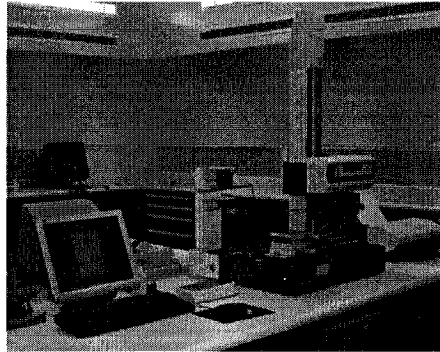
Q-switch closing frequency (kHz)	Engraving speed (mm/s)	Laser spot overlapping ratio	Current intensity (%)	Machined layer thickness (μm)	Track distance (mm)	Aperture mode (diameter of focal spot)
17	250	$O_{\text{ratio } x}=0.49$ $O_{\text{ratio } y}=0.4$	25% max	0.002	0.012	Small (30 μm)

Phase 3: After the laser machining, the roughness of the machined surfaces was measured with a formtracer (model: SV-C3000/4000, Mitutoyo, Inc., as shown in Fig.

3.3 (a)) and the surface texture was observed under an optical microscope (Olympus BX61, as shown in Fig.3.3 (b)). Then, we used the image analysis program Image-Pro Plus (version 5, Media Cybernetic Inc.) to analyze and measure the machined micro geometries. Finally, the efficiency of laser micro-machining technology on cemented carbide insert was evaluated.



(a)



(b)

Figure 3.3 (a) Olympus BX61 microscope. (b) Formtracer SV-C3000/4000

CHAPTER 4 ROUGHNESS ANALYSIS OF LASER MACHINED SURFACES

Laser beam parameters affect the roughness of laser-machined surface. Thus, it is very important to understand well laser beam parameters before machining and analyzing machining result. For most laser machining systems, the main laser beam parameters are lamp current, Q-switch frequency and Q-switch opening time (If the machine has a Q-switch), aperture size, engraving speed, feed rate and track distance, etc. The Fig. 4.1 shows the diagram of the laser generating system of the DML 40SI machine.

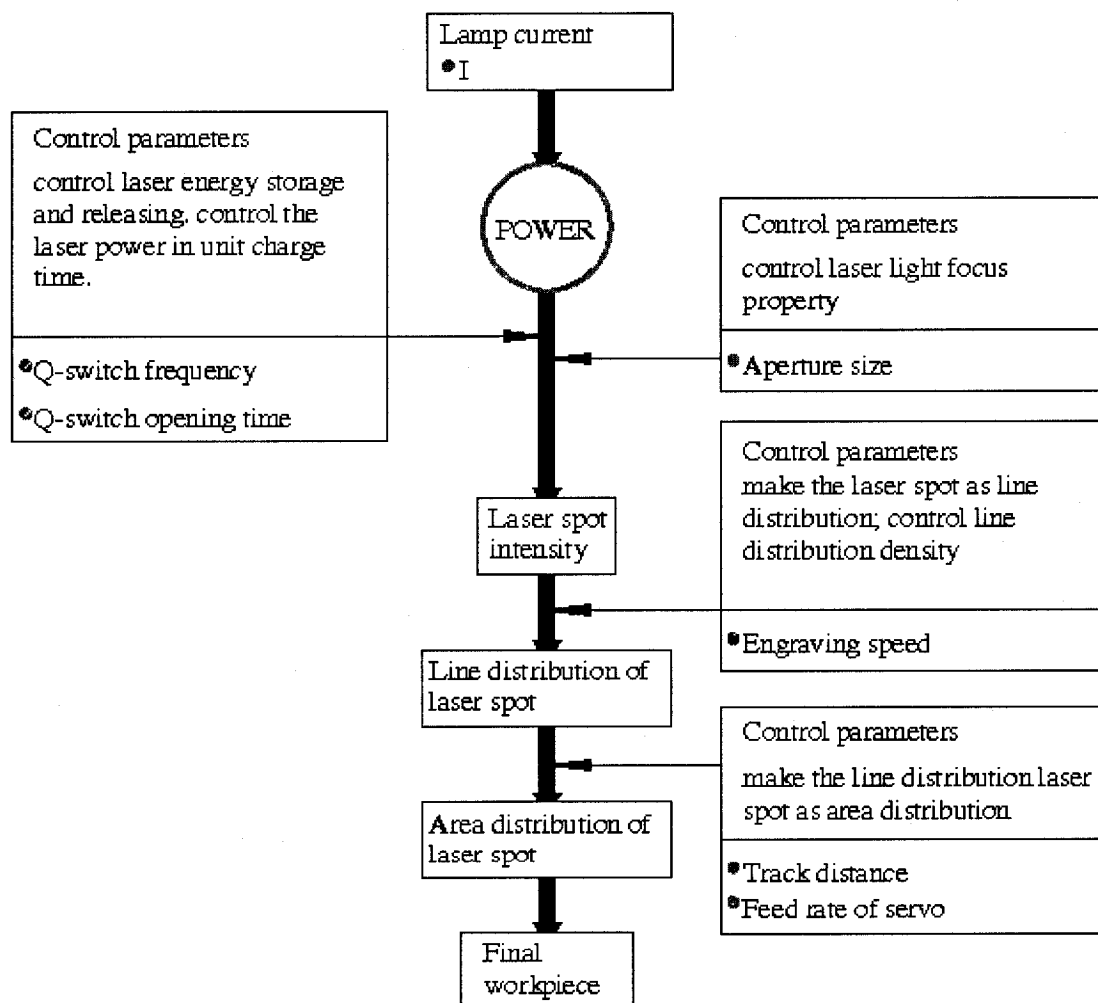


Figure 4.1 Diagram of the laser generating system of the DML 40SI machine.

As shown in Fig. 4.1, the lamp starts to pump YAG rod when the current is switched on. As soon as the energy is high enough in the YAG rod, Q-switch opens and one laser pulse is released. In order to get different laser focal spot size, mode aperture is put in the cavity as shown in Fig. 3.1 (b). With the movement and rotation of the mirrors and lens in laser scanning system, the laser beam scans the workpiece surface at a specific speed, which is called engraving speed. The distance between two neighbor-engraving tracks is called track distance. For the DML 40SI laser machine, the motion speed of the X-Y working table movement is called the feed rate. Among these parameters, the laser spot overlapping ratio and laser power intensity are most important for the machined surface roughness.

4.1 Laser spot overlapping ratio

The overlapping ratio (O_{ratio}) is the distance between the centers of two adjacent laser spots over the diameter of the spot as shown in Fig. 4.2.

$$O_{ratio} = \frac{d_{center}}{d} \quad (4.1)$$

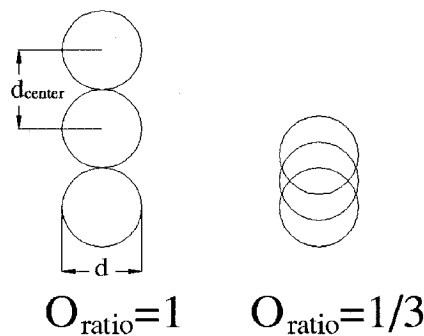


Figure 4.2 Overlapping ratio O_{ratio} .

The O_{ratio} is one of the key parameters that affect machined surface quality and machine rate. When the O_{ratio} is small, the local energy is high and the resulting laser scanning speed is low.

4.2 Effects of laser power

As shown in Fig. 4.1, the laser machining start from laser power input. High laser power will lead to big and deep laser craters.

- **Lamp current**

On DML 40SI laser machine, the laser power is adjustable by changing laser lamp current I.

- **Q-switch closing frequency and Q-switch opening time**

For DML 40SI laser machine, the parameters Q-switch closing frequency and Q-switch opening time are designed to adjust the energy of laser focal spot by controlling the energy stored and released. When the Q-switch is closed, the beam output is interrupted until a high level of population inversion and energy storage is achieved in the YAG rod.

The goal of controlling the Q-switch closing frequency is to control the amount of energy released and stored. Increasing the Q-switch-close time will charge resonator at more energy and the instantaneous laser output intensity will be increased. When Q-switch closing frequency increased or pulse length increases, the intensity of the laser beam decreases.

Fig. 4.3 illustrates the function of Q-switch closing frequency and Q-switch opening time. In Fig. 4.3, frequency $f_1 > f_2$, period B is longer than period A. When the Q-switch opening time is same, the laser beam energy in period B is higher than that in period A. Period C is as long as period B, but the Q-switch closing time in period C is shorter than that in period B, the laser beam energy in period C is less than that in period B.

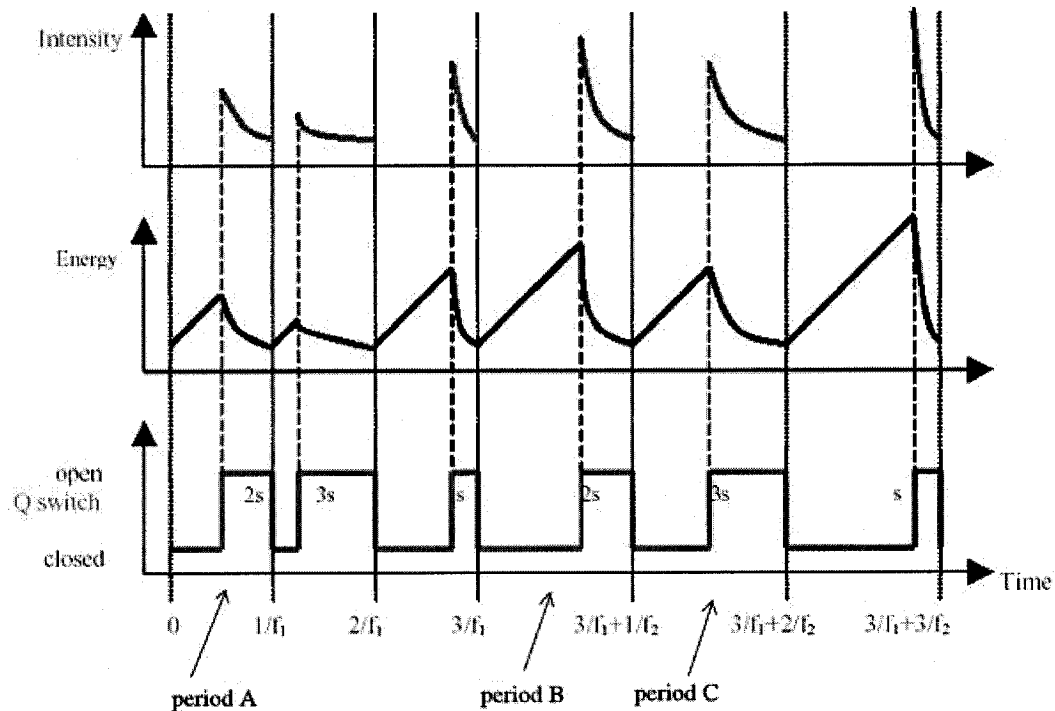


Figure 4.3 Schematic of the Q-switch function. (Manual of Laser 3D, Lasertec Co.)

For the DML 40SI laser machine, when the aperture size is 4mm and laser is in continuous wave mode, laser power is 100W. However, with the Q-switch function, the summit pulse power varies from 200kW to 60kW when Q-switch closing frequency varies from 1 kHz to 10 kHz. Because the minimal pulse length of Q-switch for DML 40SI is 90 ns, when the Q-switch closing frequency is 1 kHz, the energy of a laser pulse is 0.018 J. When the Q-switch closing frequency is 10 kHz, the energy of a laser pulse is 0.0054 J.

During our first group of experiments, the Q-switch closing frequency was varied from 4 to 50 kHz while the other parameters remained constant. These experiments were performed to investigate the influence of the Q-switch closing frequency on the roughness of the machined surface.

Fig. 4.4, Fig. 4.5, Fig. 4.6 show typical optical microscope images, profile chart and self-correlation chart of cemented carbide insert laser machined at 4 kHz and 50 kHz Q-switch closing frequency with the small aperture mode. More images of laser-machined samples are presented in Appendix A (Q-switch closing frequency = 15, 25, 30, 40 kHz)

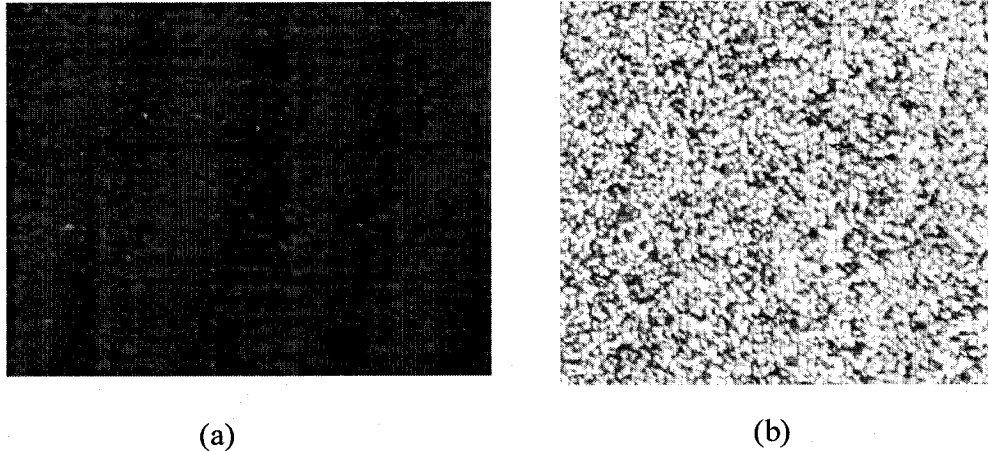


Figure 4.4 Effects of Q-switch closing frequency on cemented carbide (a) 4 kHz (b) 50 kHz (O_{ratio} is 0.33, track distance is 0.01mm, laser spot diameter is 30 μ m).

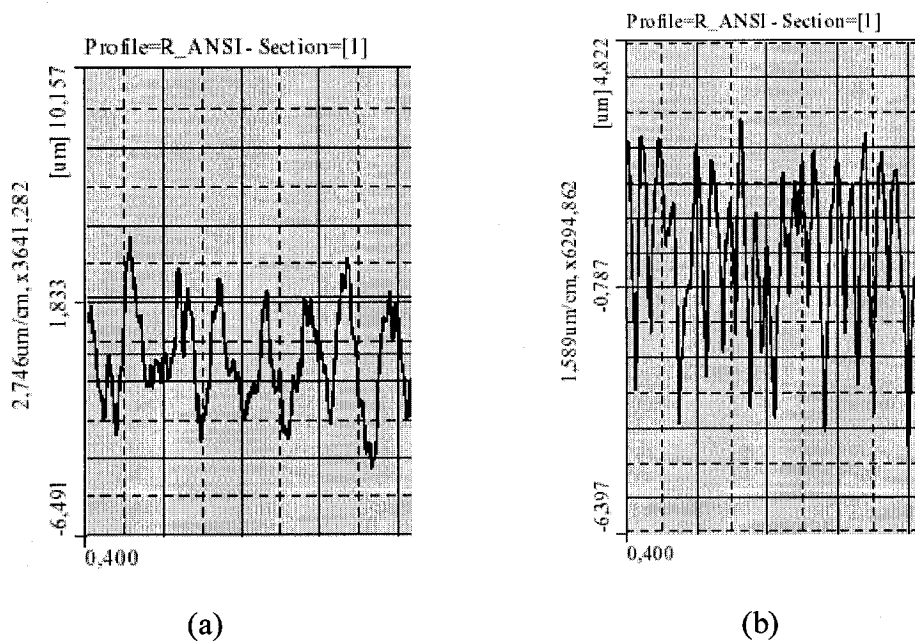


Figure 4.5 Profile of machined surface of cemented carbide (a) 4 kHz. (b) 50 kHz.

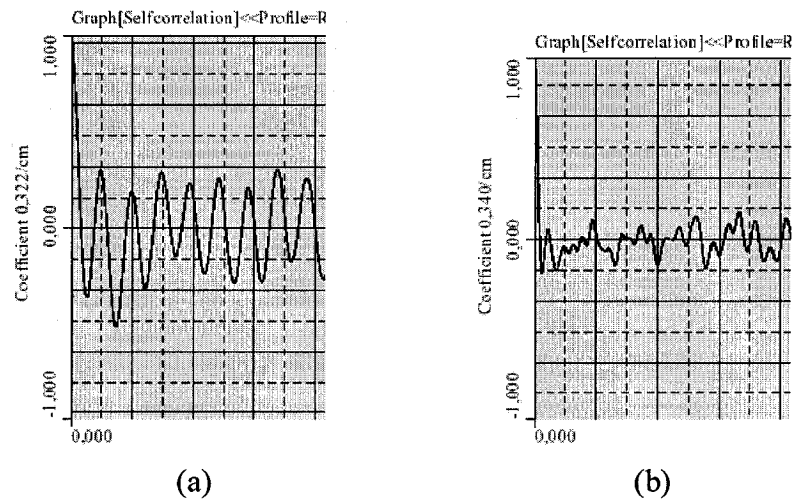


Figure 4.6 Self-correlation of machined surface of cemented carbide. (a) 4 kHz (b) 50 kHz.

1) Theoretical analysis of effects of Q-switch closing frequency for Fig. 4.4.

Fig. 4.7 is a schematic representation the 3D model of the surface texture after laser scanning where the peak and the crater shape influence the roughness of machined surface. In reality, the height of the peak is lower than predicted by simulation because of heat effects. As shown in Fig. 4.8, the heat transferred during subsequent laser pulses affects the form of the first crater. Thus, the height of peak is lower than predicted and it is difficult to predict the roughness.

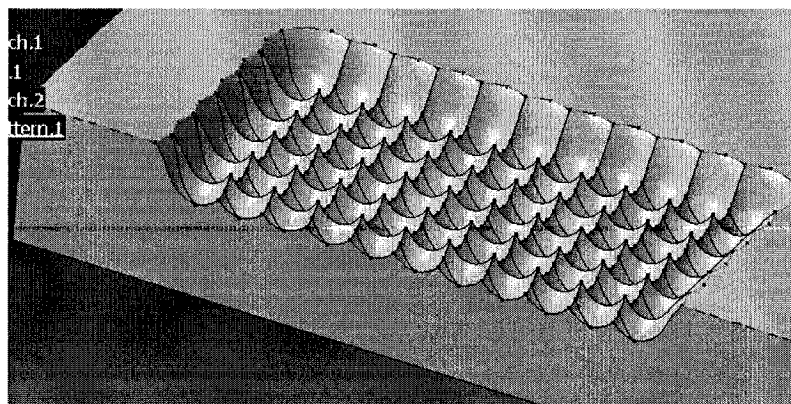


Figure 4.7 3D model of surface texture after laser scanning with $O_{\text{ratio}}=0.33$.

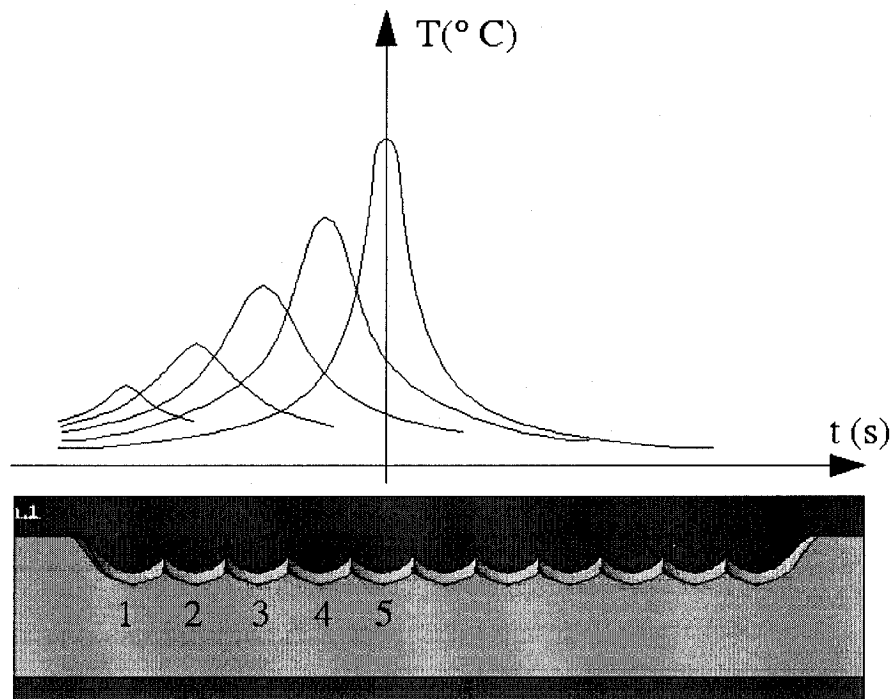


Figure 4.8 Schematic of temperature distribution during laser machining.

Because the 4 kHz Q-switch closing frequency pulse has more energy than 50 kHz pulse, the crater generated is deeper as illustrated in Fig. 4.9. Higher energy pulse will lead to deeper crater and higher temperature in the material. Thus, the measured roughness of the sample laser machined at 4 kHz Q-switch closing frequency was worse than that at 50 kHz.

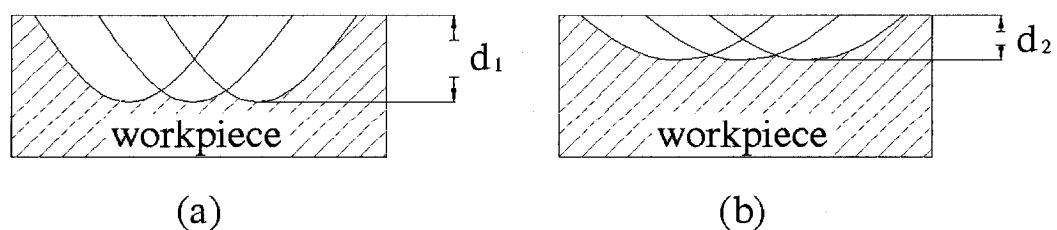


Figure 4.9 Schematic of laser machine with (a) 4 kHz and (b) 50 kHz laser spot.

Because 4 kHz laser spot has higher energy than 50 kHz laser spot has, the laser machining process with 4 kHz pulse is less sensitive to the workpiece flatness, machine vibration, etc., the material can be removed more evenly. Thus, the surface texture generated by 4 kHz laser beam is more periodic than that obtained by 50 kHz laser spot as shown in Fig. 4.6.

2) Experimental results analysis.

- **The color of the machined surface.**

As shown in Fig.4.4, the color of the machined surface changes from dark to bright when Q-switch closing frequency increases. The removed thickness of material decreases when Q-switch closing frequency increases (as observed on the machined samples). There were some scorched particles on the machined surface using the laser beam with 4 kHz Q-switch closing frequency. Above observed phenomenon conforms to the theory analysis that temperature caused by 4 kHz laser is higher than the temperature caused by 50 kHz laser when other laser beam parameters are the same.

- **Surface roughness.**

Table 4.1 and Fig. 4.10 show that the surface roughness measurements R_a are below $2.356\mu\text{m}$.

Table 4.1 Effects of Q-switch closing frequencies on surface roughness, spot size $30\mu\text{m}$.

Q-switch frequency (kHz)	Average R_a (μm)	Average R_{max} (μm)
4	1.949	17.199
15	1.156	9.157
25	1.129	9.056
30	2.356	17.907
40	1.505	10.691
50	1.092	7.120

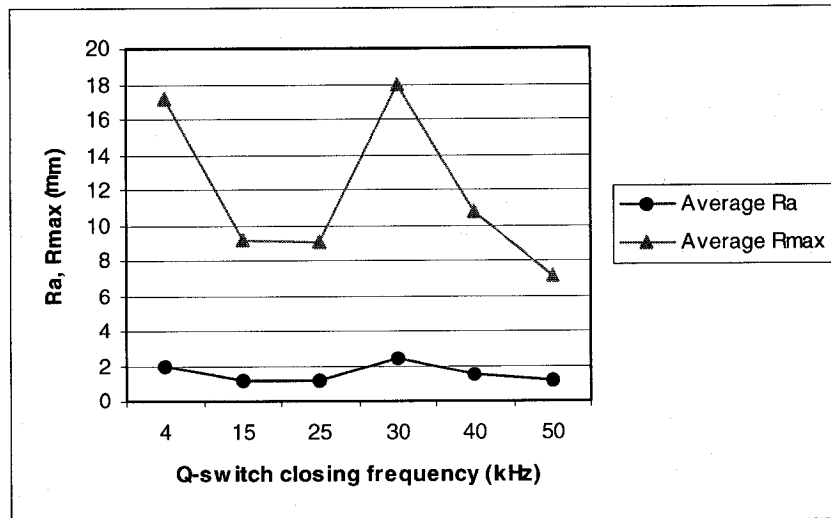


Figure 4.10 Effects of Q-switch frequencies on surface roughness, spot size 30µm.

Because the energy of 50 kHz laser spot is minimum, the crater generated by laser spot at $O_{ratio}=0.33$ is most shallow, the R_a and R_{max} values reached minimum.

Because the energy in 25 kHz laser spot is in median level and the local accumulated energy at $O_{ratio}=0.33$ is median, the material is removed evenly. R_a and R_{max} value is the second large in table 4.1. The optical microscope image, profile chart and selfcorrelation chart of the 25 kHz Q-switch closing frequency laser pulse machined surface are shown in Fig. 4.11.

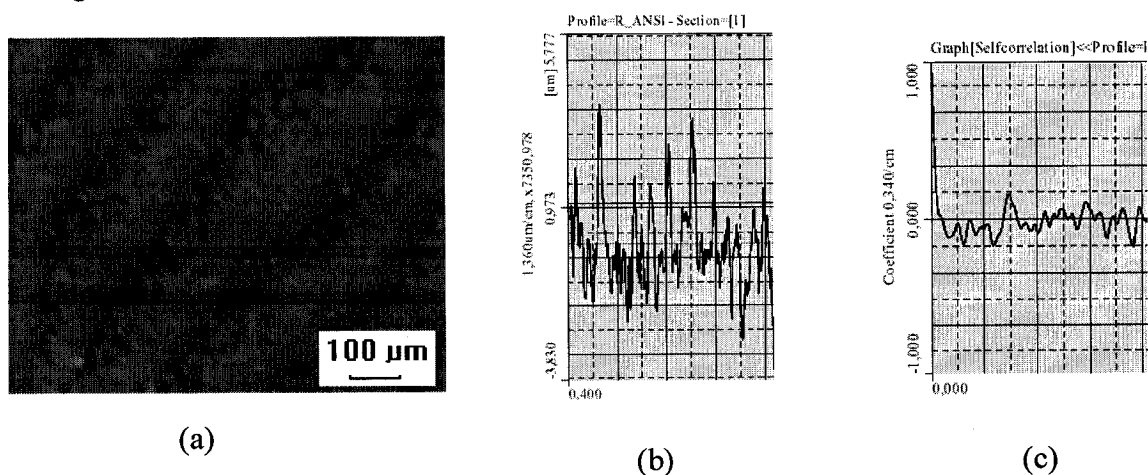


Figure 4.11 25 kHz Q-switch laser machined surface (a) optical microscope image (b) profile (c) self-correlation.

Although the laser beam energy in 30 kHz Q-switch is lower than the laser beam in 25 kHz Q-switch, the local accumulated energy is not enough to remove cemented carbide at $O_{ratio}=0.33$, the roughness reaches maximum value at 30kHz as shown in Fig. 4.10.

4.3 Effects of aperture size

In laser resonator, there are a lot of photons in off-axis mode, which is referred as in the higher mode. The higher mode photon is more difficult to be focused than lower mode photon. In order to minimize the occurrence of higher-order modes in the laser beam, an aperture is used in the cavity.

According to the Pythagora's Theorem, the number of higher mode photons (n) is given

$$\text{as: } n = \frac{1}{2} \times \frac{a^2}{L \cdot \lambda} \quad (4.2)$$

where L is length of laser cavity, λ is wavelength of the laser radiation, a is aperture size.

Using a large aperture will provide more photons in higher mode and a laser spot with a larger diameter. The heat distribution of a larger spot is more uniform over surface area. It is preferably used for welding, heat-treating and surface hatching as shown in Fig. 4.12 (b).

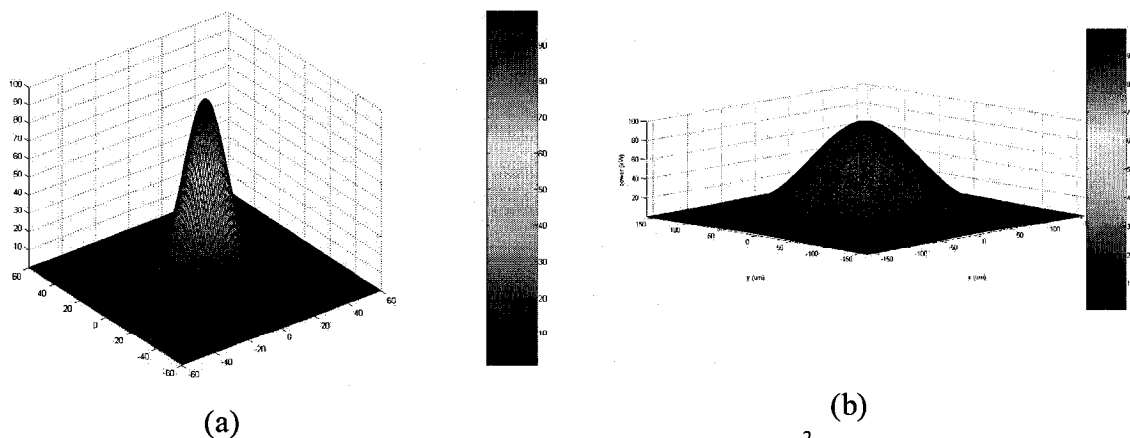


Figure 4.12 100W laser energy distribution $P = 100 \cdot \exp\left(\frac{-r^2}{r_{spot}^2}\right)$ (W) (a) 30 μ m spot (b)

80 μ m spot.

Fig. 4.13, Fig. 4.14 and Fig. 4.15 show typical optical microscope images, profile chart and self-correlation chart of cemented carbide insert laser machined at big and small aperture size. More images of laser-machined samples are presented in Appendix A.

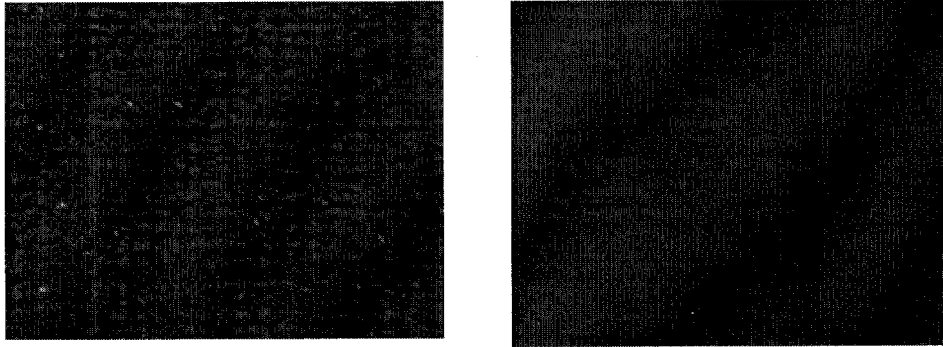


Figure 4.13 Effects of aperture size (a) 30 μ m spot (b) 80 μ m spot. Other laser beam parameters are: $f=4$ kHz, $O_{ratio}=1/3$.

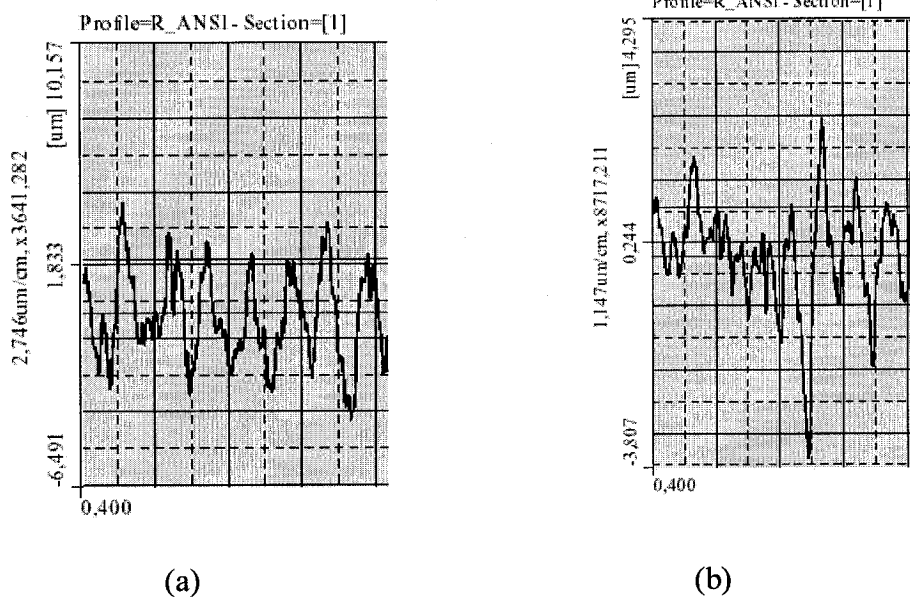


Figure 4.14 4 kHz Q-switch laser machined surface of cemented carbide (a) 30 μ m spot (b) 80 μ m spot.

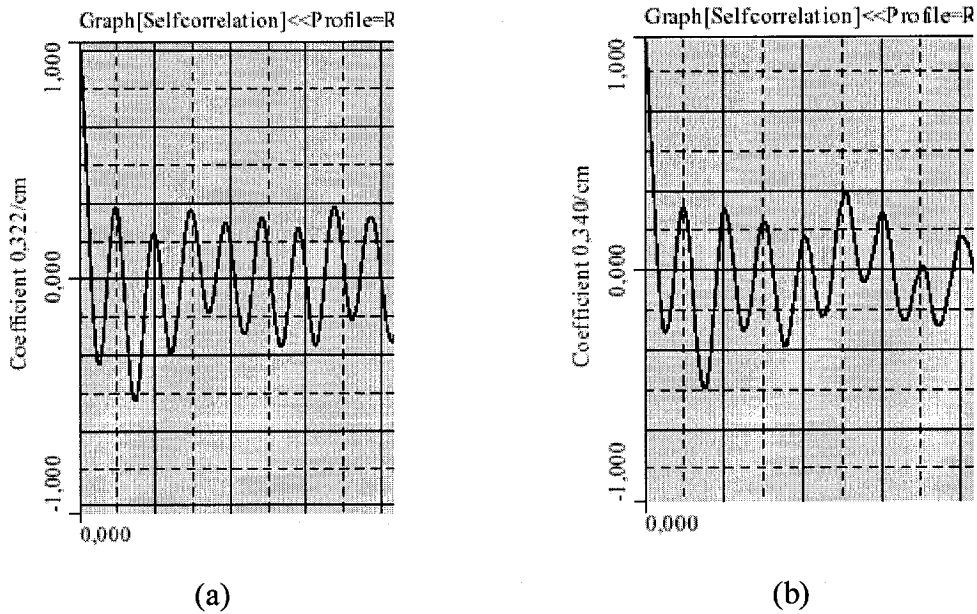


Figure 4.15 Self-correlation of 4 kHz Q-switch laser machined surface of cemented carbide (a) 30 μm spot (b) 80 μm spot.

1) Theoretical analysis of effects of aperture size

For the DML 40SI laser machine, the laser beam has a 30 μm diameter in the small aperture mode and a 70~90 μm diameter in the big aperture. Using the small aperture, the laser energy is more concentrated. The crater caused by a smaller laser spot is deeper than that caused by larger laser spot as illustrated in Fig. 4.16. The quality of the machined surface obtained by small aperture is worse than that generated by the big aperture. However, it is better to use small aperture to sculpt sharp edges and deep grooves

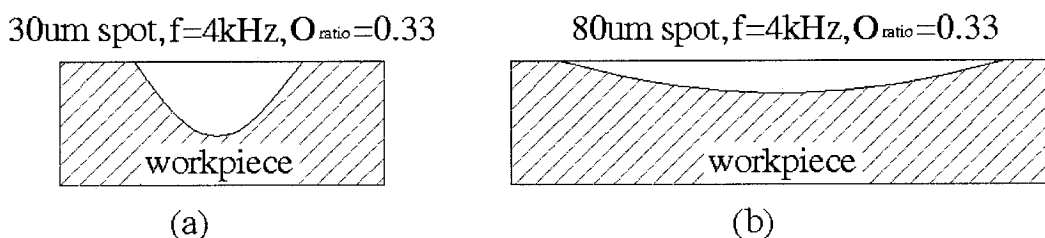


Figure 4.16 Schematic of laser machine with a) small aperture b) big aperture sizes.

2) Experimental results analysis.

Table 4.2 presents the surface roughness of machined surface with 30 μm and 80 μm laser spot.

Table 4.2 Effects of aperture size on surface roughness, O_{ratio} is 0.33.

Q-switch closing frequency (kHz)	Average Ra (μm)	
	Small spot (30 μm)	Big spot (80 μm)
4	1.949	0.828
15	1.156	0.891
25	1.129	1.065
30	2.356	1.872
40	1.505	1.155
50	1.092	0.738

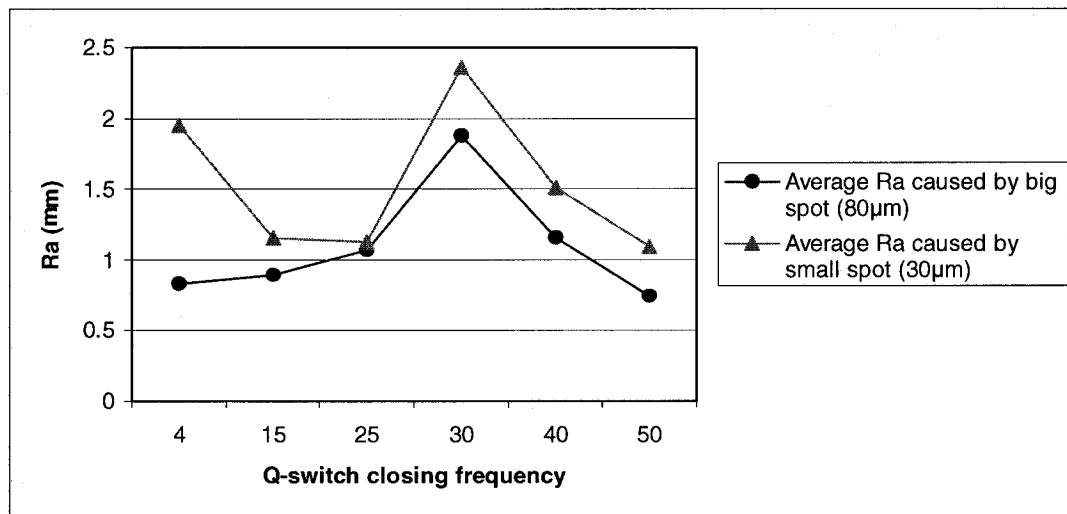


Figure 4.17 Effects of aperture size on surface roughness, O_{ratio} is 0.33.

The roughness measurements for samples machined using a big aperture are smaller than that using a small aperture as shown in Table 4.2 and Fig 4.17. These experimental results correspond to the theoretical analysis.

4.4 Effects of the engraving speed.

Engraving speed ($V_{engraving}$) is function of the laser spot overlapping ratio (O_{ratio}) for a specific scan direction and laser spot diameter.

$$V_{engraving} = O_{ratio} \times f \times d \quad (4.3)$$

where f is Q-switch closed frequency (kHz), d is diameter of laser spot. (μm), $V_{engraving}$ is engraving speed of laser beam. (mm/s)

Fig. 4.18 illustrates the laser beam engraving speed with $O_{ratio}=1$.

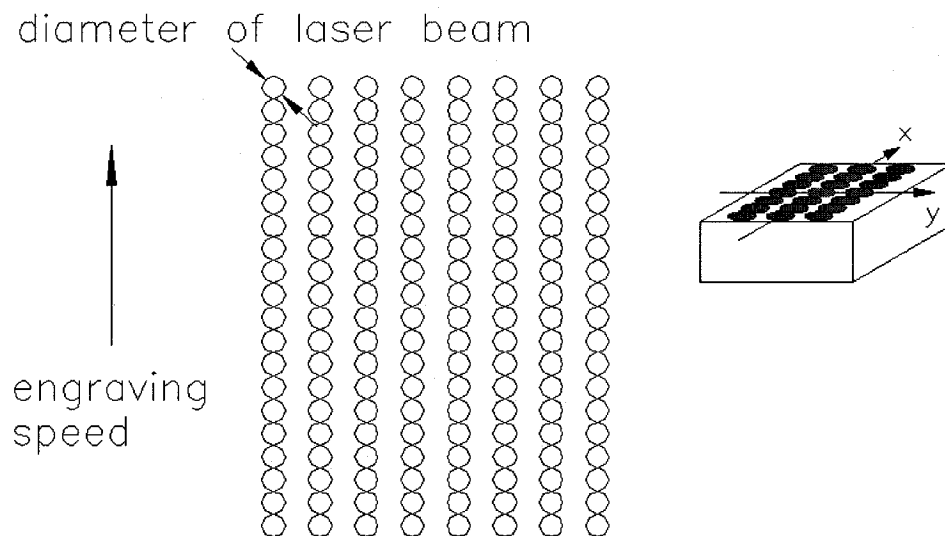


Figure 4.18 Schematic of engraving speed. ($O_{ratio}=1$)

The track of the laser spot on the machined surface is also important for the machined surface quality. The density of distribution of laser spot on the machined surface can be adjusted to obtain different machined quality. For example, when the space between two neighbor spots (s value in Fig. 4.19) or the space between two neighbor scanning tracks (t value in Fig. 4.19) is changed, different machined surface quality can be obtained.

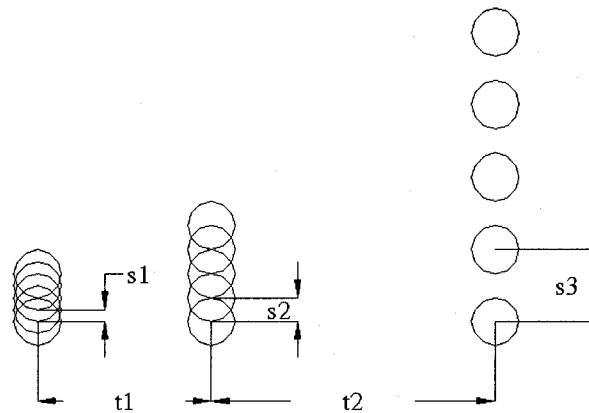


Figure 4.19 Schematic of different spaces between two neighbor spots (s_1 , s_2 , s_3) and two neighbor-scanning tracks (t_1 , t_2).

The laser beam scanning direction in two adjacent up-down layers forms laser hatching mode as shown in Fig. 4.20.

The laser-hatching mode can also be adjusted in CNC program to get different machined texture.

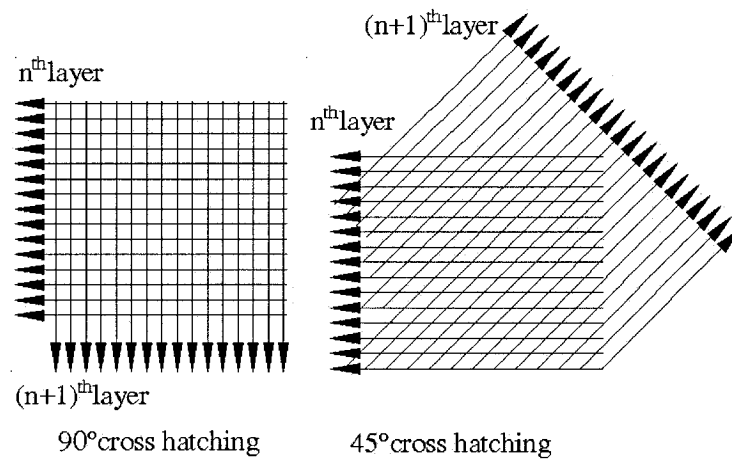


Figure 4.20 Schematic of laser hatching mode.

Another group of experiments was performed to investigate the influence of the engraving speed on the roughness of the machined surface. In the experiments with a small laser spot, the engraving speeds were 180 mm/s, 225 mm/s, 300 mm/s, 450 mm/s,

900 mm/s and 1350 mm/s. The corresponding O_{ratio} were 1/5, 1/4, 1/3, 1/2, 1, 1½. In the experiments with a big laser spot, the engraving speeds were 480 mm/s, 600 mm/s, 800 mm/s, 1200mm/s, 2400mm/s and 3600mm/s. The corresponding O_{ratio} were 1/5, 1/4, 1/3, 1/2, 1, 1½ too. During these experiments, the 90° hatching mode was used while other parameters remained constant.

1) Theoretical analysis of effects of engraving speed.

The schematic of laser machine with different engraving speed is shown in Fig. 4.21. When $V_{engraving}$ is 180 mm/s, the local energy absorbed is the highest and the machined surface is not smooth. When $V_{engraving}$ is 1350 mm/s, the craters are too discrete far from each other and the machined surface is also not smooth. The optimal machined surface will be achieved when the laser power, the $V_{engraving}$ and material properties are properly matched.

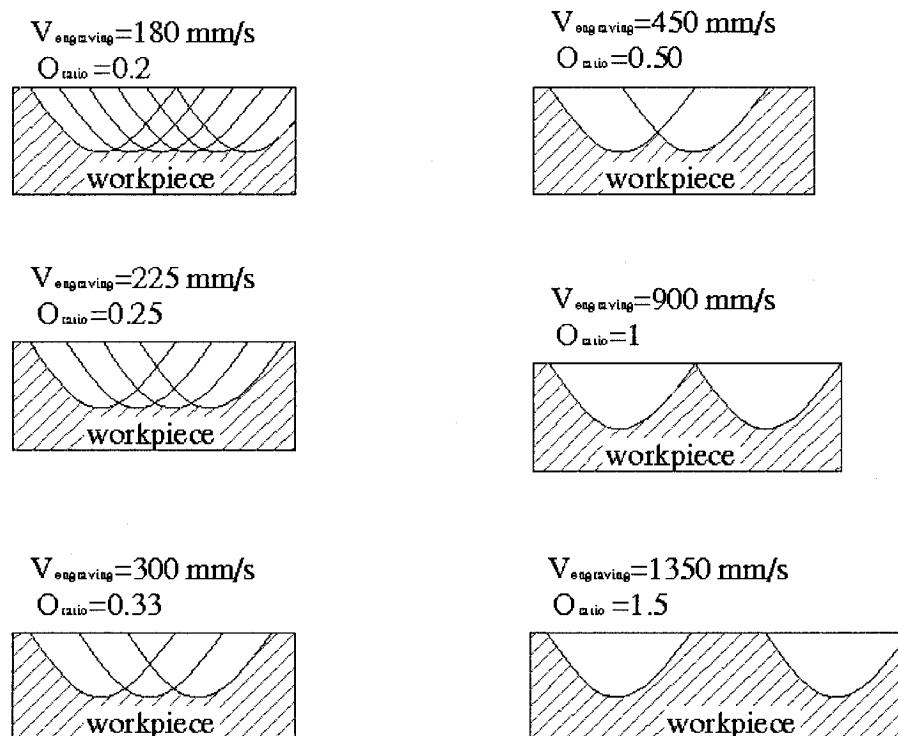


Figure 4.21 Schematic of different laser engraving speed when $f=30$ kHz, spot size $30\mu\text{m}$.

2) Experimental result analysis.

Table 4.3 and Fig. 4.22 show that the surfaces obtained with different engraving speed and with small laser spot. Surface obtained at 180 mm/s and 1350 mm/s engraving speed are rougher than the others. For the $V_{engraving}$ is 900 mm/s, the obtained roughness is minimal. For the $V_{engraving}$ in 200~300 mm/s range, the obtained roughness is second minimal.

Table 4.3 Effects of engraving speed on surface roughness, spot size 30 μ m.

Engraving speed (mm/s)	O_{ratio}	Average R_a (μ m)	Average R_{max} (μ m)
180	0.2	2.855	19.66
225	0.25	2.258	19.138
300	0.33	2.081	14.452
450	0.5	2.13	15.523
900	1	1.861	13.720
1350	1.5	3.080	21.704

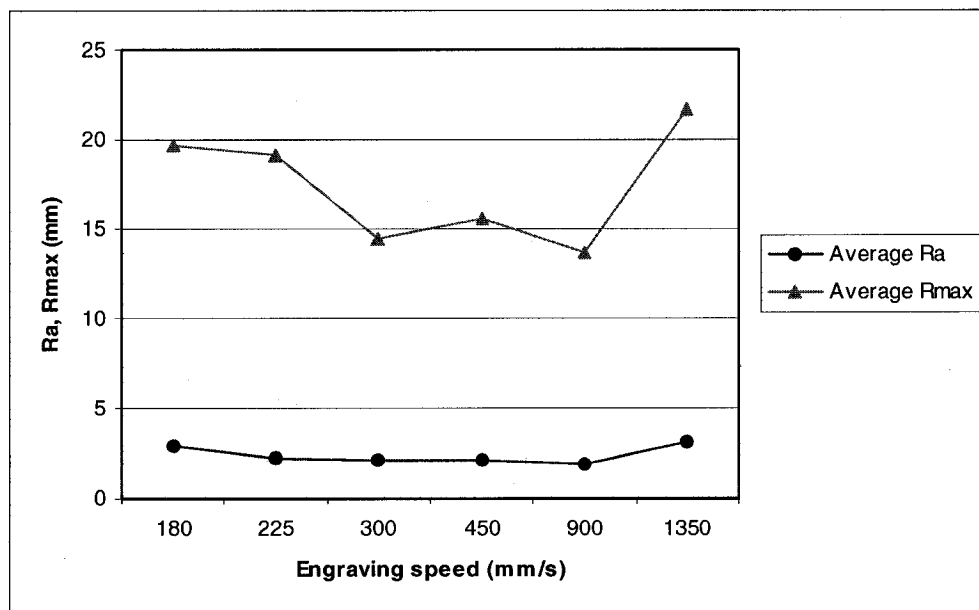


Figure 4.22 Effects of engraving speed on surface roughness, spot size 30 μ m.

4.5 Effects of servo feed rate

The speed of servo is designed for control the moving speed of working table. Adjusting this parameter to shorten the work piece positioning time can control the machining rate. Some CNC system allows X-Y working table moving in one axis while laser spot moving in other axis. For DML 40SI laser machine, X-Y working table and laser beam can not move at same time.

If people choose high feed speed, the start and stop will produce large inertia force and vibration. These factors will affect the quality of machined surface.

4.6 Effects of the track distance

The *Track distance* (D) is the space between two adjacent laser tracks. It is always recommended to use the distance between two-laser pulses for DML 40SI machine.

$$D = \frac{V_{engraving} \left(\frac{mm}{s} \right)}{f(hz) - 1} \quad (4.4)$$

The value can be approximate by $D \approx \frac{V_{engraving}}{f} \approx O_{ratio} \times d$ (4.5)

O_{ratio} : overlapping ratio.

d : diameter of laser spot.

If the track distance is too small, the two adjacent laser traces overlap too much and the local energy absorbed will be too high for a smooth machined surface. The effects of track distance are as same as the effects of the engraving speed. The schematic of track distance is shown in Fig. 4.23.

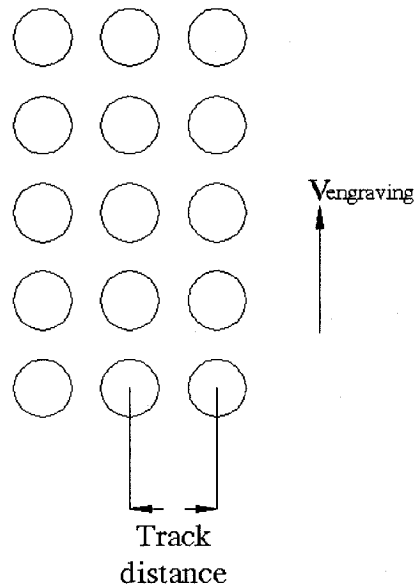


Figure 4.23 Schematic of track distance.

4.7 Thickness of machined layer per pulse

Every time Q-switch opens, the laser beam will shoot the workpiece and one layer of material will be removed. The machined layer thickness can be obtained by adjusting the focal position. Because the surface spot size determines the surface power intensity and the depth of penetration, the optimum cutting can be obtained by having the minimum spot size slightly below the surface as shown in Fig. 4.24. $2\mu\text{m}$ layer thickness is used in all experiments.

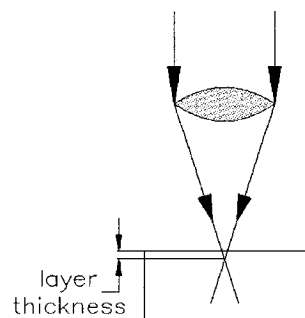


Figure 4.24 Schematic of the thickness of machined layer .

4.8 Conclusion

From the different machining experiments, the following conclusions on the effects of laser beam parameters could be given:

- 1) O_{ratio} and laser power intensity are the two most important parameters during laser machine. If O_{ratio} is too small, the local energy absorbed is too much, then the machined result is not good. If O_{ratio} is too big, the laser spots are too discrete from each other, the local energy absorbed is too little and the machined result is not good also. The surface roughness is a complicate function of laser power and O_{ratio} . If the experimental data were enough, a diagram of roughness with laser power intensity and laser spot overlapping ratio would be obtained as shown in Fig. 4.24.

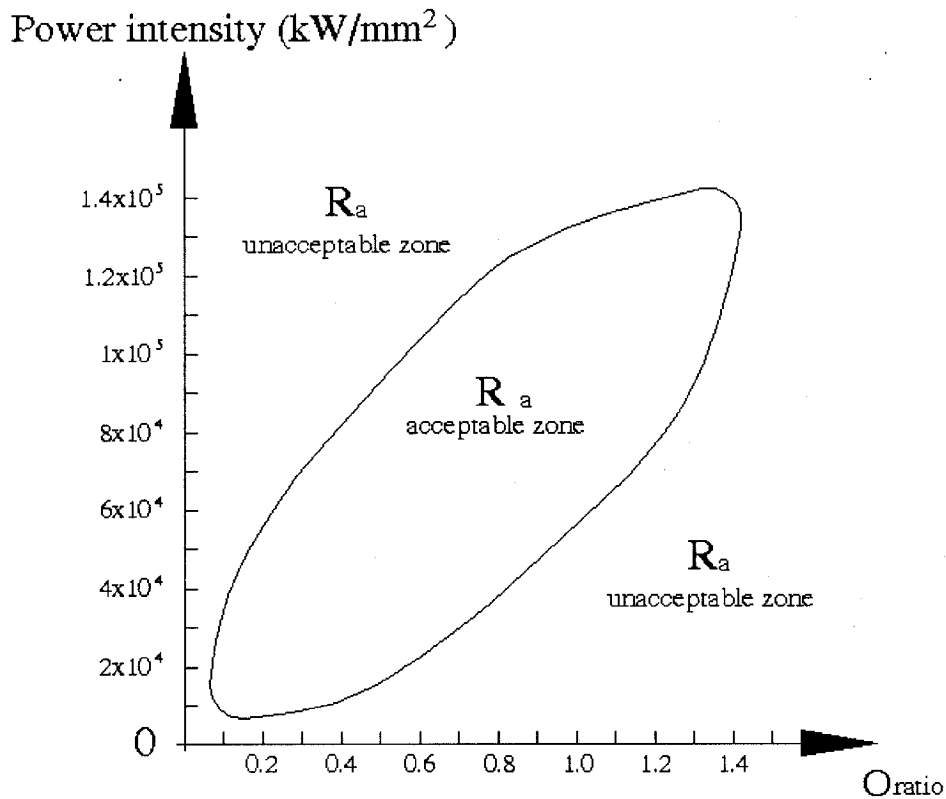


Figure 4.24 Diagram of I- O_{ratio} for cutting tool material X.

As shown in I- O_{ratio} chart, there are two zones for roughness. In Ra unacceptable zone, the obtained surface is not good because of too more local energy absorbed. Based on the information in Fig. 4.24, a lot of research could be done. Such as, optimal machining could be designed and investigated by using fuzzy logic method.

- 2) Big aperture laser beam is good for scanning surface. The roughness caused by small aperture laser beam is high than that caused by big aperture laser beam.
- 3) $V_{engraving}$ is the function of laser spot overlapping rate and laser spot diameter.

$$V_{engraving} = O_{ratio} \times f \times d.$$
 If $V_{engraving}$ is too small then laser spot overlaps too much, the local energy absorbed is too high to obtain a good surface. If $V_{engraving}$ is too big then laser spot distribute too discretely to get a good surface.
- 4) If X-Y working table and laser beam move at the same time, then the feed rate affect the surface quality through controlling laser trace overlapping rate.
- 5) The track distance should be as same as the space distance between two adjacent spots in engraving direction.
$$D \approx \frac{V_{engraving}}{f} \approx O_{ratio} \times d.$$
- 6) Different parameters combination has to be considered in order to make laser machining process not only be capable to remove material well but also be insensitive to material property, machine vibration, surface flatness tolerance, etc.
- 7) The optimum cutting can be obtained by having the minimum spot size below the surface. The thickness of machined layer is $2\mu\text{m}$ for DML 40SI laser machine.
- 8) For one material, different groups of laser beam parameters can be chosen to obtain a similar value. Using DML 40SI laser machine for example, for cemented carbide, $f=17\text{kHz}$, $O_{ratio\ x,y}=1$, $V_{engraving}=510\text{ mm/s}$, current=25%, trace distance=0.030mm, $30\mu\text{m}$ laser spot, cross and unidirectional hatching are an one of the acceptable choices.

CHAPTER 5 ANALYSIS OF LASER MACHINED MICRO-GEOMETRIES

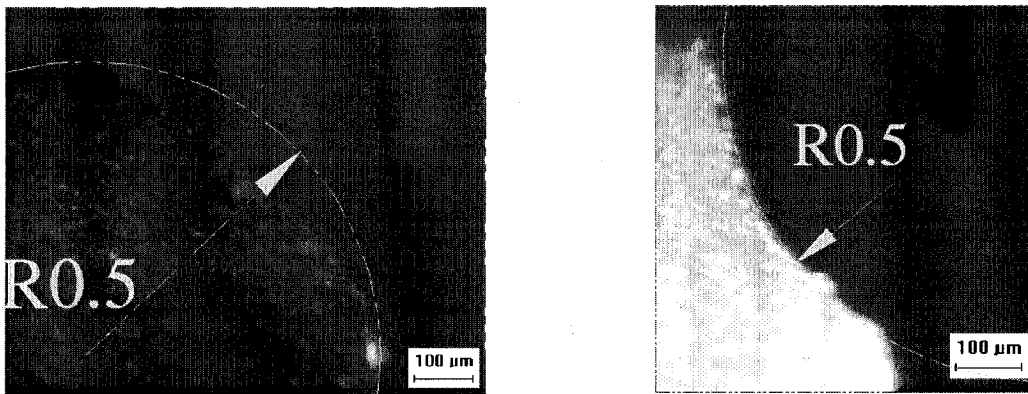
Different micro-geometries on cemented carbide inserts and a micro-mould of a micro drill for biomedical engineering were laser machining. The O_{ratio} was set at 0.49 while other machining parameters are shown in table 5.1.

Table 5.1 Laser beam parameters for machining of micro-geometry on cemented carbide inserts

Q-switch closing frequency (kHz)	Engraving speed (mm/s)	Current intensity	Machined layer thickness (μm)	Track distance (mm)	Aperture Mode (laser spot diameter (μm))	Hatching mode
17	250	25% I_{max}	0.002	0.015	Small (30)	Cross hatching and unidirectional

5.1 Machining of micro-geometries

1. Round cutting edge.



(a)

(b)

Figure 5.1 Round cutting edge machined by DML40SI laser machine, desired radius=0.5mm (a) positive cutting edge (b) negative cutting edge.

Fig. 5.1 shows the profile of machined round cutting edge R0.5mm. The hidden line is the designed profile. For positive cutting edge (Fig. 5.1 (a)), the curvature of cutting edge profile obtained is more like a chamfer. The maximum error is about 14%. When the radius of round cutting decreases, the obtained maximum error increases. It is because that the material is removed layer by layer. The profile of a laser machined round cutting edge is illustrated in Fig. 5.2. When the laser beam starts to ablate the lower layer, heat will still burn the previous layer leading to error. The steeper the surface, the less energy will be absorbed by the lower layer of material. This will lead to a lower material removal rate and the smoothness of the machined round surface decrease.

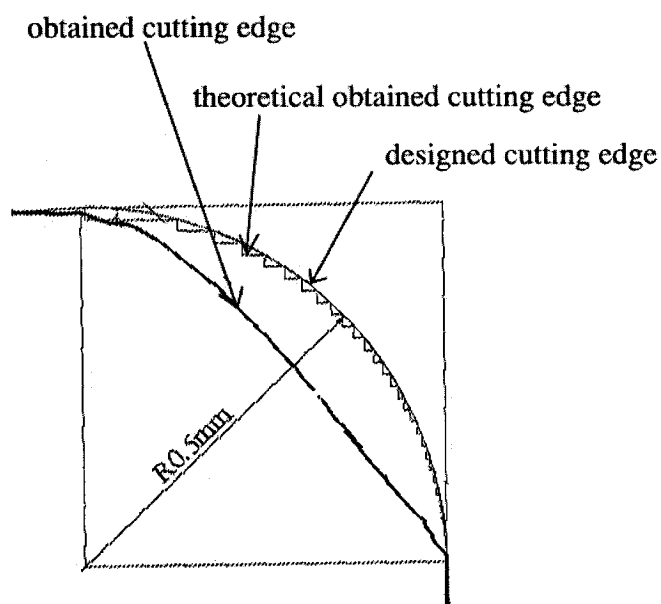


Figure 5.2 Comparison of laser machined cutting edge to desired cutting edge.

For negative cutting edge (Fig. 5.1(b)), the curvature of cutting edge profile obtained is more like a chamfer. The maximum error is about 1%. This phenomenon is related to optical measuring sensor system and laser side burning.

In order to make a more accurate round cutting edge, the following methods are suggested to use:

- 1) Use anti-vibration fixture to completely fix the carbide insert on X-Y working table.
- 2) Choosing precise calibrate equipment to make the cutting edge precisely position on X-Y working table.
- 3) Using higher engraving speed 400mm/s for DML 40 SI laser machine.
- 4) Choosing other more precise laser machine in market to do laser machining cutting tool material experiment.

2. Semi-circular profile groove

Fig 5.3 shows semi-circular micro groove R0.1mm where the hidden line is the desired profile. The maximum geometry error is $\sim 13\%$ located at the bottom of groove. The wider kerf obtained (i.e., $230\mu\text{m}$) is due to side burning as shown in Fig 5.4. The narrower the designed value, the more serious the side burning. The bottom profile is more like an ellipse can be explained as bad heat conduction in the bottom of the groove and accumulated heat makes the groove deeper.

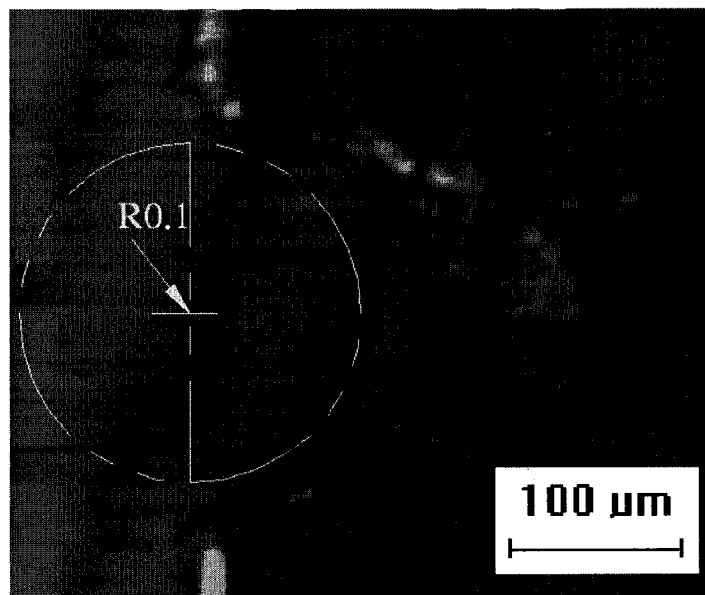


Figure 5.3 Semi-circular profile micro-groove laser machined using DML40SI machine. Desired radius=0.10mm.

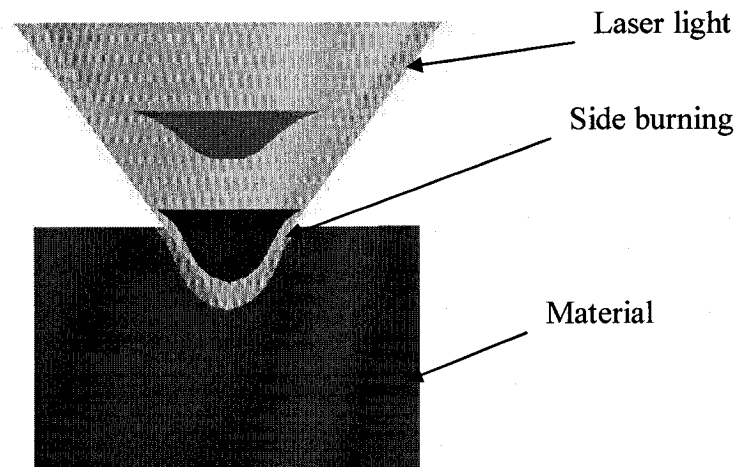


Figure 5.4 Schematic of side burning.

3. Rectangular profile groove.

During the laser machining of rectangular profile grooves, the critical parameter is the ratio of depth to width as shown in Fig. 5.5. If the ratio of depth to width is too big, the profile of groove is more like triangle as shown in Fig. 5.6.

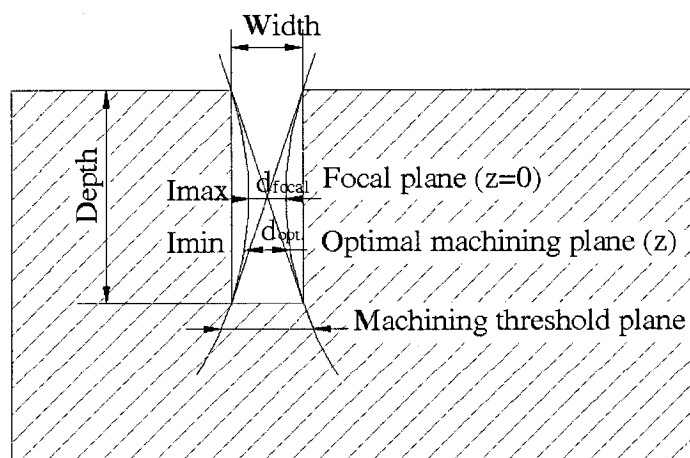


Figure 5.5 Relation of width and depth of machined microstructure.

Fig. 5.6 shows an optical microscope image of a machined rectangular groove where the desired width of 0.2mm and a depth of 0.75mm (ratio=3.75). The hidden line is the designed profile. The width of the rectangular groove is precisely laser machined with a error of 2%. The bottom profile is not satisfied. The profile of the groove is more like rectangle.

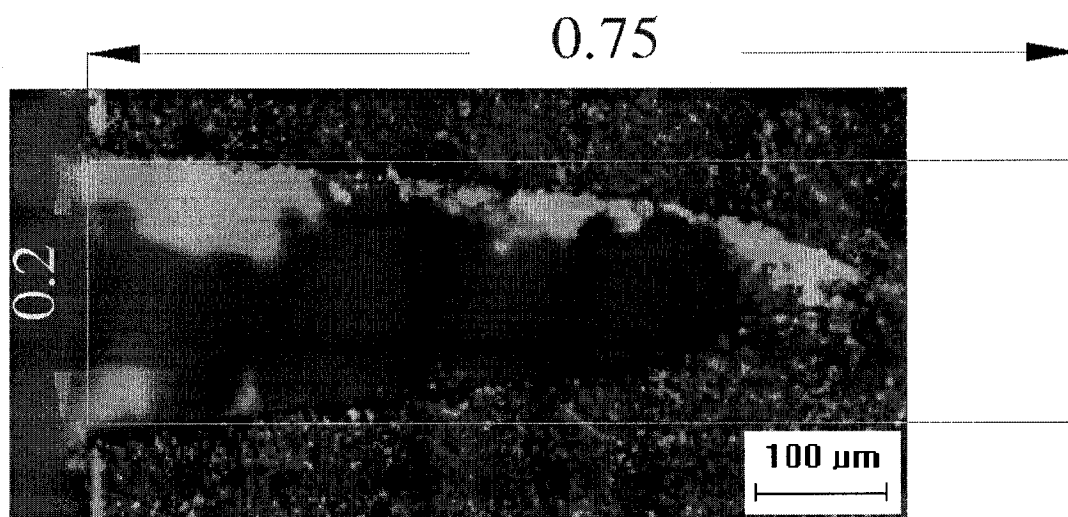


Figure 5.6 Rectangular micro grooves, desired width=0.2mm, desired depth=0.75mm.

For DML 40SI laser machine, the ratio of $\frac{depth}{width}$ is about $\frac{1}{2.5}$ for get a better rectangular groove.

4. Micro-cylindrical pocket

Fig. 5.7 shows an optical microscope image of a desired micro-cylindrical pocket where desired radius of 0.2mm and depth of 0.15mm are shown with the hidden line. The hidden line is the designed profile. Error is less than 1%. The top circular profile of micro pocket is done well and the geometry error is less than 1%. Accumulated heat at the bottom makes the bottom surface concave.

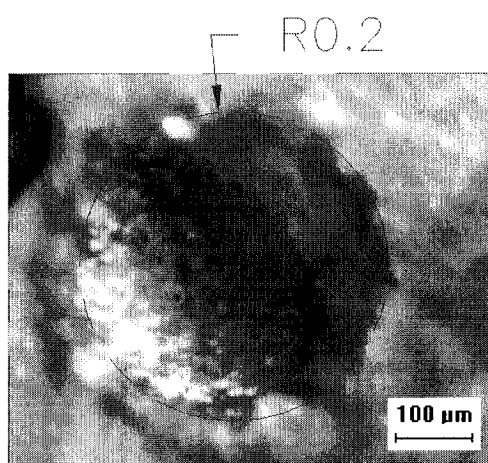


Figure 5.7 Micro-cylindrical pocket machined using DML40SI laser machine, desired radius=0.2mm, desired depth=0.3mm.

5. Square pocket:

Fig. 5.8 shows optical microscope image of a machined square pocket 1.0x1.0mm where the hidden line is the desired dimension. The hidden line is the designed profile. The geometry is precise with an error of less than 1.0%.

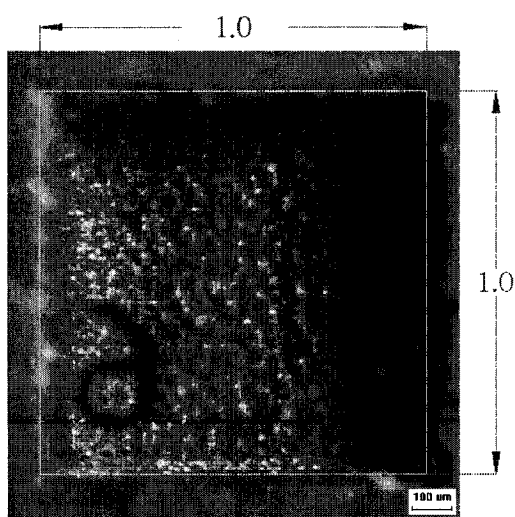


Figure 5.8 Micro square pocket machined by DML40SI laser machine, 1.0 x 1.0 mm, desired depth 0.5mm.

Fig. 5.9 shows 3D model of surface texture of the wall and bottom of the machined square pocket and the error of width caused by side burning.

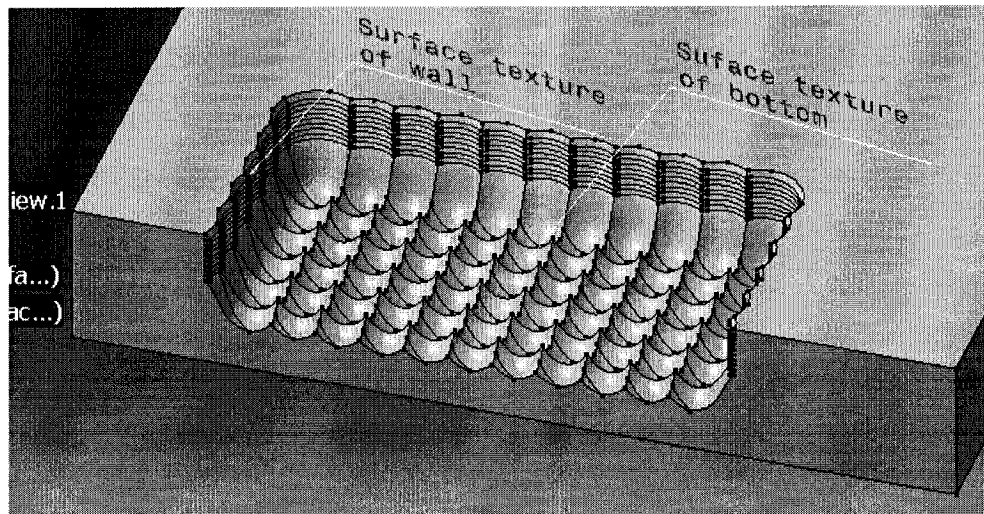


Figure 5.9 Schematic of surface texture of the wall and bottom of the machined square pocket.

6. Micro drill:

Fig. 5.10 shows a CAD drawing of a micro drill for biomedical applications. The head of the micro drill is a R0.45mm sphere and the drill body is a R0.4mm cylinder. This tool is so micro that is time costly to be processed by metal cutting method. Using mould technology, it can be made fast and in large quantity.

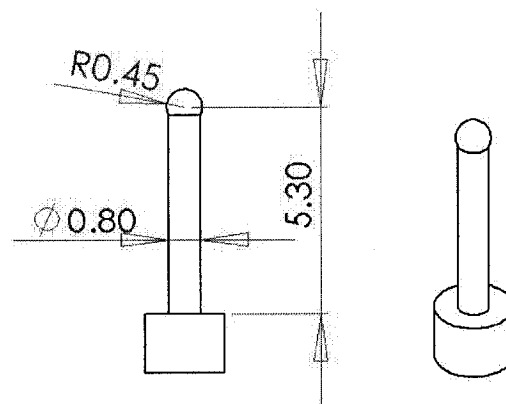


Figure 5.10 Micro drill CAD drawing.

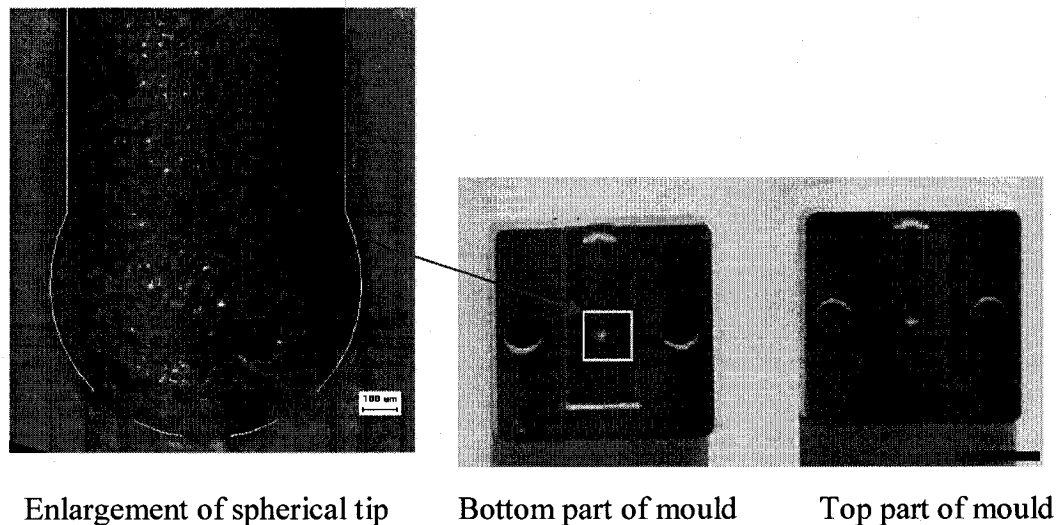


Figure 5.11 Laser machined mould for micro-drill fabrication.

In the Fig. 5.11, the drawn line is the desired profile which is matching well with the machined micro mould, error is less than 1%. The machined surface roughness is 2.615 due to used 0.5 O_{ratio} is too big for cemented carbide insert.

5.2 Conclusion

After observing the machined workpiece, following conclusions could be obtained:

1. Using laser technology to machine cutting-edge and other micro-geometry is a feasible method. DML40SI can be used to obtain make micro geometry when it is above.
2. Material property and micro geometry characteristic are important for the laser beam parameters determination. Due to sided burning, when the wanted geometry is a positive geometry, “-” dimension tolerance has to be used. When the wanted geometry is a negative geometry, “+” dimension tolerance has to be used.

3. In order to get better machining result, it is better to use different machining parameters for different local place in a workpiece through modifying CNC program.

CHAPTER 6 CONCLUSION AND RECOMMENDATIONS

Laser machining technology was explored to machine cutting tool. The driving factors this exploration is to introduce laser machining technology into cutting tool manufacturing field but also to solve the existing problem during using the traditional processing methods to manufacture cutting edge. DML 40 SI Q-switch laser machine, which is the first set laser machine bought by l'école Polytechnique de Montréal from Lasertec company, was used to manufacture experimental samples. Although this laser machine is still in running and adjustment period, machining experiment were still achieved satisfied due to the good experimental arrangement advised by my director Mr. Marek Balazinski and co-director Mr. Daniel Therriault and fixing the machine breakdown in time by Mr. Sylvain Simard. Through optical microscope observation and analysis, the conclusions and recommendations are given as following.

Using laser technology to machine micro-geometries on cemented carbide inserts is a feasible method. When the radius of cutting edge is larger than $100\mu\text{m}$ or the size of chamfer of the T land is larger than $100\mu\text{m}$, DML40SI laser machine can do the processing well. If other more precise laser machine were chosen, the smaller size and more precise dimension could be obtained. This technology not only could be used as new feasible processing method, but also it can be used as a new technology in laboratory. For example, the aim of researches on cutting edge or grooved chip beaker is to obtain better cutting result and not reduce the life of cutting tool at the same time. In order to obtain different cutting data, it is necessary to prepare a lot of inserts with different geometries. With the help laser machining technology, experimental efficiency could be increased and experimental cost could be decreased.

The machined surface quality depends on the assemble effects of lame current, aperture mode, Q-switch closing frequency, Q-switch opening time, engraving speed and track distance. Among these parameters, O_{ratio} and laser power intensity are the most important.

$$O_{ratio} = \frac{d_{center}}{d} \text{ (equation 4.1), } V_{engraving} = O_{ratio} \times f \times d \text{ (equation 4.3),}$$

$$D = \frac{V_{engraving}}{f-1} \text{ (equation 4.4), } D \approx \frac{V_{engraving}}{f} \approx O_{ratio} \times d \text{ (equation 4.5) are specially}$$

concluded as an important supplement for DML 40SI laser machine operation manual.

For the laser machining, laser beam parameters should be adjusted according to type of materials or structure of geometries. For cemented carbide work piece, geometry with flat surface, laser beam parameter can be chosen as $f=17\text{kHz}$, $V_{engraving}=510\text{mm/s}$, $\text{current} I=25\%I_{\text{max}}$, $\text{trace distance}=0.03\text{mm}$, $30\mu\text{m}$ laser spot, cross and unidirectional hatching.

I- O_{ratio} chart (as shown in Fig. 4.24) concept is concluded as an important researching method for investigating the effects of laser beam parameters on cutting tool materials. With the help of I- O_{ratio} chart, the research on roughness of machined surface and the research on effect of laser beam mode (i.e. Gaussian mode and Doughnut mode) can be done more easily than using other parameters, like laser spot diameter, engraving speed and track distance.

6.1 Recommendations

Human needs lead to the development of novel technology in order to improve the human's living and working condition are improved continuously. The following are some imaged perspective research of application of laser micro machining technology on cutting tool.

Laser technology can be used to prepare mill or drill tool. Fig. 6.1 shows DML 80 fine cutting technology, it can be used to cutting 3D model. With CNC program design, DML 40SI laser ablation technology can be used to prepare cutting edge or micro geometry on milling tool or drilling tool as shown in Fig. 6.2.

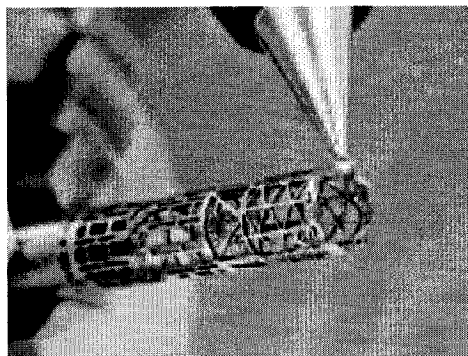


Figure 6.1 Laser 80 fine cutting technology. (Lasertec Company)

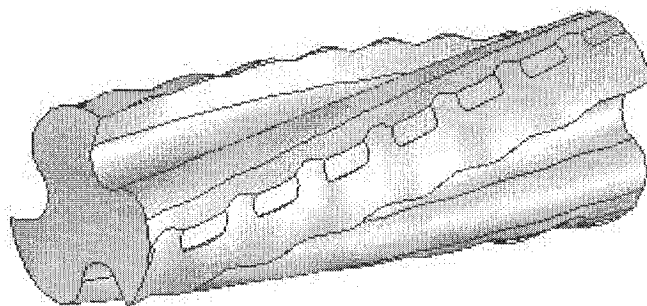


Figure 6.2 Illustration of 3D model of cutting edge machined by laser.

Cutting edge with variable radius. This design is established based on working life problem of the cutting insert. Figure 6.3 shows edge wear of insert. According to the position and size of edge wear, we can make an insert with variable radius or variable chamfer size of insert.

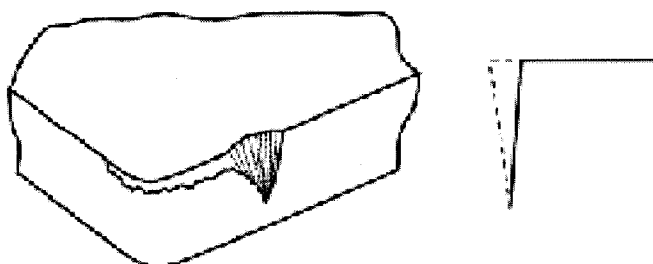


Figure 6.3 Illustration of edge wear of insert.(Balazinski M.)

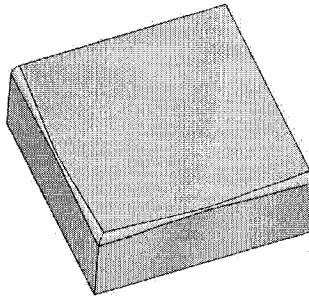


Figure 6.4 Illustration of insert of varying radius cutting edge.

Local strengthened-insert. This design is based on the crater wear of insert as shown in Fig. 6.5.

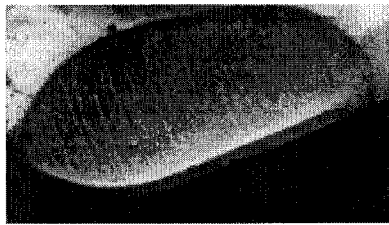


Figure 6.5 Example of crater wear of insert. (Balazinski M.)

It is possible to laser machine a pocket on the top surface of insert, using high-hardness to strengthen this specific location in order to increase the work life.

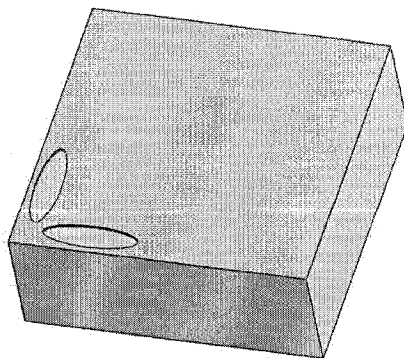


Figure 6.6 Example of local strengthened insert.

REFERENCE

- Abdelmoneim M.E.S., Scrutton, R.F., Tool edge roundness and stable build-up formation in finish machining. 1974. Trans. ASME 96, 1258~1267.
- Albrecht P., 1960, New developments in the theory of metal cutting process: Part I—the ploughing process in metal cutting. 1960. Trans. ASME, J. Eng. Ind.82, 348~357.
- Albrecht, P., 1960. New developments in the theory of metal cutting process: Part II—The theory of chip formation. Trans. ASME, J. Eng. Ind. 83, 557~568.
- Albrecht, P., 1965, Dynamics of the metal cutting process. Trans. ASME, J. Eng. Ind.87, 429-441.
- A.O. Schmidt, 1969, Tools and engineering materials with hard, wear-resistant infusion. Journal Eng. Ind. 91, 549-552.
- Arsecularatne J. A., Fowle R. F., 1998, Prediction of chip flow direction, cutting forces and surface roughness in finish turning, Journal of manufacturing science and engineering, Vol.120, 1~12.
- Atkins A. G., Tabor D., 1966, Proc. Roy. Soc. (A), 292.
- Backer, W.R, Marshall, E.R., Shaw, M.C., 1952. The size effect in metal cutting. Trans. ASME 74, 61~72.
- Balazinski M., Fabrication Mécanique Avancée version 1.0. École Polytechnique de Montréal.
- Balazinski M., 1993, Control of metal-cutting process using neural fuzzy controller. IEEE 1993, 161~166.
- Balazinski M., E. Czogala, S. Gravelle, 1995, Automatic tool selection using a fuzzy decision support system. IEEE 1995. 615~620.
- Basov N.G., Kroklin O.N. and Popov Y. M., 1961, Production of negative temperature state p-n junctions of degenerate semiconductors. *Sov. Phy. JETP* 13, 1961, 1320.

- Bube K.R., Miller A.Z., Howe A., Antoni B., 1979, Influence of laser-trim configuration on stability of small thick-film resistors, *Laser in modern industry*, Soc. of Mfg. Eng., Dearborn, MI, 1979, 245~250.
- Bouzakis K.-D., Michailidis N., Vidakis N., Efstathiou K., Leyendecker T., Erkens G., Wenke R., Fussal H.-G, 2000, Optimisation of the cutting edge radius of PVD coated inserts in milling considering film fatigue failure mechanisms. *Surface and Coating Technology* 133-134,2000, 501-507.
- Braga D.U., Diniz A. E., Miranda G.W.A., Coppini N.L., Using a minimum quantity of lubricant (MQL) and a diamond coated tool in the drilling of aluminum-silicon alloys, *Journal of materials processing technology*, 2002, 122/1, 127~138.
- Brinksmeier E., Walter A., Janssen R., Diersen P., Aspects of cooling lubrication reduction in machining advanced materials, *Proceedings of the institution of mechanical engineers*, 1999, 2/3 part B, 769~778.
- Buljan S. T., Sarin V. K., 1981, Machining performance of ceramic tools, *American Society for Metals, Metals Park, Ohio 44073, Cutting tool materials*, 335~348.
- Carlsaw H. S., Jaeger J. C., 1959, *conduction of heat in solids*, 2nd edition, Oxford U. P., New York.
- Choi J.P., Lee S. J., 2001, Efficient chip breaker design by predicting the chip breaking performance, *International Journal of Advanced Manufacturing Technology*, Vol.17, 489~497.
- Cline H.E., T.R. Anthony, 1977, Heat treating and melting with a scanning laser or electron beam, *Journal of Applied Physics*, Vol. 48. 3895~ 3900.
- Chryssolouris George, 1991, *laser machining: theory and practice*, Springer-Verlag, Newyork.
- Doi, S., Kato, S., 1956. Chatter vibration of lathe tools. *Trans. ASME* 78, 1127~1134.
- Draper C. W., 1982, Laser surface alloying: The state of the art.. *Journal of Metals*, June 24-32.
- Ernst H., Merchant M.E.,1941, Chip formation, friction and high quality machined surfaces, *Trans. of A.S.M. , Surface Treatment of metals*, 335~336.

- Ewing J.J, Brau C.A., 1974, Laser action on the bands of KrF and XeCl, *Appl. Phys. Lett.* 27, 1975, 350.
- Fang N., 2003. Slip-line modeling of machining with a rounded-edge tool—Part I : new model and theory. *J. Mech. Phys. Solids.* 715~742.
- Fang N., 2003. Slip-line modeling of machining with a rounded-edge tool—Part II : analysis of the size effect and the shear strain-rate. *J. Mech. Phys. Solids.* 743~762.
- Fei J., Jawahir I.S.. A Fuzzy Classification Technique for predictive assessment of chip breakability for use in intelligent machining. 2nd IEEE Int. Conf. on Fuzzy Systems, March, 1993.
- Geusic J.E., Marcos H.M. and Van Uitert L.G., 1964, Laser oscillation in Nd. Doped yttrium aluminium, yttrium gallium and gadolinium garnets, *Appl. Phys. Lett.* 4, 1964,182.
- Gitin M., 1996, Diode pumped lasers in nick of time, *Photonics Spectra*, 122.
- Gunter K.L., Sutherland J.W., An experimental investigation into the effect of process conditions on the mass concentration of cutting fluid mist in turning, *journal of cleaner production*, 1999, 7/5, 341~350.
- Hall R.N., Fenner G. E., Kingsley J. D., Soltys T.J., Carlson R.O., 1962, Coherent light emission from GaAs junctions. *Phys. Rev. Lett.* 9 (1962) 366.
- Hands D.M., Sheehan J., Wong B., Lick H.B., Comparison of metalworking fluid mist exposures from machining with different levels of machine enclosure, *American Industrial Hygiene Association Journal*, 1996 ,57/12, 173~178.
- Henriksen E. K., 1954, Balanced design will fit the chip breaker to the job, *American Machinist*, 98(4), 118~124.
- Henriksen E. K., 1955, Findings and directions in chip breaker research, *Proc. 23rd Ann. Mtg. Of ASTE*, los Angeles, California.
- Hess P., 1993, New insights into laser induced polymer ablation. *Lambda Highlights* 42.
- H.S. Rajasekhara and P.A. Molin, 1985, Development of hard cutting tool edges by laser processing. *Transaction of NAMRI/SME*, 386-393.

Hsu M. J. and Molian P., 1989, Machining characteristics of laser tungsten surface-alloyed M2 high speed steel.. *Wear*, 132, 123-137.

ISO 3685 1993 Tool life testing with single – point tools.

ISO 4957 1980 Tool steel.

Jawahir I.S. , An investigation of three-dimensional chip flow in machining of steels with grooved chip forming toolinserts, *Trans. NAMRI/SME* ,1991, 222~231.

Jawahir I.S., Fei J. A comprehensive evaluation of tool insert for chip control using fuzzy modeling of machinability parameters. *Trans. NAMRI/SME Vol.21* 1993, 205~213.

Joseph ElGomayel, Joseph Gamini Pinto, March, 1977, *Symp. Soc. Carbide and Tool Engg.*, 218~225.

John F. R., 1971, *Effects of high-power laser radiation*, Academic Press, New york, London.

Johan Meijer, 2002, laser micromachining, *Micromachining of engineering maerials*, edited by Joseph McGeough, Marcel Dekker, Inc.

Kaplan A.F.H., 1998, *Laser marking. Handbook of Eurolaser Academy*, Vol. 2, ed D. Shuöcker. Chapman and Hall.

Kaldor S., Ber A., lenz E., 1979, *On the mechanism of chip Breaking*, ASME, 1979, Vol. 101,241~249.

K.-D Bouzakis, N. Michailidis, S. Hadjiyiannis, K. Efstathiou, E. Pavlidou, G. Eekens, S. Rambadt, I. Wirth, 2001, Improvement of PVD coated inserts cutting performance, through appropriate mechanical treatments of substrate and coating surface. *Surface and coating technology*, 146-147, 443-450.

K.-D Bouzakis, N. Michailidis, G. Skordaris, S. Kombogiannis, S. Hadjiyiannis, K. Efstathiou, E. Pavlidou, G. Erkens, S. Rambadt, I. Wirth, 2003, Optimisation of the cutting edge roundness and its manufacturing procedures of cemented carbide inserts, to improve their milling performance after a PVD coating deposition, *Surface and coatings technology*, 163-164, 625-630.

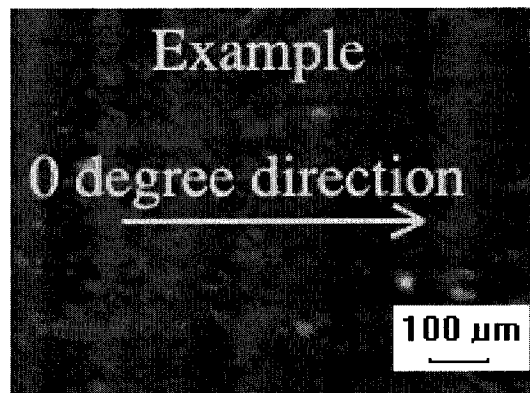
- Kim K.W., Sin H.C., 1996, Development of a thermo-viscoplastic cutting model using finite element method. *Int. J. Machine Tools manufacture*. 1996, Vol. 36,379~397.
- Kim T. H., Seong B. G., Titanium nitride laser-beam surface-alloying treatment on carbon tool steel, 1990, *Journal of Materials Science*, Vol.25, 3583~3591.
- Kim Y. W., Strutt P. R., Nowotny H., 1979, Laser melting and heat treatment of M2 tool steel: a microstructural characterization, *Metallurgical Transactions A.*, 881~886.
- Klopstock H., 1925, Recent investigation in turning and planning a new form of cutting tool. *Trans. ASME* Vol. 47, 345~377.
- Lasers : Operation, Equipment, Application and Design*, by the staff of Coherent, Inc. (New York: McGraw-Hill, 1980).
- Lee, E.H., Shaffer, B.W., 1951. The theory of plasticity applied to a problem of machining. *Trans. ASME* 73, 405~413.
- Lueth R.C., 1974, *Fracture Mechanics of Ceramics*, R.C. Bradt *et al.*, Ed., Plenum Press, p 791-806.
- Machado A.R., Wallbank J., The effect of extremely low lubricant volumes in machining, 1997, *Wear*, 210, 76~82.
- Machinability Data Handbook*, Metcut Research Associates Inc., Cincinnati Ohio, 1980.
- Machinery Handbook* . Edition 26th.
- Maiman T. H., 1960, Stimulated optical radiation in ruby. *Nature* 6 August.
- Manjunathaih, J., Endres, W.J., 2000. A new model and analysis of orthogonal machining with an edge-radiused tool. *Trans. ASME, Journal Manuf. Sci. Eng.* 122, 384~390.
- Mayer, Jr., J. E., and Stauffer, D. J., Effects of tool edge hone and chamfer on wear life. *Manufacturing Engineering Transactions (SME)*, Vol. 3, 1974, 5-15.
- Mazumder J., 1983, Laser welding, *Laser Material Processing*, ed M. Bass, North-Holland, Amsterdam, 1983, ch. 3, 113~ 200.
- Mckenna P.M., Tool Materials—Cemented Carbides, in *Powder Metallurgy*, J. Wulff, Ed., 1942, 454~469.

- Merchant, M.E., 1944. Basic mechanics of the metal cutting process. Trans. ASME66, A168~A175.
- Milton C. Shaw, 1984, Metal Cutting Principles. Oxford Science Publications.
- Milton C. Shaw, 2005, Metal Cutting Principles. Second edition. Oxford Science Publications.
- Miyazawa H., Takeuchi S., Miyake S., Murakawa M., 1996, Sintered diamond cutting inserts with chip breaker prepared by laser technique, Surface and Coating technology Vol.86~87, 797~802.
- Miyoshi A., Hara A. J., 1965, J. Japan Soc. Powder and Power Met., Vol. 12, 78.
- Moissan H., The Electrical Furnance, V. Lenher, Trans., Chemical Publishing Company, 1904.
- Nakayama K., A study on chip-breaker, Bull. JSME ,1962, Vol.5, No.17,142~150.
- Nakayama, K. , Tamura, K.,1968, Size effect in metal cutting force. 1968. Trans. ASME, J. Eng. Ind. 90, 119~126.
- Nakayama K., 2004, Chip form Geometry, Journal of JSPE, 38, 592~598.
- Nakayama K., Arai M., Comprehensive chip form classification based on the cutting mechanism, 1992, Ann. CIRP Vol.41, 71~74.
- Nathan M.I., William P. Dumke, Gerald Burns, Fredrick H. Dill Jr., Gordon Lasher, 1962, Stimulated emission of radiation from GaAs p-n junctions, *Appl. Phys. Lett.* 1, (1962), 62.
- Oxley, P.L.B., 1989, The Mechanics of Machining, Halsted Press. A strain hardening solution for the 'shear angle' in orthogonal metal cutting. Int. J. Mech. Sci., Pergamon Press, Vol. 3, 68-79.
- Patel C.K.N., 1964, Continuous wave laser action on vibrational-rotational transitions of CO₂ *Phy. Rev. A* 136 (1964), 1187.
- Porat R., Ber A., 1990, New approach of cutting tool materials-Cermets, Ann. of CIRP, Vol.39.
- Quist T. M., Rediker R.H., Keyes R.J., Krag W. E., Lax B., McWhorter A.L., Zeigler H.J., 1962, Semiconductor maser of GaAs, *Appl. Phys. Lett.* 1, 91.

- Rahman M., Kumar A. S., Salam M.U., Experimental evaluation on the effect of minimal quantities of lubricant in milling, *Int. J. of machine tools and manufacture*, 2002, 42/5, 539~547.
- Rajasekhara H. S., Molian P. A., 1985, Development of hard cutting tool edges by laser processing, *Trans. of NAMRI/SME*, 386~393.
- Roy J. Schimmel, Jairam Manjunathaiah, William J. Endres, 2000, Edge Radius Variability and Force Measurement Considerations. *Trans. ASME, J. Manuf. Sci. Eng.* 2000, 122, 590~593.
- Schnerwitz, G., Z, 1932, Messung von Schneidenkrümmungs-radien.. für Instrumentenkunde, 52 Jahrgang, Erstes Heft, 1932, p. 1.
- Schroeter K., U.S. Patent 1,549,615, 1925.
- Seaman F.D., 1977, Role of shielding gas in high power CO₂ CW laser welding, *SME Tech Paper no. MR77-982*, Society of manufacturing engineering, Dearborn, MI, 1977.
- Shehata G.H. and Molin P.A., 1991, Cutting performance of a Nd/YAG Laser Alloyed Carbon Tool Steel With Ti/BN. *Transaction of NAMRI/SME*, 170-176.
- Shehata G. H., Moussa A. M. A., Molian P. A., 1993, Nd:YAG laser alloying of high-speed steel tools with BN and Ti/BN and the effects on turning performance, *Wear*, Vol.170, 199~210.
- Shinozuka J., Obikawa T., Shirakashi T., 1996, Chip breaking Analysis from the viewpoint of the optimum cutting tool geometry design, *Journal of Materials Processing Technology*, Vol.62, 345~351.
- Singh J., 1995, Laser beam and photon-assisted processes for surface treatments. *Materials and Processes for Surface and Interface Engineering*. 1995, 347~406.
- Smart R.F., 1982, Performance of tool materials: the user's view. *Towards Improved Performance of Tool Materials*. The Metals Society London, 1982.
- SME Technical Papers*, Review on Hard Turning and CBN Cutting Tool, *Proceeding of the 1st International Machining and Grinding Conference*, MR95-214, 951-962.

- Sokolnikoff I.S., Redheffer R. M., Mathematics of physics and modern engineering, McGraw-Hill, New York, 1958).
- Spaans C., Van Geel P. F. H. J., 1969, Break mechanism in cutting with a chipbreaker, Ann CIRP Vol. 18,87~92.
- Steen W.M., 2003, Laser Material Processing, third edition, Springer-Verlag London Limited 2003.
- Sven Ekemar, 1977, Coated Indexable Cemented Carbide Inserts—A Development in Progress, presented at SME's Westec'77 Conference, March 1977.
- Thiele, J.D., Melkote, S.N., Peascoe, R.A., Watkins, T.R., 2000, Effect of cutting-edge geometry and workpiece hardness on surface residual stresses in finish hard turning of AISI 52100 steel. 2000. Trans. ASME, J. Manuf. Sci. Eng. 122, 642~649.
- Tönshoff H. K., Wobker H.-G., Brunner G., 1995, CBN grinding with small wheels, Ann. of CIRP, Vol.44, 311~316.
- Trent E. M., 1959, I.P.E.J, vol. 38, 105.
- Trent E.M., 1984, Metal cutting, second edition, Butterworths
- Um J. Y., Chow L.C., Jawahir I.S., Experimental investigation of the application of the spray cooling method in stainless steel machining, ASME, Manufacturing Engineering Division, MED, Manufacturing Science and Engineering, 1995, 2/1, 165~178.
- Wakabayashi T., Sato H., Inasaki I., Turning using extremely small amount of cutting fluids, JSME, 1998, SeriesC, 41/1, 143~148.
- Wilgoss R.A., Megaw J.H.P.C. , Clarke j. N., 1979, Assessing the laser for power plant welding, Weld Met. Fabr., March, 1979, 117.
- Willam J. Endres. 2002. The effect of corner radius and edge radius on tool flank wear. Journal of Manufacturing Processes. V4. 89-96.
- William R Pfouts,2000, Cutting edge coating. Manufacturing Engineering. July, 2000; 125,1; Wilson Applied Science & Technoloy Abstracts, Page 98.

APPENDIX A: PHOTOS AND EXPERIMENTAL RESULTS OF MACHINED SURFACE FOR EXPERIMENTS DISCUSSED IN CHAPTER 4



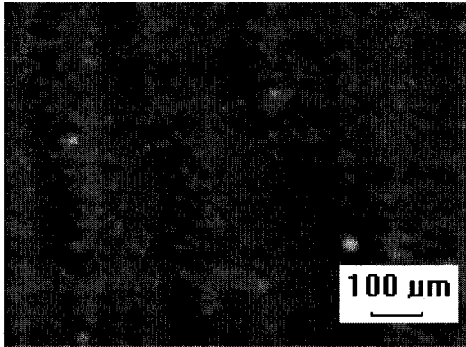
0° direction is roughness measuring direction.

1. Experiment 1

Table Appendix A.1 Experiment parameters to investigate *Q-switch closing frequency*. (Small laser spot)

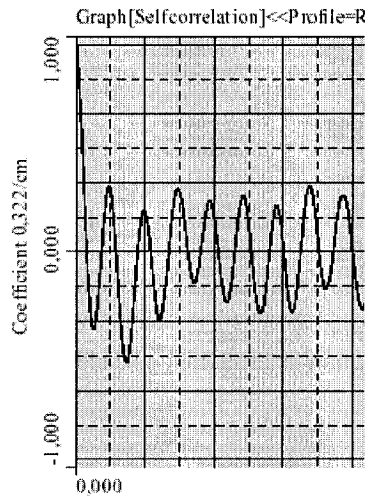
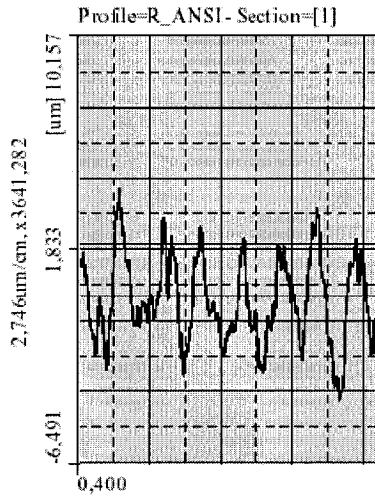
Parameter studied	Independent variable		Experiment parameters constant				Hatching Mode
	Q-switch closing frequency (kHz)	$O_{ratio(x, y)}=0.33$ Engraving speed (mm/s)	Current intensity	Machined layer thickness (μm)	Track distance (mm)	Aperture Mode (Spot diameter μm)	
Q-switch closing frequency	4	40	25% Max	0.002	0.01	Small (30)	Cross and unidirectional
	15	150					
	25	250					
	30	300					
	40	400					
	50	500					

Sample a1

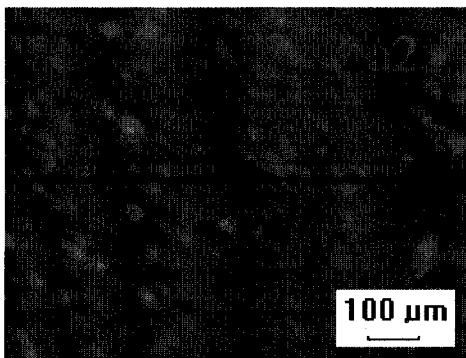


Parameter SumTable

	Profile=R_ANSI - Section=[1]	Average Value
Ra (um)	1,979	1,979
Rmax (um)	15,193	15,193
Rz (um)	11,940	11,940
Rt (um)	15,856	15,856

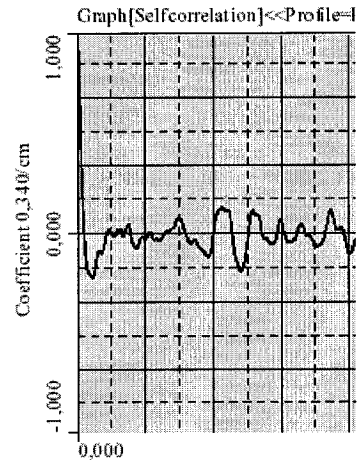
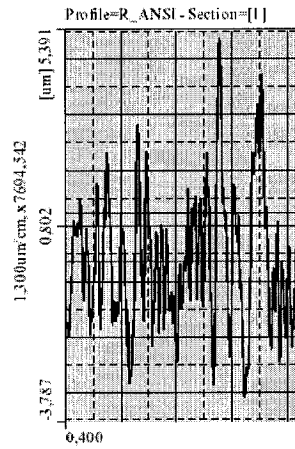


Sample a2

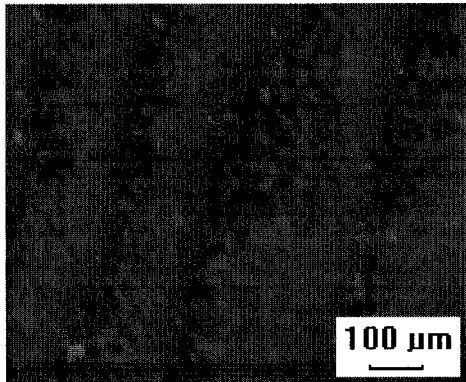


Parameter SumTable

	Profile=R_ANSI - Section=[1]	Average Value
Ra (um)	1,126	1,126
Rmax (um)	8,349	8,349
Rz (um)	7,348	7,348
Rt (um)	8,741	8,741

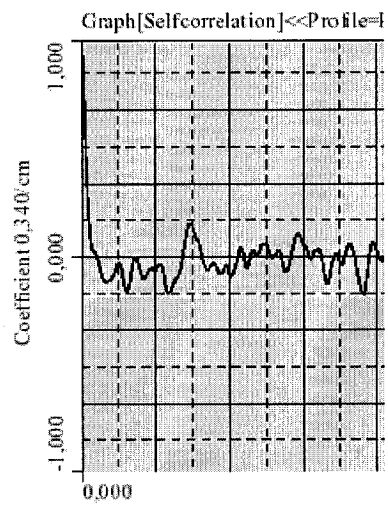
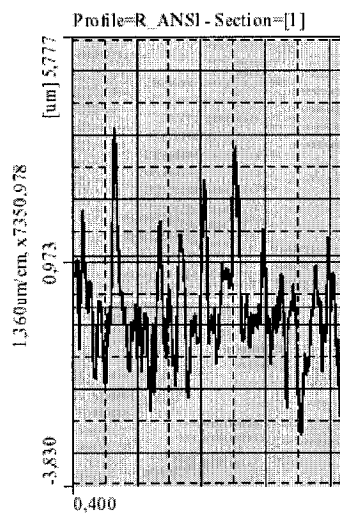


Sample a3

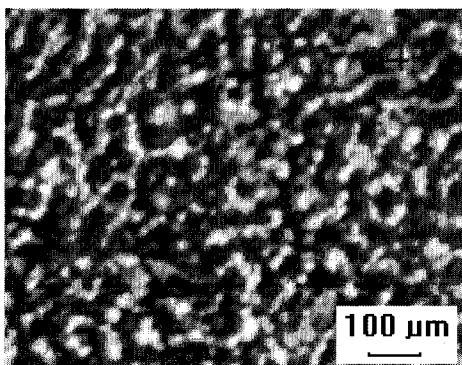


Parameter Sum Table

	Profile=R_ANSI - Section=[1]	Average Value
Ra (um)	1,094	1,094
Rmax (um)	9,060	9,060
Rz (um)	7,732	7,732
Rt (um)	9,150	9,150

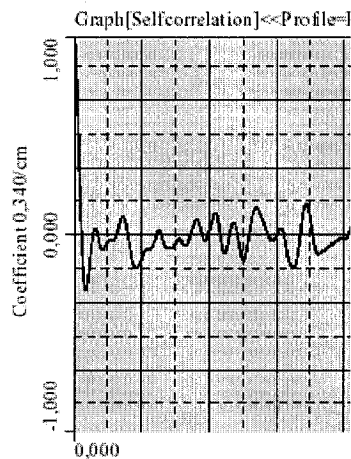
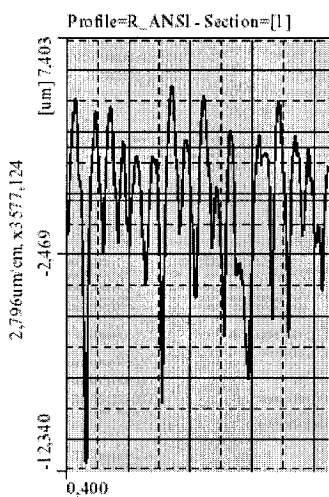


Sample a4

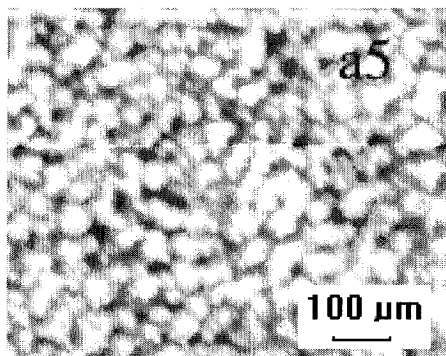


Parameter Sum Table

	Profile=R_ANSI - Section=[1]	Average Value
Ra (um)	2,394	2,394
Rmax (um)	17,078	17,078
Rz (um)	16,369	16,369
Rt (um)	18,802	18,802

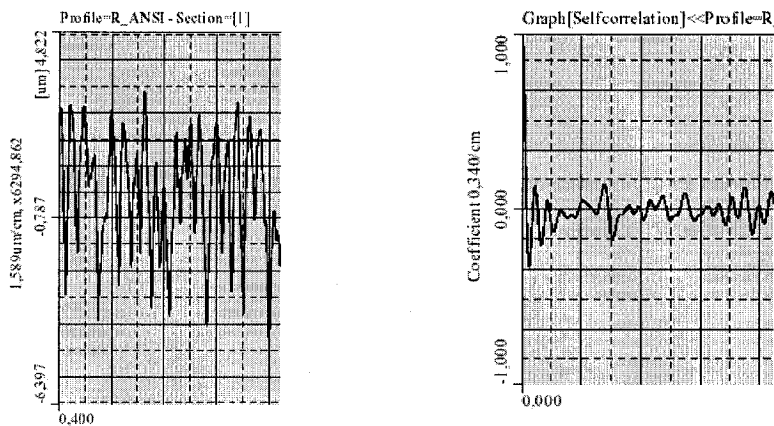


Sample a5

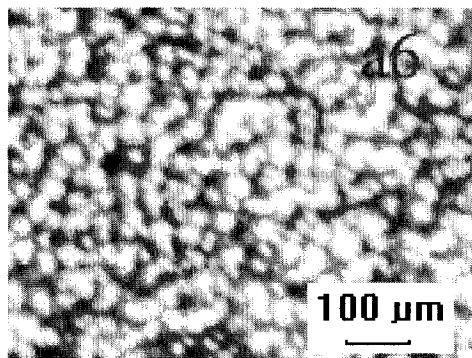


Parameter Sum Table

	Profile=R_ANSI - Section=[1]	Average Value
Ra (um)	1,512	1,512
Rmax (um)	10,660	10,660
Rz (um)	9,434	9,434
Rt (um)	10,685	10,685



Sample a6



Parameter Sum Table

	Profile=R_ANSI - Section=[1]	Average Value
Ra (um)	1,120	1,120
Rmax (um)	7,500	7,500
Rz (um)	6,597	6,597
Rt (um)	7,722	7,722

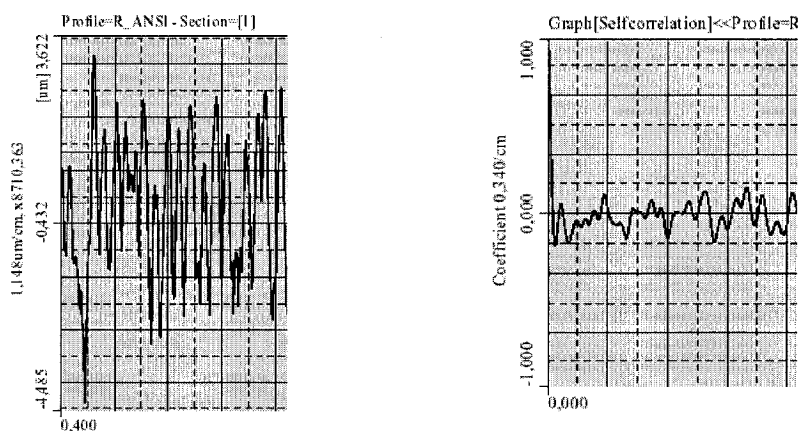


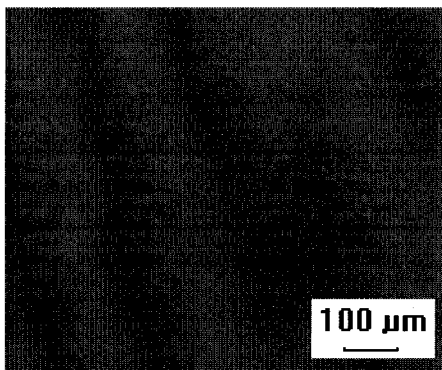
Figure APP.A-1 Microscope photos of test for verifying *Q-switch closing frequency*. (Small laser spot). a1: 4kHz; a2: 15kHz; a3: 25kHz; a4: 30kHz; a5: 40kHz; a6: 50kHz.

2. Experiment 2

Table Appendix A.2 Experiment parameters of test for verifying *Q-switch closing frequency*. *Q-switch closing frequency*. (Big laser spot)

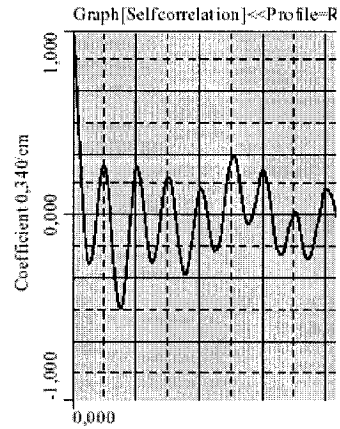
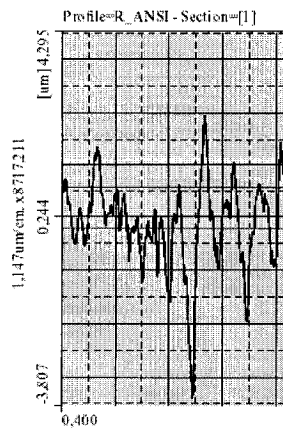
Parameter studied	Experiment parameters						Hatching Mode
	Independent variable		Current intensity	Machined layer thickness (μm)	constant		
	Q-switch closing frequency (kHz)	$O_{ratio(x)}=0.33$ $O_{ratio(y)}=0.125$ Engraving speed mm/s					Track distance (mm)
Q-switch closing frequency	4	40	25% Max	0.002	0.01	Big (80)	Cross and unidirectional
	15	150					
	25	250					
	30	300					
	40	400					
	50	500					

Sample A1

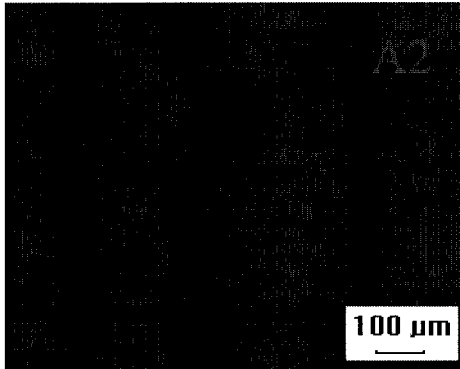


Parameter SumTable

	Profile=R_ANSI - Section=[1]	Average Value
Ra (um)	0,874	0,874
Rmax (um)	6,349	6,349
Rz (um)	5,875	5,875
Rt (um)	7,716	7,716

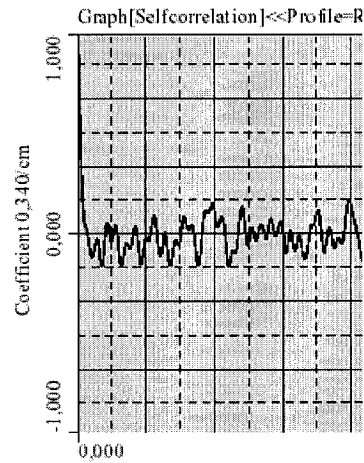
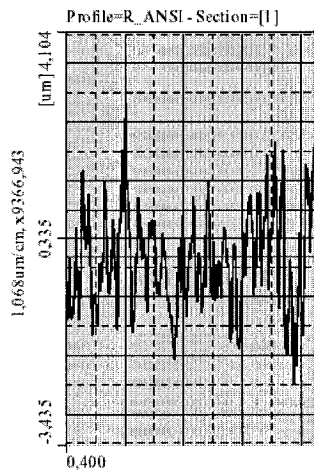


Sample A2



Parameter Sum Table

	Profile=R_ANSI - Section=[1]	Average Value
Ra (um)	0,866	0,866
Rmax (um)	6,528	6,528
Rz (um)	5,692	5,692
Rt (um)	7,180	7,180

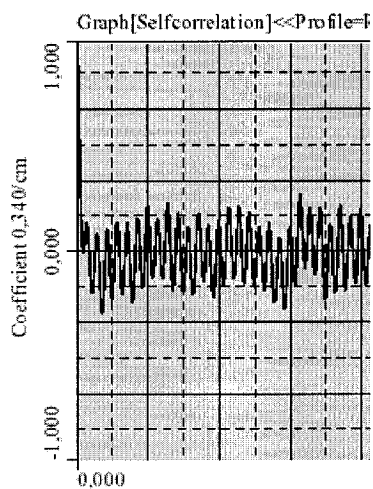
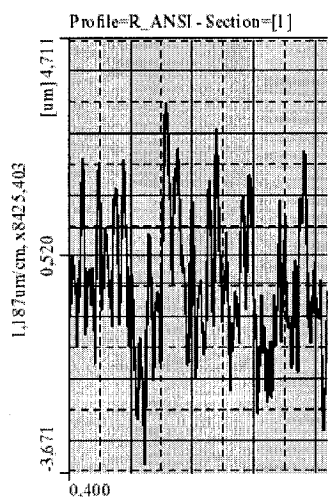


Sample A3

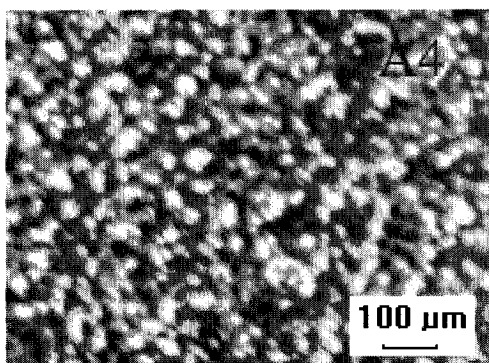


Parameter Sum Table

	Profile=R_ANSI - Section=[1]	Average Value
Ra (um)	1,089	1,089
Rmax (um)	7,377	7,377
Rz (um)	6,883	6,883
Rt (um)	7,983	7,983

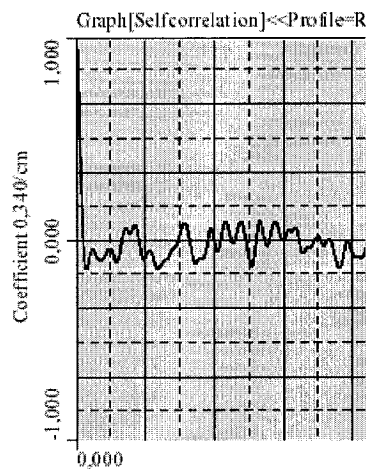
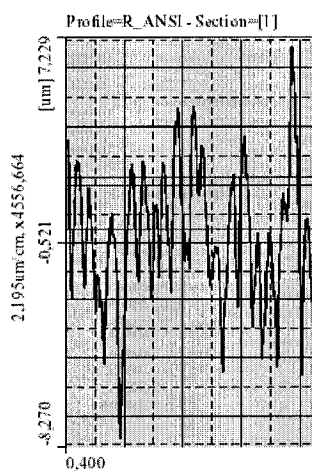


Sample A4

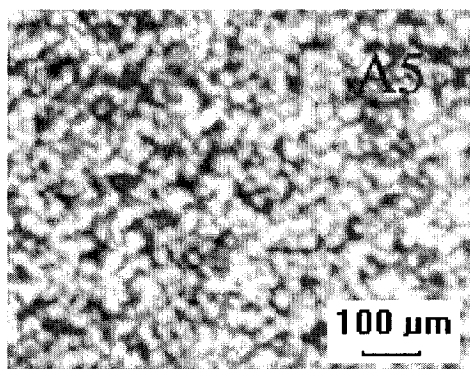


Parameter SumTable

	Profile=R_ANSI - Section=[1]	Average Value
Ra (um)	1,946	1,946
Rmax (um)	14,760	14,760
Rz (um)	11,902	11,902
Rt (um)	14,760	14,760

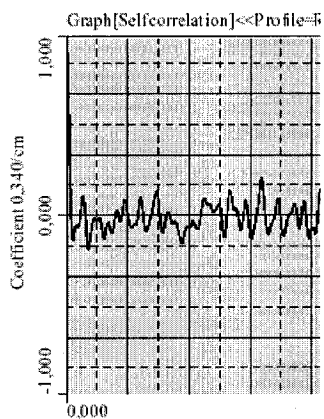
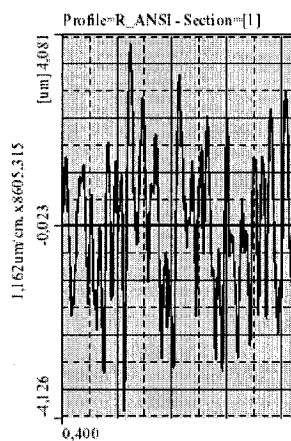


Sample A5

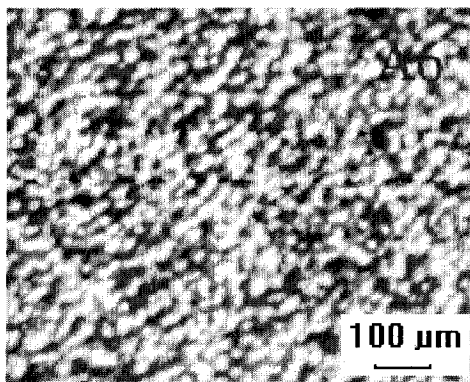


Parameter SumTable

	Profile=R_ANSI - Section=[1]	Average Value
Ra (um)	1,144	1,144
Rmax (um)	7,816	7,816
Rz (um)	6,802	6,802
Rt (um)	7,816	7,816



Sample A6



Parameter SumTable

	Profile=R_ANSI - Section=[1]	Average Value
Ra (um)	0,747	0,747
Rmax (um)	6,043	6,043
Rz (um)	4,993	4,993
Rt (um)	6,345	6,345

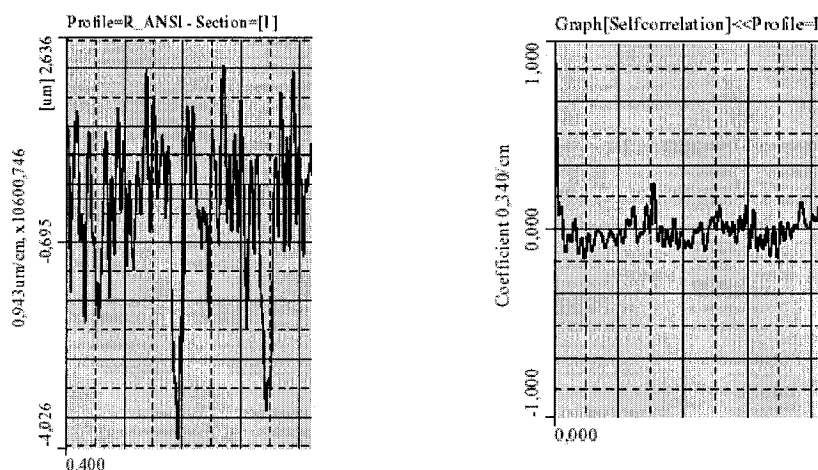


Figure APP.A-2 Microscope photos of test for verifying *Q-switch closing frequency*. (Big laser spot). A1: 4kHz; A2: 15kHz; A3: 25kHz; A4: 30kHz; A5: 40kHz; A6: 50kHz.

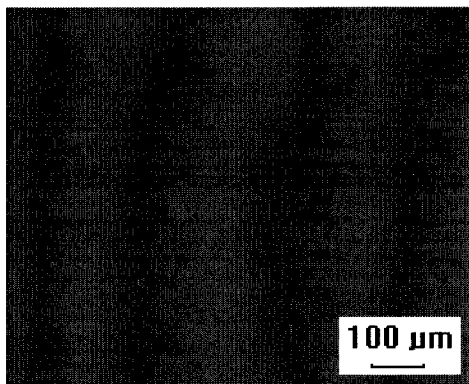
3. Experiment 3

Table Appendix A.3 Experiment parameters of test for verifying *engraving speed*.

(Small laser spot)

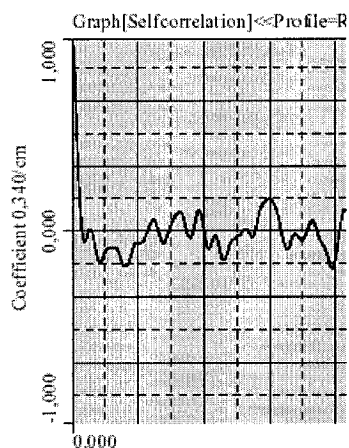
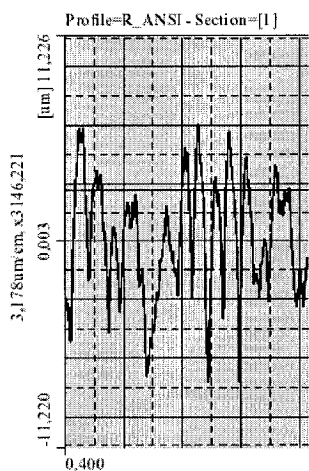
Parameter studied	Experiment parameters							
	Independent variable				constant			
Q-switch closing frequency (kHz)	$O_{ratio(x)}$	$O_{ratio(y)}$	Engraving speed (mm/s)	Current intensity	Machined layer thickness (μm)	Track distance (mm)	Aperture Mode (Spot diameter μm)	
Engraving speed	30	0.2	0.33	180	25% Max	0.002	0.01	Small (30)
	30	0.25	0.33	225				
	30	0.33	0.33	300				
	30	0.5	0.33	450				
	30	1	0.33	900				
	30	1.5	0.33	1350				
								Cross hatching and unidirectional

Sample b1

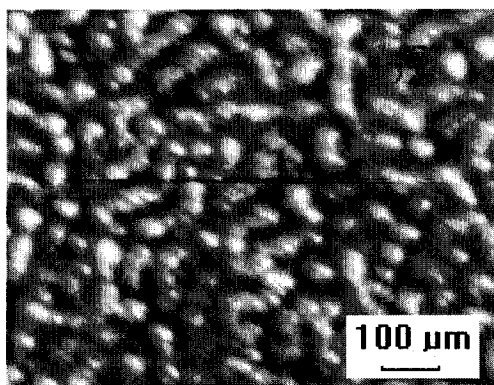


Parameter SumTable

	Profile=R_ANSI - Section=[1]	Average Value
Ra (um)	2,737	2,737
Rmax (um)	19,036	19,036
Rz (um)	16,664	16,664
Rt (um)	21,377	21,377

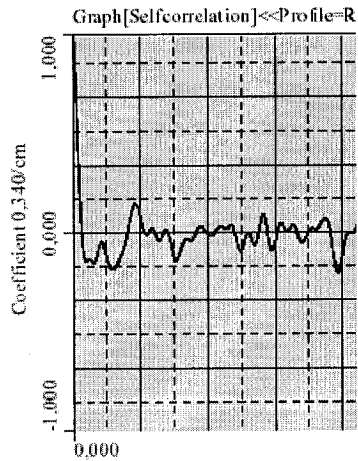
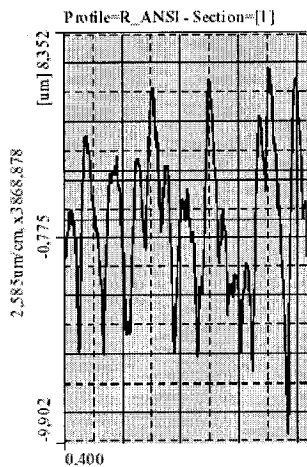


Sample b2

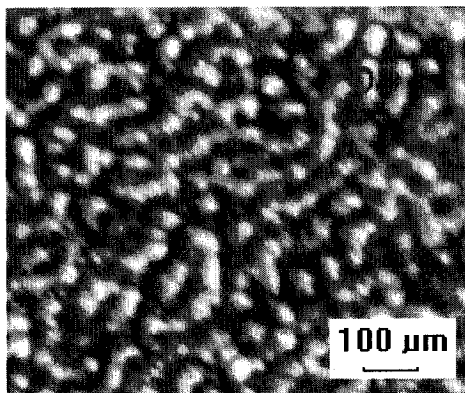


Parameter SumTable

	Profile=R_ANSI - Section=[1]	Average Value
Ra (um)	2,209	2,209
Rmax (um)	16,273	16,273
Rz (um)	13,202	13,202
Rt (um)	17,384	17,384

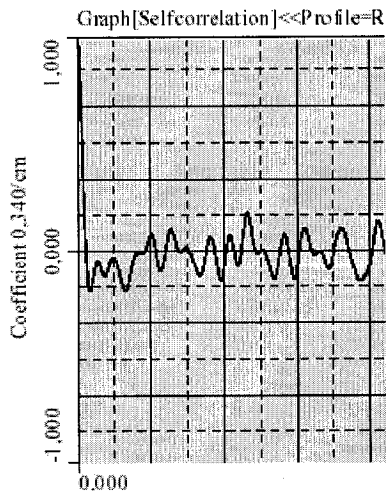
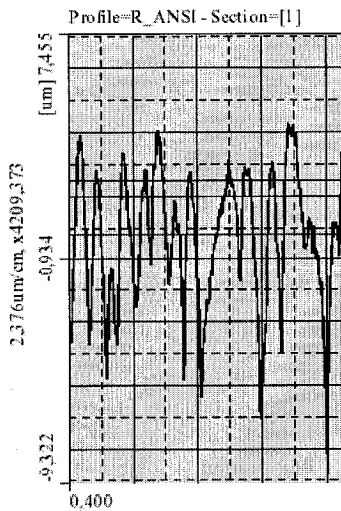


Sample b3

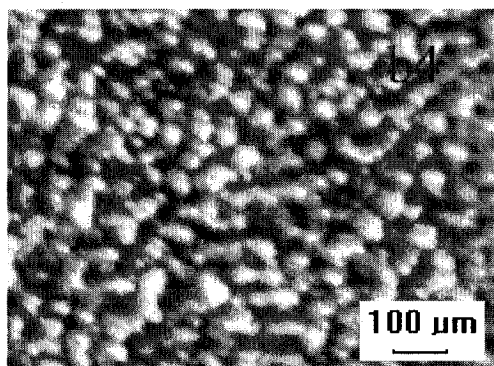


Parameter Sum Table

	Profile=R_ANSI - Section=[1]	Average Value
Ra (um)	2,040	2,040
Rmax (um)	13,046	13,046
Rz (um)	11,958	11,958
Rt (um)	15,978	15,978

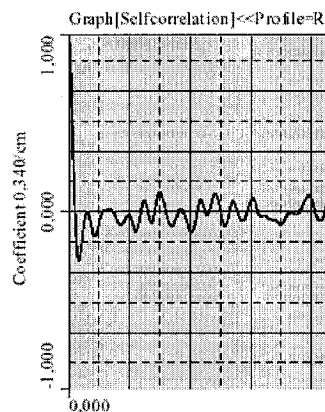
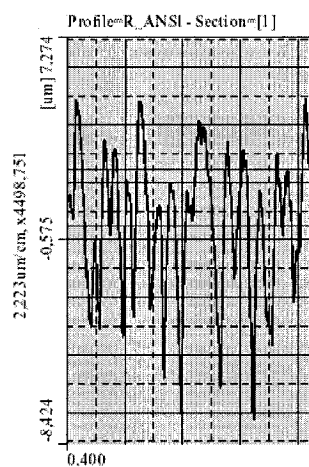


Sample b4

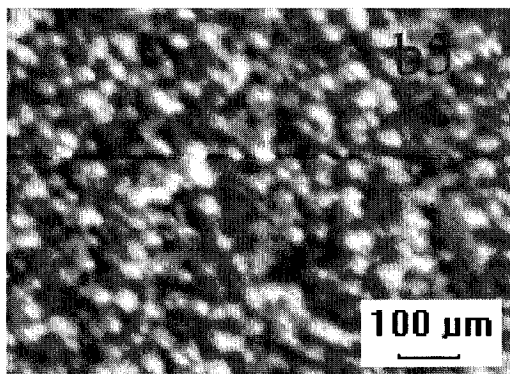


Parameter SumTable

	Profile=R_ANSI - Section=[1]	Average Value
Ra (um)	2,103	2,103
Rmax (um)	14,950	14,950
Rz (um)	13,081	13,081
Rt (um)	14,950	14,950

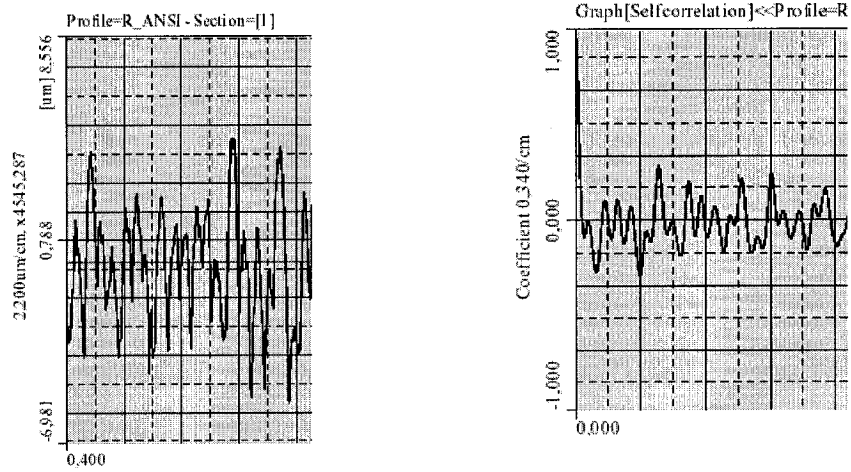


Sample b5

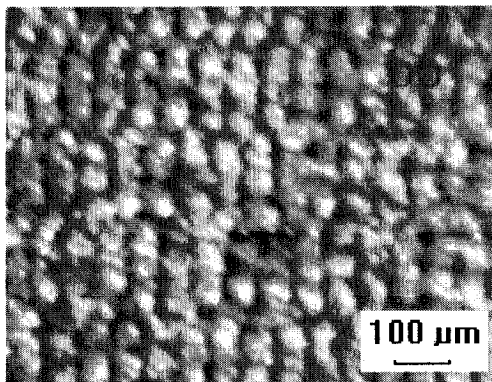


Parameter SumTable

	Profile=R_ANSI - Section=[1]	Average Value
Ra (um)	1,899	1,899
Rmax (um)	13,594	13,594
Rz (um)	12,060	12,060
Rt (um)	14,797	14,797



Sample b6



Parameter Sum Table

	Profile=R_ANSI - Section=[1]	Average Value
Ra (um)	2,985	2,985
Rmax (um)	17,779	17,779
Rz (um)	16,860	16,860
Rt (um)	19,278	19,278

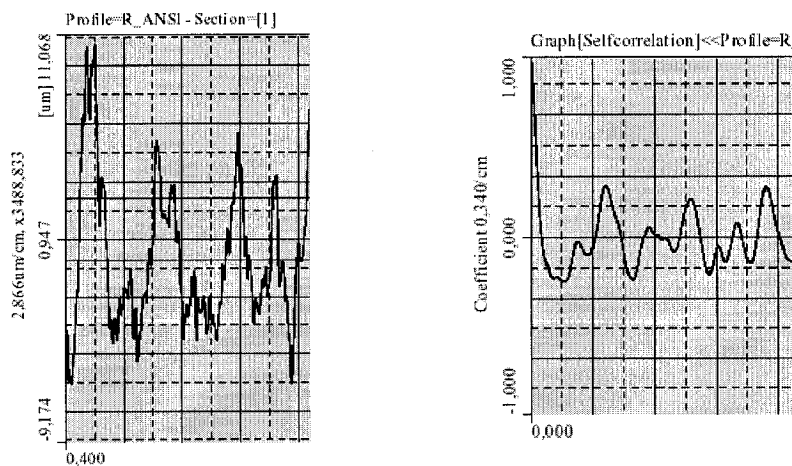


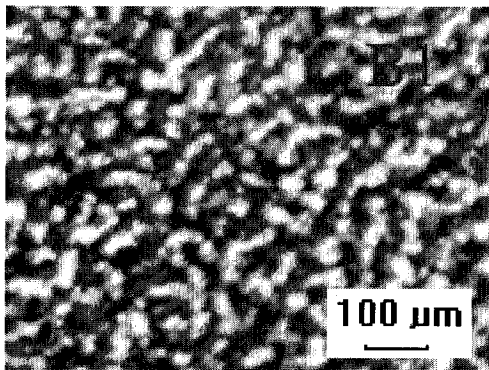
Figure APP.A-3 Microscope photos of test for verifying *engraving speed*. (Small laser spot) b1:180mm/s; b2:225mm/s; b3:300mm/s; b4:450mm/s; b5:900mm/s; b6:1350mm/s

4. Experiment 4

Table Appendix A.4 Experiment parameters of test for verifying *engraving speed*. (Big laser spot)

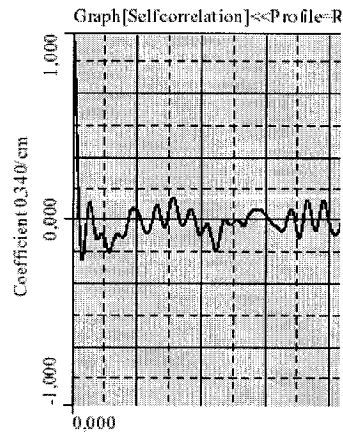
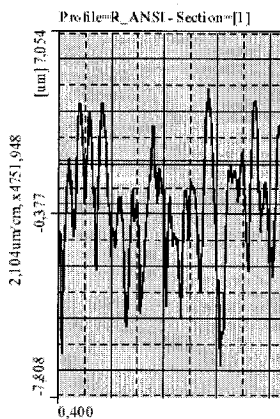
Parameter studied	Experiment parameters				Current intensity	constant			Hatching mode
	Independent variable					Engraving speed (mm/s)	Machined layer thickness (µm)	Track distance (mm)	
Engraving speed	30	0.2	0.125	480	25% Max	0.002	0.01	Big (80)	Cross hatching and unidirectional
	30	0.25	0.125	600					
	30	0.33	0.125	800					
	30	0.5	0.125	1200					
	30	1	0.125	2400					
	30	1.5	0.125	3600					

Sample B1

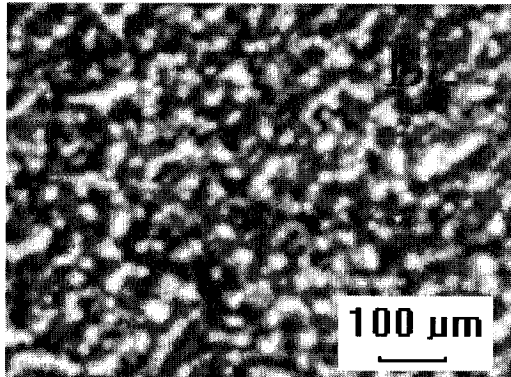


Parameter SumTable

	Profile=R_ANSI - Section=[1]	Average Value
Ra (µm)	1,872	1,872
Rmax (µm)	14,154	14,154
Rz (µm)	11,901	11,901
Rt (µm)	14,154	14,154

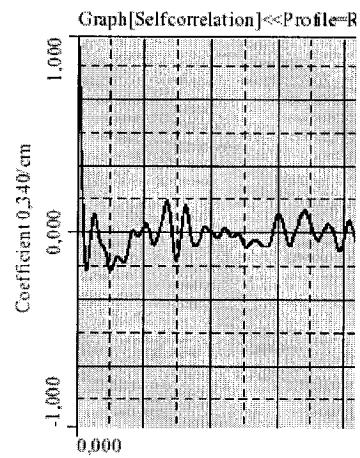
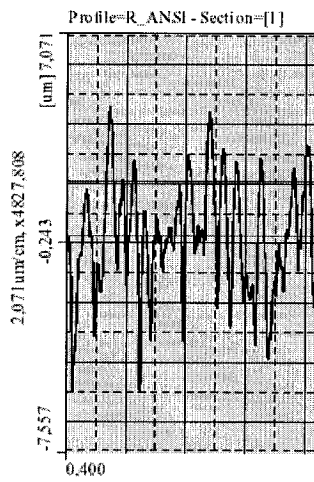


Sample B2

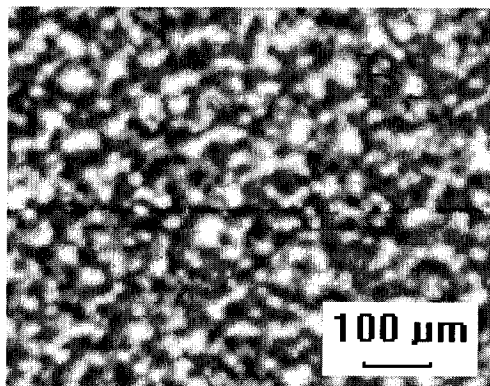


Parameter SumTable

	Profile=R_ANSI - Section=[1]	Average Value
Ra (um)	1,857	1,857
Rmax (um)	13,475	13,475
Rz (um)	12,228	12,228
Rt (um)	13,931	13,931

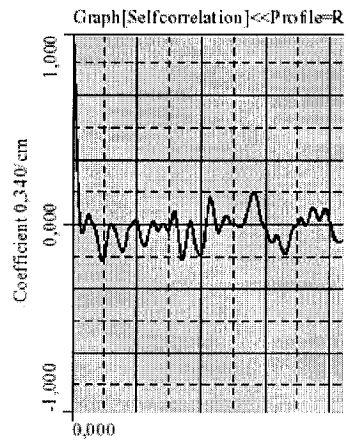
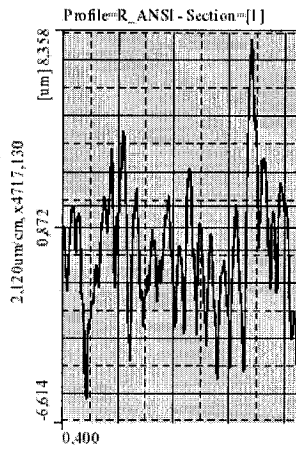


Sample B3

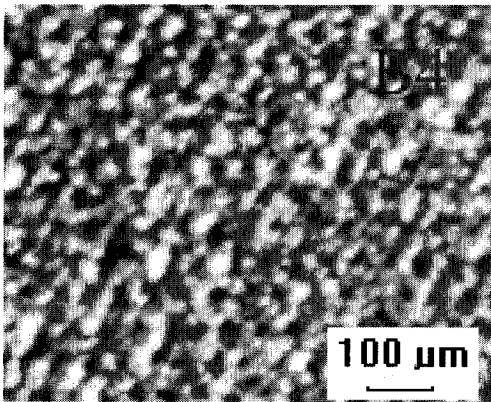


Parameter SumTable

	Profile=R_ANSI - Section=[1]	Average Value
Ra (um)	1,705	1,705
Rmax (um)	13,677	13,677
Rz (um)	11,379	11,379
Rt (um)	14,258	14,258

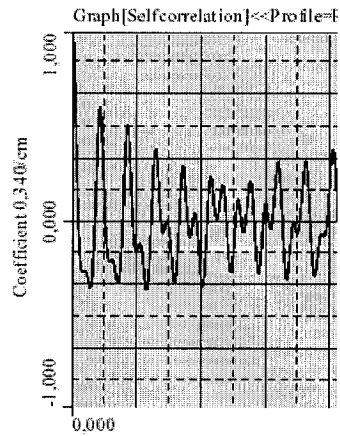
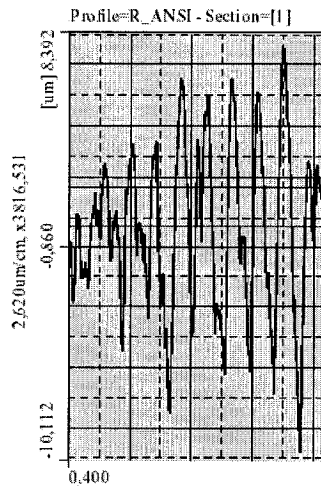


Sample B4

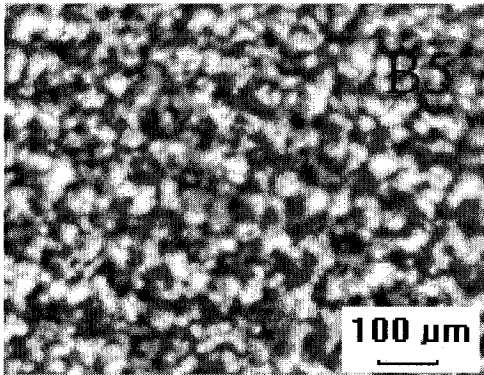


Parameter Sum Table

	Profile=R_ANSI - Section=[1]	Average Value
Ra (um)	2,127	2,127
Rmax (um)	17,455	17,455
Rz (um)	13,170	13,170
Rt (um)	17,623	17,623

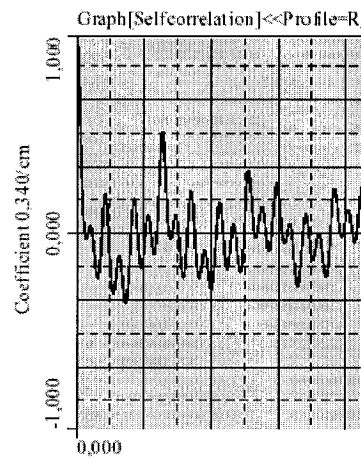
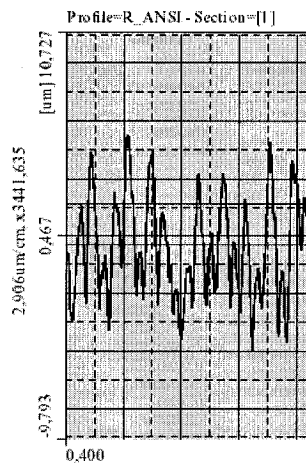


Sample B5

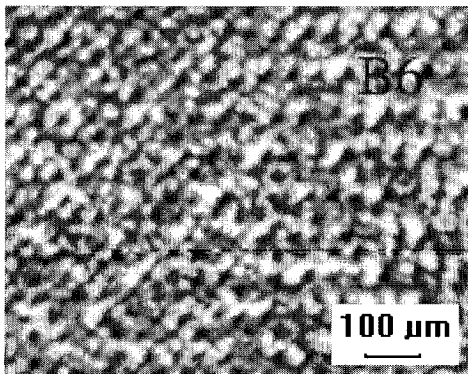


Parameter SumTable

	Profile=R_ANSI - Section=[1]	Average Value
Ra (um)	2,133	2,133
Rmax (um)	19,061	19,061
Rz (um)	14,172	14,172
Rt (um)	19,543	19,543



Sample B6



Parameter SumTable

	Profile=R_ANSI - Section=[1]	Average Value
Ra (um)	2,040	2,040
Rmax (um)	15,572	15,572
Rz (um)	12,124	12,124
Rt (um)	15,654	15,654

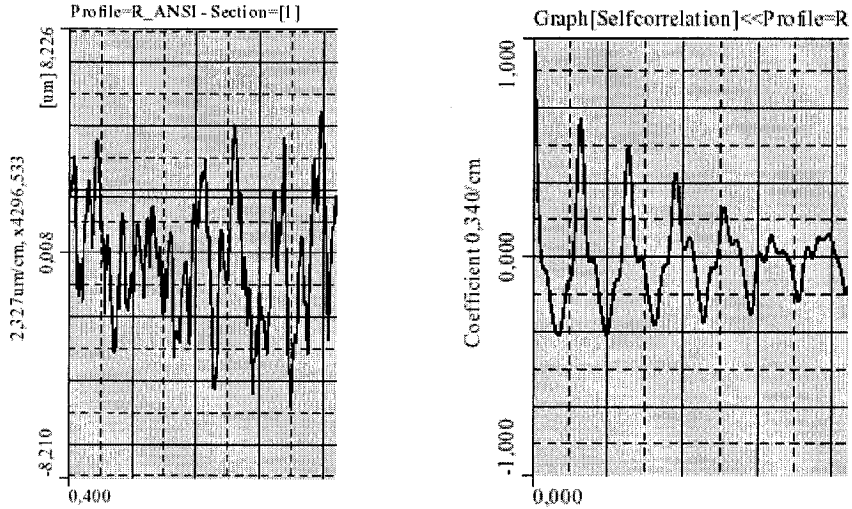


Figure APP.A-4 Microscope photos of test for verifying *engraving speed*. (Big laser spot) B1:480mm/s; B2:600mm/s; B3:800mm/s; B4:1200mm/s; B5:2400mm/s; B6:3600mm/s

APPENDIX-B PHOTOS OF MICRO-GEOMETRIES DISCUSSED IN CHAPTER 5

During our experiments, laser machined micro geometries on cemented carbide inserts and made a micro mould for a micro drill. The machining parameter is:

Q-switch closing frequency (kHz)	Engraving speed (mm/s)	Current intensity	Machined layer thickness (μm)	Track distance (mm)	Aperture mode Diameter of laser beam (μm)	Hatching mode
17	400	25%	0.002	0.01	Small (30)	Cross hatching and unidirectional

Experiment 1: Round cutting edge.

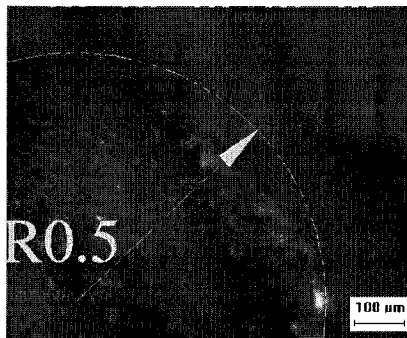


Figure APP.B-1.1 Positive round cutting edge, desired radius=0.5mm, error <14%.

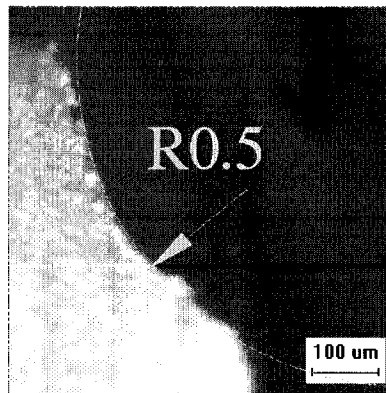


Figure APP.B-1.2 Negative round cutting edge, desired radius=0.5mm, error <1%.

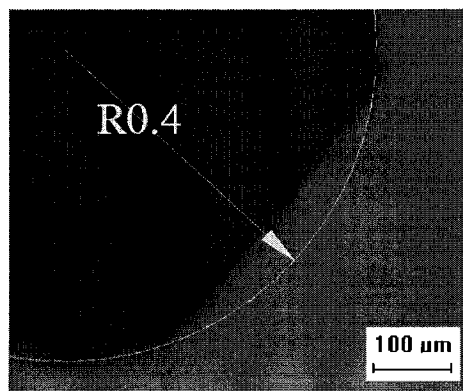


Figure APP.B-1.3 Round cutting edge, desired radius=0.4mm, error<10%.

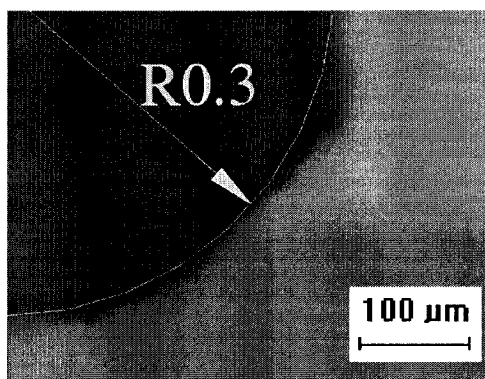


Figure APP.B-1.4 Round cutting edge, desired radius=0.3mm, error<10%..

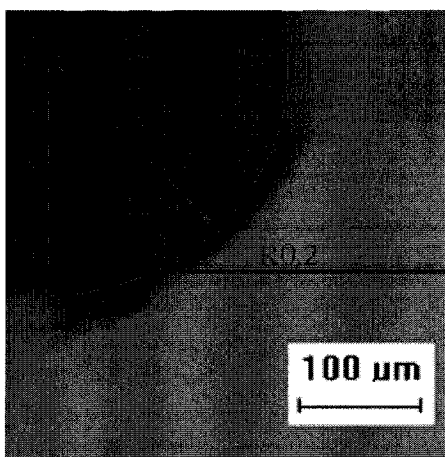


Figure APP.B-1.5 Round cutting edge, desired radius=0.2mm, error<10%.

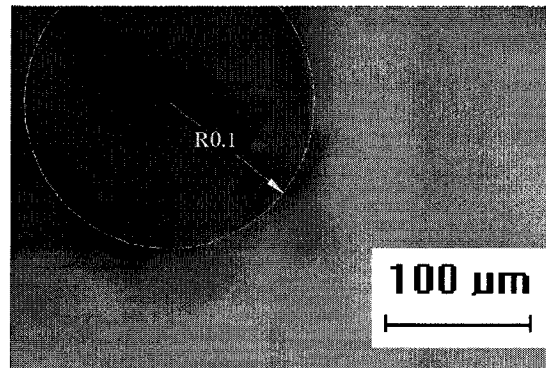


Figure APP.B-1.6 Round cutting edge, desired radius=0.1mm, error<15%.

Experiment 2: Semi-circular profile groove.

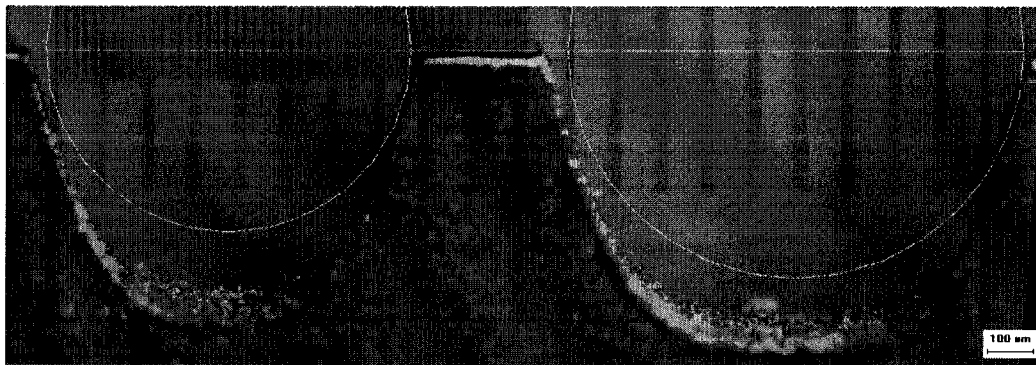


Figure APP.B-2.1 Semi-circular profile micro groove, desired radius=0.5,0.4mm, error< 12%.

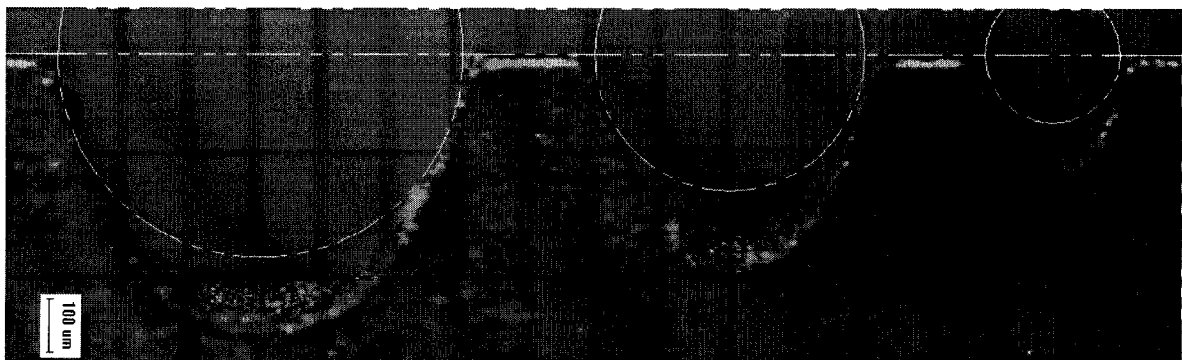


Figure APP.B-2.2 Semi circle profile micro groove, desired radius=0.1, 0.2, 0.3 mm, error <12%.

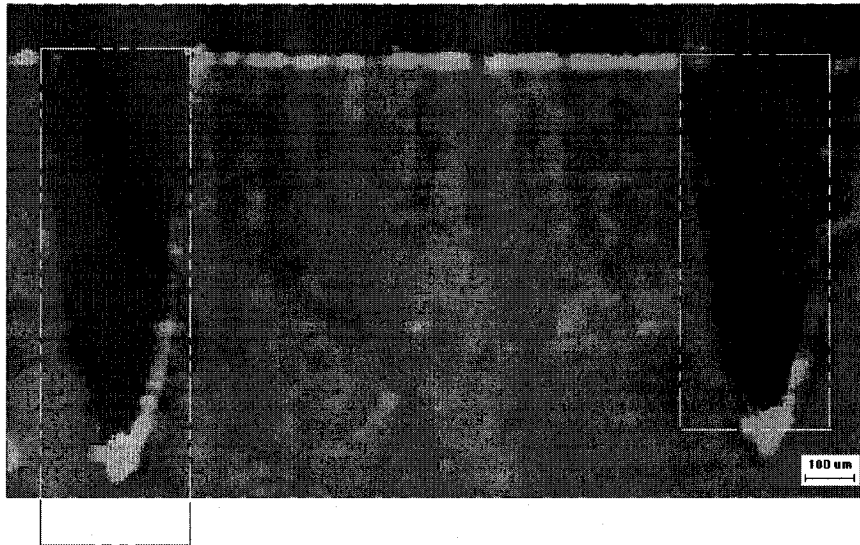
Experiment 3: Rectangle profile groove.

Figure APP.B-3.1 Rectangle profile micro groove, desired width=0.3mm. desired depth=0.75mm, 0.5mm.

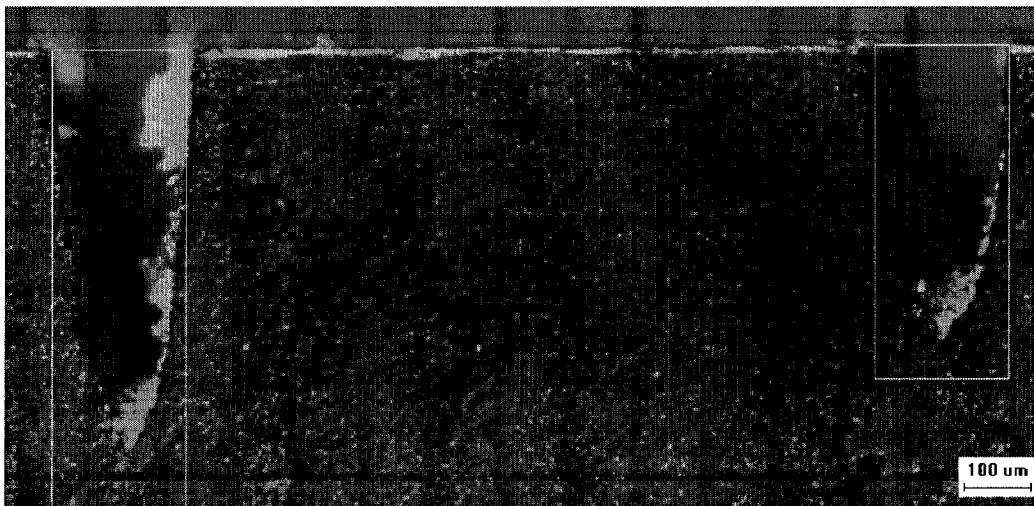


Figure APP.B-3.2 Rectangle profile micro groove, width=0.2mm, desired depth 0.75mm, 0.5mm.

Experiment 4: Micro-cylindrical pocket

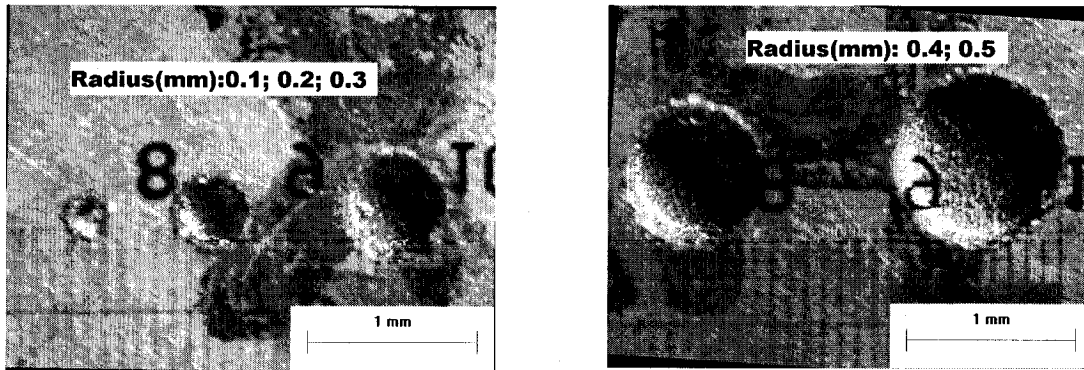


Figure APP.B-4 Micro-cylindrical pocket. Desired radius are $R=0.1\text{mm}$, $R=0.2\text{mm}$, $R=0.3\text{mm}$, 0.4mm , 0.5mm .

Experiment 5: Micro rectangle pocket

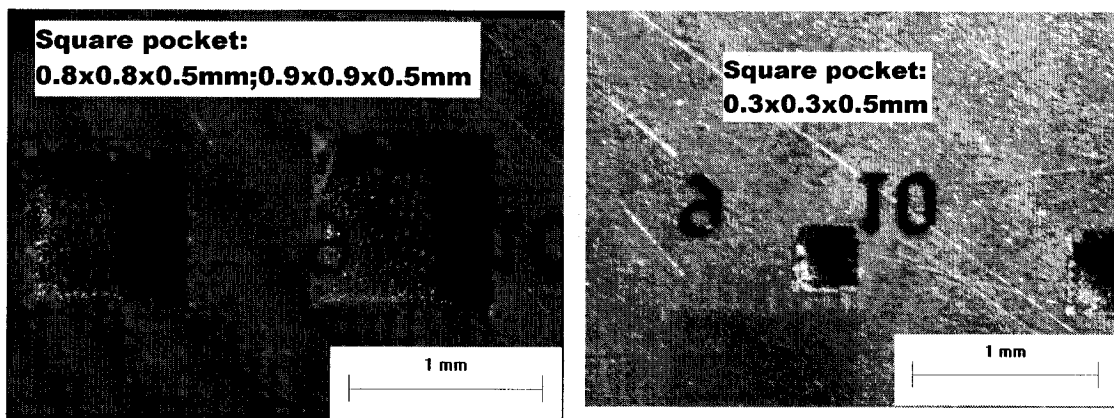


Figure APP.B-5 Micro square pocket. Desired size are $0.9\times 0.9\text{ mm}$, $0.8\times 0.8\text{mm}$, $0.3\times 0.3\text{mm}$, depth 0.5mm .